

An energy recovery device for small-scale seawater reverse
osmosis desalination

by

Alfredo Sergio Bermudez Contreras

A Doctoral Thesis

Submitted in partial fulfilment of the requirements
for the award of
Doctor of Philosophy of Loughborough University

9th December 2009

© by Alfredo Sergio Bermudez Contreras 2009

Certificate of originality

This is to certify that I am responsible for the work submitted in this thesis, that the original work is my own except as specified in acknowledgements, footnotes or references, and that neither the thesis or the original work contained therein has been submitted to this or any other institution for a degree.

Signed: Alfredo Bermudez

Date: 09 December 2009

Abstract

This work presents the concept development, implementation and first practical demonstration of a new pressure intensifier for energy recovery in small-scale seawater reverse osmosis systems, and the simplified system configuration it requires. The new concept has great potential to reduce the specific energy consumption of small-scale seawater reverse osmosis systems. A mathematical analysis to study pressure intensifiers for energy recovery in reverse osmosis applications was developed. The analysis was used in the design and modelling of the energy recovery device. A first prototype was built and subsequently demonstrated in a system desalinating seawater over a wide range of electrical input power stretching between 286 and 1196 W, producing up to 286 L/h of freshwater with specific energy consumptions in the range of 3.5 to 4.5 kWh/m³. The flat specific energy characteristic makes the device attractive for renewable-energy-powered systems without energy storage. The prototype implementation was realised through modifying a Clark pump, but the new concept is fundamentally different. The new device recovers energy from the concentrate stream, which it then uses to suck in and pressurise seawater, relying purely on its piston area ratio, and thus eliminating the need for a low-pressure feed pump.

Acknowledgements

I wish to express my gratitude to Murray Thomson for his support, encouragement and useful guidance throughout this project. I thank him for the long discussions we engaged in, particularly towards the end of this project. They have been of enormous value.

I also wish to acknowledge the financial support of Mexico's National Council for Science and Technology (CONACYT), which has given me the opportunity of getting involved in this most interesting field.

To my loved ones, many thanks for your help and support.

Alfredo Bermudez

December 2009

Contents

Certificate of originality	ii
Abstract	iii
Acknowledgements	iv
Contents	v
List of figures	ix
List of tables	xi
List of symbols and abbreviations	xii
Chapter 1 Overview	1
1.1 Water and energy	1
1.2 Reverse osmosis basics	2
1.3 Energy recovery for reverse osmosis	3
1.4 The Clark pump	4
1.5 This project	4
1.6 Relevance	6
Chapter 2 Literature and technology review	8
2.1 Desalination	8
2.1.1 Desalination industry	8
2.1.2 Salinity of the source: brackish or seawater	9
2.1.3 Implications for desalination	10
2.1.4 Water quality target: literature and guidelines	10
2.1.5 Seawater desalination technologies	11
2.1.5.1 Evaporation	12
2.1.5.2 Multiple effect distillation (MED)	13
2.1.5.3 Multistage flash distillation (MSF)	13
2.1.5.4 Vapour compression (VC)	14
2.1.5.5 Comparison	14
2.2 Reverse osmosis	16
2.2.1 Osmotic processes	16
2.2.2 Continuous process	17
2.2.3 Water transport	18
2.2.4 Salt transport	19
2.2.5 History and technology progress	20
2.2.6 Membrane materials	22
2.2.7 Membrane configurations	23
2.2.8 Concentration polarisation	27
2.2.9 Membrane fouling	28
2.2.10 Pretreatment	29
2.3 Energy for desalination	29
2.3.1 Energy consumption and CO ₂ emissions	29
2.3.2 Desalination and renewable energy	30

2.3.2.1	Solar thermal.....	31
2.3.2.2	Photovoltaics.....	33
2.3.2.3	Wind.....	34
2.3.2.4	Wave power	34
2.3.2.5	Renewable energy variability and reverse osmosis	36
2.4	Energy recovery	38
2.4.1	Energy recovery economics	39
2.4.2	Classification of brine-stream energy recovery	40
2.4.3	Pelton wheel	41
2.4.4	Hydraulic turbo booster	43
2.4.5	Dual work exchanger energy recovery (DWEER)	44
2.4.6	PX Pressure Exchanger (PX)	45
2.4.7	Booster pump	46
2.4.8	High-pressure pump	46
2.4.9	Integrated pump and energy recovery (IPER)	47
2.4.10	Energy recovery for small-scale seawater reverse osmosis.....	47
2.4.11	Pumps with built-in energy recovery	48
2.4.12	Hydraulic motor	49
2.4.13	Device selection	49
Chapter 3	The Clark pump	54
3.1	Concept.....	54
3.2	Mechanics	55
3.3	Basic system configuration	55
3.4	Injection configuration	58
Chapter 4	The challenge and initial investigations	61
4.1	State of the art summary.....	61
4.2	Motorised pump efficiency observation	62
4.3	Thesis objectives.....	63
4.4	Many possibilities	63
4.5	Initial selection.....	65
4.6	Generalised configuration	67
Chapter 5	Generalised analysis of pressure intensifiers for energy recovery	68
5.1	Pistons	68
5.2	Piston area ratio	68
5.3	Area ratio of the Clark pump	70
5.4	Device equations.....	70
5.4.1	Energy recovery	70
5.4.2	RO membranes	72
5.5	System equations.....	72
5.5.1	Flow balances.....	73
5.5.2	Pressure differences.....	74
5.6	Analysis.....	74
5.6.1	Permeate flow rate	75
5.6.2	Recovery ratio	76

5.6.3	Membranes' feed pressure	78
5.6.3.1	Area ratio $r_a > 1$	78
5.6.3.2	Area ratio $r_a < 1$	79
5.6.3.3	Area ratio $r_a = 1$	80
5.6.4	Device comparison	81
5.7	Area ratio of the new device	82
5.8	System operation description	83
Chapter 6	System modelling and performance predictions	85
6.1	Simulink model	85
6.2	Effect of piston area ratio	86
6.3	Selection	88
6.4	Performance predictions	89
6.4.1	Area ratio $r_a = 0.96$	89
6.4.2	Energy flows at $r_a = 0.96$	91
6.4.3	Comparison to the basic Clark pump	93
6.4.4	Area ratio $r_a = 0.90$	94
6.4.5	Energy flows at $r_a = 0.90$	97
Chapter 7	Prototype implementation	99
7.1	New chamber arrangement	99
7.2	New area ratio	101
7.3	Internal flows in the standard Clark pump	101
7.4	Modifying the Clark pump	105
7.4.1	Main flows	105
7.4.2	Valve gear	105
7.4.3	Practical modifications	106
7.4.4	Control flows	108
7.5	Preliminary tests	109
7.6	The pressure exchanger-intensifier	111
Chapter 8	Testing and results	114
8.1	General arrangement	114
8.2	Successful operation	116
8.3	Test setup details	116
8.4	Results	118
8.4.1	Product flow	118
8.4.2	RO membranes performance	120
8.4.3	Membranes feed pressure	121
8.4.4	Flows in the modified Clark pump	122
8.4.5	Energy balance	125
8.4.6	Uneven operation	126
8.5	Revised modelling	127
Chapter 9	Conclusions	130
9.1	Energy recovery for small-scale SWRO	130
9.2	Mathematical analysis of pressure intensifiers	130
9.3	New system configuration	131

9.4	Improved system efficiency	131
9.5	New device concept	132
9.6	Prototype implementation	132
9.7	First practical demonstration	132
9.8	Practical issues	133
9.9	Alternative implementation	134
9.10	Closing statement	135
Publications.....		136
References.....		137
Appendix A	Testing data	146

List of figures

Figure 1.1 Reverse osmosis schematic	3
Figure 1.2 System configuration with the new energy recovery device.....	5
Figure 2.1 Global installed desalination capacity	8
Figure 2.2 Membrane and thermal desalination installed capacity worldwide ..	12
Figure 2.3 Osmosis	16
Figure 2.4 Reverse osmosis.....	17
Figure 2.5 Schematic of a reverse osmosis process.....	18
Figure 2.6 Specific flux and salt passage evolution for seawater membranes .	21
Figure 2.7 Evolution of net driving pressure for brackish water membranes	21
Figure 2.8 Evolution of energy consumption for seawater reverse osmosis	22
Figure 2.9 Spiral wound module fabrication	26
Figure 2.10 Sankey diagram of a PV-RO system using batteries	37
Figure 2.11 Sankey diagram of a seawater PV-RO system with energy recovery	38
Figure 2.12 Approaches to energy recovery and transfer	40
Figure 2.13 System using a Pelton wheel	42
Figure 2.14 System using a hydraulic turbo booster	43
Figure 2.15 System using a DWEER	44
Figure 2.16 System using a PX.....	45
Figure 2.17 Energy consumption for various energy recovery approaches	51
Figure 3.1 Schematics of a Clark pump	54
Figure 3.2 Basic configuration of a system with a Clark pump	56
Figure 3.3 Energy flows in Spectra Watermakers' system	57
Figure 3.4 Injection system configuration of the Clark pump.....	59
Figure 4.1 Potential for specific energy reduction	62
Figure 4.2 Spectrum of geometries	64
Figure 4.3 Generalised system configuration	67
Figure 5.1 Flows and piston areas in the three intensifiers	69
Figure 5.2 Piston areas in a Clark pump	70
Figure 5.3 Flow rates and pressures in a device with $r_a < 1$	71
Figure 5.4 Flows and pressures	73
Figure 5.5 Permeate and high-pressure pump flow rates	75
Figure 5.6 Freshwater recovery ratio	77
Figure 5.7 Effect of pressure drop for $r_a > 1$	79
Figure 5.8 Effect of pressure drop for $r_a < 1$	80
Figure 5.9 Inlet pressure versus area ratio for $\Delta P_{RO} = 0$	82
Figure 5.10 New system configuration	83
Figure 6.1 Simulink high-level structure of the system model	85
Figure 6.2 Effect of the area ratio at various motor speeds.....	87
Figure 6.3 Operation with $r_a = 0.96$	90

Figure 6.4 Specific energy flows at 1196 W input power.....	92
Figure 6.5 Simulation results of operation at 10% recovery ratio	94
Figure 6.6 Operation with $r_a = 0.90$ (red) and $r_a = 0.96$ (blue)	95
Figure 6.7 The proposed device and system configuration	96
Figure 6.8 Energy flows at $r_a = 0.90$ and 1196 W	98
Figure 7.1 New chamber arrangement.....	100
Figure 7.2 Comparison of the new arrangement and the Clark pump	101
Figure 7.3 Schematic of a Clark pump	102
Figure 7.4 Reciprocation valve gear and internal flows in a Clark pump	103
Figure 7.5 Reciprocation valve gear in the Clark pump	106
Figure 7.6 Reciprocation valve gear reconfiguration	107
Figure 7.7 Separation of the valve block	107
Figure 7.8 The modified Clark pump	108
Figure 7.9 Arrangement for preliminary testing	110
Figure 7.10 Independent movement of the rod and high-pressure piston	111
Figure 7.11 Attaching the pistons and new rod	111
Figure 8.1 Prototype test arrangement.....	114
Figure 8.2 The test rig	115
Figure 8.3 Product flow	118
Figure 8.4 Specific energy	119
Figure 8.5 Effect of feed pressure on product flow	120
Figure 8.6 RO membranes feed pressure	121
Figure 8.7 Inlet-to-exhaust flow ratio in the modified Clark pump.....	123
Figure 8.8 Pressure-driven leak	124
Figure 8.9 Specific energy flows during the test at 1196 W	126
Figure 8.10 Revised model predictions	128
Figure 8.11 Sankey diagram of revised energy flows at 1196 W	129
Figure 9.1 Alternative configuration.....	135

List of tables

Table 2.1 Practical energy consumption in seawater desalination	14
Table 4.1 Capabilities of the device layouts	66
Table 5.1 High-pressure pump flow rate	76
Table 5.2 Comparison of the pressure intensifiers	81
Table 6.1 Model constants	86
Table 6.2 Typical values	88
Table 6.3 Model predictions with $r_a = 0.96$ at 1196 W of input power.....	91
Table 6.4 Model predictions with $r_a = 0.90$ and $r_a = 0.96$ at 1196 W of input power	97
Table 8.1 Test rig hardware	117
Table A.1 Averaged data for all tests	146

List of symbols and abbreviations

A	Area on the seawater side of pistons in the ERD
A_m	Membrane area
B	Area on the concentrate side of pistons in the ERD
C	Concentrate flow
C_{avg}	Average concentration in the feed-brine channel
C_f	Concentration of the feed
C_p	Concentration of the permeate
CA	Cellulose acetate
CP	Clark pump
DC_{in}	Electrical DC power input
DWEER	Dual work exchanger energy recovery
E	Exhaust flow
ED	Electrodialysis
ER	Energy recovery
ERD	Energy recovery device
F	Forces
HPB	Hydraulic Pressure Booster
HP	High-pressure seawater flow
IPER	Integrated pump and energy recovery
K_s	Salt permeability coefficient of the membrane
K_w	Water permeability coefficient of the membrane
MCP	Modified Clark pump
MED	Multiple effect distillation
MPPT	Maximum power point tracker
MSF	Multistage flash distillation
NDP	Net driving pressure
P_c	Concentrate pressure
P_e	Exhaust pressure
P_f	RO membranes feed pressure
P_i	ERD seawater inlet pressure

P_p	Permeate pressure
PEI	Pressure exchanger intensifier
PV	Photovoltaics
PX	PX Pressure Exchanger
ΔP_{RO}	Pressure drop across the membranes
ΔP_{SW}	Pressure difference between the seawater chambers in the modified Clark pump
ΔP_{ER}^{f-c}	ERD pressure difference (high pressure – concentrate pressure)
π_{avg}	Average osmotic pressure in the feed-brine channel
π_f	Osmotic pressure of the RO membranes' feed
π_p	Osmotic pressure of the permeate
Q_c	Concentrate flow
Q_e	Exhaust flow
Q_f	RO membranes' feed flow
Q_h	High-pressure pump flow
Q_i	ERD seawater inlet flow
Q_{leak}	Internal leakage flow in the modified Clark pump
Q_p	Permeate flow
Q_s	Salt flow through the membrane
Q_t	ERD seawater high-pressure flow
r_a	ERD piston area ratio
RO	Reverse osmosis
RR	Freshwater recovery ratio
S	Seawater input flow
SEC	Specific energy consumption
SMSF	Solar multistage flash distillation
SW	Seawater
SWRO	Seawater reverse osmosis
T_{SW}	Seawater temperature
TDS	Total dissolved solids
Vc	Concentrate valve
VC	Vapour compression
Vp	Permeate valve

Chapter 1 Overview

1.1 Water and energy

Many regions of the world are facing enormous water shortages. In 2005, half a billion people lived in water-scarce and water-stressed countries (UN-Water, 2005); many of them are forced to drink contaminated water, which often causes disease and can lead to their early death. Population growth and the pollution of natural sources of freshwater are causing a significant and on-going reduction in the worldwide per capita availability of clean drinking water. Increasing water demands for agriculture, industry and tourism lead to further shortages.

Similar factors apply to energy. With highly volatile oil prices and in view of the great costs that fossil fuels pose on the environment, alternative renewable energy sources must be increasingly included in the energy mix. However, despite the enormous growth rates of some renewables like wind and solar in the past decades, their contributions in absolute terms must still grow considerably.

In the provision of both water and energy two goals must be globally adopted:

- First is the conservation of currently available resources. This alone, however, will not be sufficient.
- Second is the production of freshwater and energy from alternative sources like sea or brackish water and renewable energy.

Desalination of sea and brackish water already plays a major role in the provision of freshwater for domestic, agricultural and industrial uses in many parts of the world and is a thriving industry that has doubled its capacity to almost 50 million m³/d in the last ten years or so (see section 2.1.1). Reverse osmosis (RO) and various thermal methods dominate the industry. Whilst highly successful in delivering freshwater, desalination is a very energy-intensive

process, already consuming vast quantities of fossil fuels worldwide (see discussion in section 2.3). As a result, desalination is a major contributor to CO₂ emissions and will undeniably play a part in global warming.

Fortunately, the areas where water shortage is most acute often have good renewable energy resources, which could be used to power desalination. This has long been recognised and many pilot demonstrations of renewable-energy powered desalination have been built. Seawater reverse osmosis (SWRO) powered by wind or solar energy is regarded amongst the most promising options, particularly for small-scale installations producing freshwater in the range of tens of cubic meters per day (section 2.3.2).

1.2 Reverse osmosis basics

Reverse osmosis can be compared to a filtration of salts that achieves the separation by means of a semipermeable membrane (the filtration medium, see Figure 1.1). The membrane allows water through but opposes the passage of salts. Reverse osmosis membranes can also reject all particulate and colloidal matter, bacteria, viruses and dissolved organic matter. The energy required to achieve the separation of salts and water is supplied to the process in the form of pressure, which must exceed the osmotic pressure of the seawater to push freshwater through the membrane. Pressures of around 50 bar or higher are typical in seawater reverse osmosis.

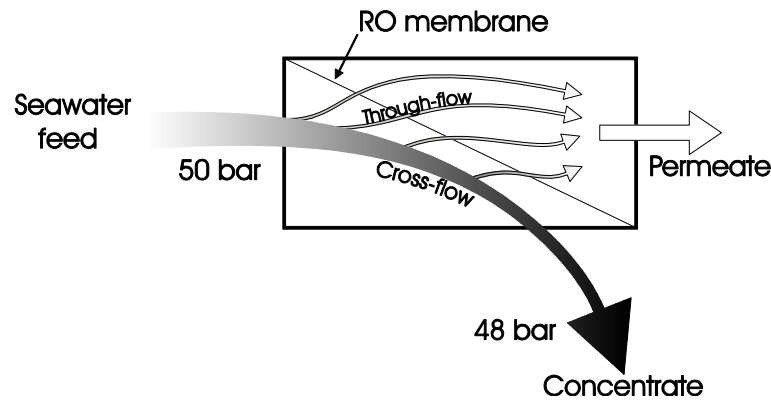


Figure 1.1 Reverse osmosis schematic

In seawater reverse osmosis, unlike dead-end filtration, not all the water in the feed goes through the membrane. Normally, only 30-45% of the feed flow is recovered as freshwater; this is referred to as the permeate or product. The rest of the seawater ends up in the concentrate or brine stream, which serves to flush the salts out of the membrane to prevent these from accumulating on the membrane surface.

1.3 Energy recovery for reverse osmosis

The pressure drop across the feed-brine channel of the reverse osmosis membranes is very small, of the order of 1-2 bar. As a result, the concentrate carries a large share of the energy in the seawater feed. Recycling this energy back into the process improves the overall efficiency of the operation. Amongst the mainstream seawater desalination technologies, reverse osmosis with energy recovery has the lowest energy requirements per unit of freshwater produced (see Table 2.1). This energy is known as the specific energy consumption (SEC) and is used to measure the efficiency of RO operations.

In recognition of this, brine-stream energy recovery is common practice in large SWRO plants. However, energy recovery is often overlooked in small-scale

applications to reduce capital costs and as a result, such systems are often very energy wasteful.

1.4 The Clark pump

The Clark pump from Spectra Watermakers (www.spectrawatermakers.com, accessed 17 July 2009), discussed in detail in Chapter 3, is an efficient energy recovery device for small-scale seawater RO, originally developed for desalinators onboard small yachts. It is a small-scale pressure intensifier that uses the reciprocating motion of two pistons connected by a rod inside a cylindrical housing (see Figure 3.1, page 54) to recover energy from the concentrate stream in a RO process.

In its basic implementation, a Clark pump requires only one low-pressure pump (Figure 3.2), which makes it possible to operate a small RO system from a single battery (Smith, 2000).

To increase the water production per Clark pump beyond that of its basic implementation, an injection system configuration with a high-pressure pump can be used (Figure 3.4). Such a configuration has been demonstrated desalinating seawater using photovoltaics to power a system without any energy storage (Thomson, 2003). In this demonstration, the system desalinated seawater efficiently despite fluctuations of the solar resource but the overall complexity of the system and the low efficiency of the low-pressure pump remained outstanding issues.

1.5 This project

To address the issues highlighted by Thomson's demonstration (2003), this thesis aimed at identifying a different pumping approach that improved the overall system efficiency while also allowing for a simpler system configuration.

The implementation of these concepts, however, required a different approach to energy recovery, which is the main subject of this work.

The rest of this thesis describes the background (Chapter 2 and Chapter 3) and theoretical concept development (Chapter 4, Chapter 5 and Chapter 6) of a first prototype of a new pressure intensifier for brine-stream energy recovery in small-scale SWRO and the system configuration required (Figure 1.2). This thesis also presents the practical implementation of the prototype (Chapter 7) and the testing results recorded (Chapter 8). The device uses only the energy in the concentrate to suck in seawater and intensify its pressure above the pressure of the concentrate. The concept implementation was carried out using a Clark pump's hardware and thus the prototype is mechanically similar to a Clark pump. However, its arrangement and operation is fundamentally different.

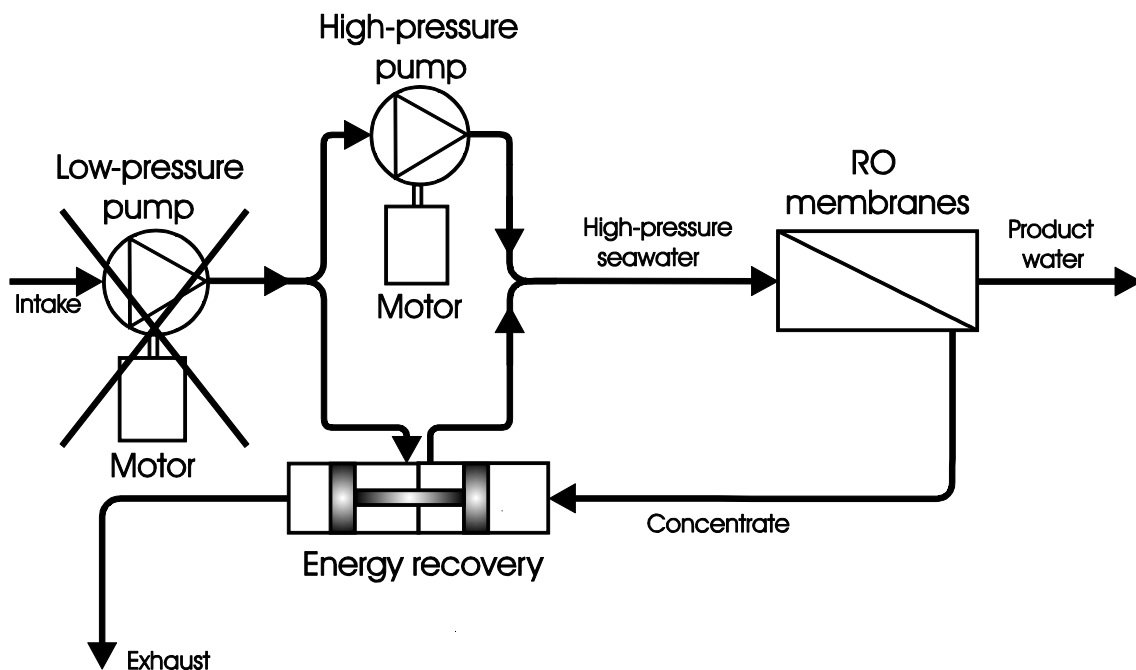


Figure 1.2 System configuration with the new energy recovery device

Unlike the Clark pump configurations (Figure 3.2 and Figure 3.4), a system with the new energy recovery device does not require a low-pressure pump, which simplifies the system configuration, and has the potential to improve the overall system efficiency by using only one motorised high-pressure pump. The

prototype of the energy recovery concept was demonstrated in a system desalinating seawater, with specific energies between 3.5 and 4.5 kWh/m³ over a wide range of input power and freshwater flow rates up to 286 L/h.

1.6 Relevance

The energy recovery concept and system configuration presented in this thesis are a new option for energy recovery in SWRO and have great potential to reduce the overall energy consumption in small-scale systems. The rationale behind the approach is shown in section 4.2. The results of the system modelling (section 6.4.1) show that specific energies below 3 kWh/m³ can be obtained over wide ranges of input power.

Recognising this potential, a prototype was built and subsequently demonstrated within a system desalinating seawater. To the knowledge of the author, the work of this thesis is the first practical demonstration of this device and system configuration.

The specific energies recorded during testing were very respectable for a small system and even more so for a first prototype, but due to the approach taken for implementation, these values were higher than predicted in the simulations. The causes for this are identified and explained (sections 7.2 and 8.4), and are readily fixable. In consequence, the great potential for energy consumption reduction remains unchanged.

Both the system modelling and the practical tests showed relatively flat specific energy consumption characteristics over a wide range of input power. Therefore the device and system configuration described in this thesis are well suited for applications with fluctuating power inputs like renewable-energy powered SWRO systems without energy storage.

Whilst the concept demonstration carried out in this thesis was performed in a small-scale system, there are no obvious limitations to extend its use to larger

systems as long as positive displacement high-pressure pumps are used. For larger systems, however, there are already several successful commercial energy recovery options making the work in this thesis most relevant for small-scale applications.

Chapter 2 Literature and technology review

2.1 Desalination

2.1.1 Desalination industry

Mankind have been separating salt from water for centuries either to produce salt or to obtain freshwater. Desalination refers to the latter: the physical separation of salts and water in a saline solution to produce freshwater. However, it was not until World War II that greater research efforts in desalination were undertaken and their continuation has led to the thriving industry that desalination is today. Figure 2.1 shows the fast growth of this industry worldwide in the last four decades. The installed capacity is mostly concentrated in large desalination plants capable of producing in excess of tens of thousands of cubic meters daily (Pankratz, 2008). Desalination is widely used in the provision of water for municipal, agricultural and industrial uses, and has enabled development in numerous areas around the world, notably the Middle East.

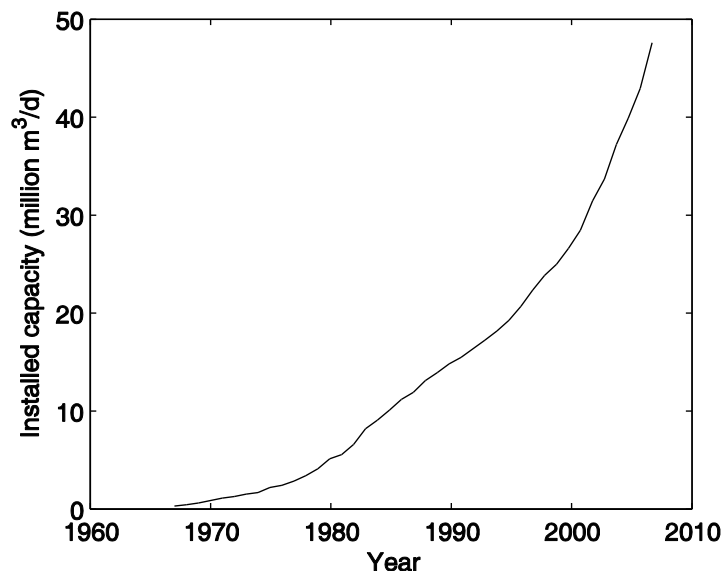


Figure 2.1 Global installed desalination capacity.
Data from Pankratz (2008)

2.1.2 Salinity of the source: brackish or seawater

The selection of a desalination method depends largely on the salinity of the water source. To make a distinction between the various water sources, it is necessary to first discuss salinity and how it is measured.

Salinity refers to the concentration of dissolved salts in water. Throughout the literature, salinity is reported in different units. Mass-to-volume and mass-to-mass ratios are the most common. The desalination industry uses parts per million (ppm) and mg/L as standard to report total dissolved solids (TDS) and they are often used interchangeably due to their numerical similarity. Strictly speaking, this practice is incorrect especially for waters of higher concentration like seawater.

Authors in the desalination field classify water according to its salinity. The desalination industry makes a clear distinction between brackish water and seawater. The former has an upper concentration limit of about 10 000 mg/L and its components vary greatly depending on the minerals present in the ground where it is sourced. This may lead to waters with higher concentrations of particular components, like Arsenic or Boron, requiring special treatment when desalinating water.

Seawater, on the other hand, has a more uniform composition with sodium and chloride ions accounting for most of the mass of dissolved solids. Seawater salinity, with an overall average of 34 000 mg/L, ranges from averages as low as 28 000 mg/L in the Baltic Sea to 44 000 mg/L in the Red Sea and even higher values in enclosed water bodies like the Dead Sea. Local seawater concentrations vary too with evaporation, precipitation and proximity to river estuaries (Medina San Juan, 2000; El-Dessouky and Ettouney, 2002).

2.1.3 Implications for desalination

Salinity plays a role in the selection of desalination method in that desalination of lower salinity water can be achieved with less energy and this should be taken advantage of whenever possible. Thus, thermal desalination methods, which rely on a phase change to separate water from salt, have energy requirements largely independent from water salinity and hence are better suited for seawater desalination. Electrodialysis (ED), relying on a potential difference to separate dissolved ions from water, works best for brackish water. Reverse osmosis works efficiently for both brackish and seawater desalination.

Regarding the selection of a desalination method, the various desalination technologies yield water of varying qualities. Thermal methods achieve purities well beyond that required for human consumption in one pass and some form of remineralisation may even be required. This makes thermal methods also well suited to produce high-purity water for industrial applications.

Electrodialysis and reverse osmosis can both produce water suitable for human consumption. They can also achieve very high purities but they may require more energy or additional process stages to achieve very low product water salinities.

2.1.4 Water quality target: literature and guidelines

In the desalination literature an upper limit of 500 mg/L of total dissolved solids is often quoted as the maximum allowed concentration of total dissolved solids in drinking water. This value is normally, and wrongly, attributed to the World Health Organization (WHO) in their *Guidelines for drinking-water quality* (WHO, 2003). The WHO say that “reliable data on the possible effects associated with the ingestion of TDS in drinking-water are not available, and no health-based guideline value is proposed.” (WHO, 2008; p. 444). Some authors (Mathew et al., 2000; Richards and Schäfer, 2002) dealing with water supply for remote

areas in Australia suggest that there could be links between drinking water of poor quality and health problems like diabetes, kidney and gastric disorders.

The WHO's Guidelines suggest that 600 mg/L is the upper TDS limit for drinking water to be considered good based on palatability (see also WHO, 2003) and that values higher than 1000 mg/L make water significantly unpalatable. The Guidelines also suggest that high concentration of dissolved solids may also indirectly affect consumers as excessive scaling may form on hardware and appliances to handle water with a high TDS content. The WHO also recommend against very low dissolved solids concentrations in drinking water as this may be again of poor taste.

For the purpose of this thesis, the 500 mg/L figure will be adhered to as the upper limit for acceptable concentration of dissolved solids in drinking water because this is widely accepted in the industry and is within what the WHO recommend.

2.1.5 Seawater desalination technologies

Mainstream seawater desalination is performed either thermally or by means of membranes. The growth of the industry saw first the development of thermal methods followed by the development of membranes for desalination in the second half of the last century. Figure 2.2 presents the evolution of the installed capacity of thermal and membrane desalination worldwide since the 1980s and shows that membrane technologies have already overtaken the thermal methods. The pie chart in this figure shows the relative installed capacity shares of the main desalination technologies in 2008. Burol (2000), Wangnick (2004) and Kalogirou (2005) provide good overviews of all major desalination technologies. Desalination textbooks like those by Spiegler and El-Sayed (1994) and El-Dessouky and Ettouney (2002) present in-depth descriptions of these technologies. The following sections describe briefly the mainstream seawater desalination technologies.

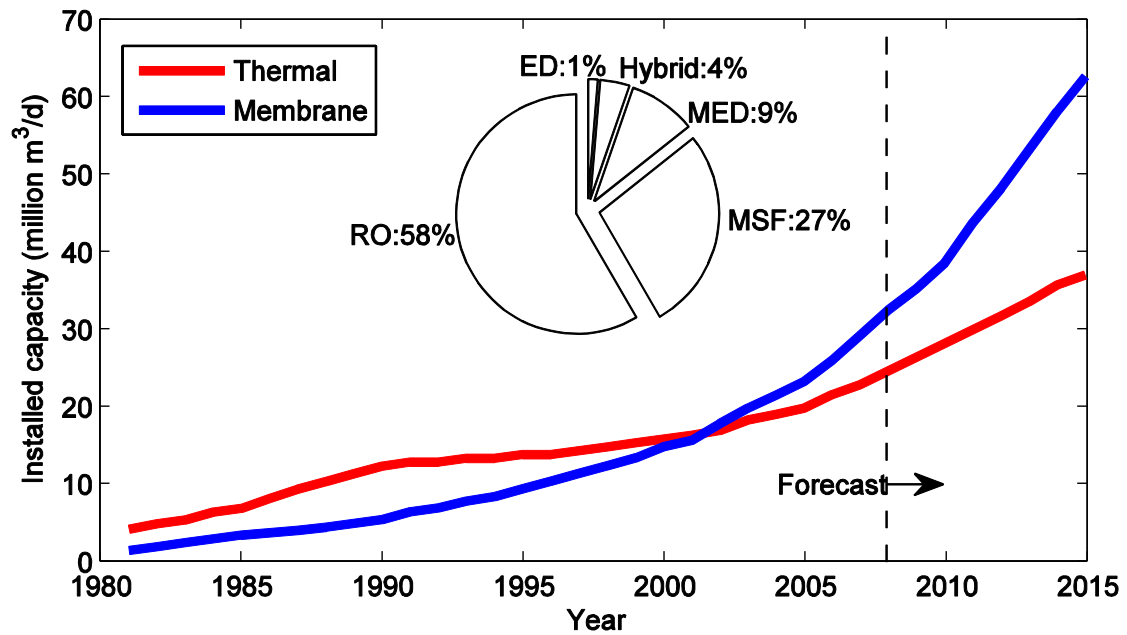


Figure 2.2 Membrane and thermal desalination installed capacity worldwide. RO, reverse osmosis; ED, electrodialysis; MED, multiple effect distillation; MSF, multistage flash. Data from the Global Water Intelligence via Economist.com (2008) and from Pankratz (2008)

2.1.5.1 Evaporation

The simplest method of desalination is evaporation, where heat is supplied to seawater to produce water vapour which is then condensed and collected. This produces high-purity water and leaves behind a concentrated brine, mirroring the natural water cycle. The latent heat required for water evaporation is in excess of 600 kWh per cubic meter of freshwater produced (El-Dessouky and Ettouney, 2002). To condense the water vapour, the latent heat is transferred to an external cooling medium, making evaporation without energy recuperation very inefficient. Industry recognised this and developed methods to recuperate heat, resulting in the technologies presented below.

2.1.5.2 Multiple effect distillation (MED)

In MED, the latent heat of the steam produced in one still (called “effect”) is used to heat up the brine in a second effect that is kept at lower pressure. This causes the steam from the first effect to condense while producing steam in the second effect, which is in turn used to heat up the brine in a third effect at even lower pressure and so on. In this way, the heat supplied in the first effect is used to subsequently produce steam in all other effects. The warm condensate from the effects is used to preheat the incoming seawater, recovering part of the sensible heat too. Energy recuperation in MED makes it significantly more efficient than evaporation (see the comparison in section 2.1.5.5).

However, some salts present in seawater dissolve less readily at higher temperatures, which causes the formation of mineral scale deposits that reduce the heat transfer efficiency between the steam and the brine. To reduce scale formation, the maximum temperature of seawater has to be limited.

2.1.5.3 Multistage flash distillation (MSF)

MSF also consists of a number of cascading stills (now called “stages”) at progressively lower pressure, but energy recuperation is approached in a different way.

In MSF, the seawater is heated to saturation and then enters the first stage through a valve, reducing its pressure. This causes the seawater to boil rapidly (flash) without supplying additional heat to the stage, unlike MED. The brine from the first stage is fed to the second stage through another valve, causing further flashing and so on. The steam is condensed within the stage where it was produced using the incoming seawater on its way to the heating section prior to entering the first effect. Since no heat is exchanged with the brine, scale formation is reduced.

MSF plants account for the largest share of thermal desalination worldwide and the second largest share of all technologies after reverse osmosis (Figure 2.2).

2.1.5.4 Vapour compression (VC)

Steam produced in a still is at the same temperature and pressure as its brine. Compressing the steam externally increases its temperature and pressure. The compressed steam can then be used to heat up the brine it originated from, while condensing. The warm condensate is also used to heat up the incoming seawater.

Compared to MSF and MED, this approach reduces the number of effects required as the latent heat from the steam is recuperated and kept within the effect.

2.1.5.5 Comparison

Table 2.1 presents the energy requirements of the technologies described above. In this table, an electrical equivalent of thermal energy is used. This is calculated as the electricity that the steam used for desalination would have produced had it been used in a turbine generator (Wangnick, 2004).

**Table 2.1 Practical energy consumption in seawater desalination.
Data from El-Dessouky and Ettouney (2002) and Wangnick (2004)**

	Specific energy consumption (kWh/m ³)
Evaporation	627 (thermal)
Multiple effect distillation	7.5
Multistage flash distillation	15.5
Vapour compression	8 – 14
Reverse osmosis	4 – 7

It is clear that MED, MSF and VC are much more efficient than simple evaporation. Reverse osmosis has even lower energy requirements. This is possible because RO does not involve a phase change to achieve separation.

Practical size is also an important consideration. Unlike MED and MSF, the modular nature of RO allows it to cater for virtually any desired production capacity, including the very small end of the spectrum (less than 50 m³/d).

Additionally, RO systems can cope better with the variable operation patterns and conditions often found in small plants, although manufacturers do not recommend this. For instance, small reverse osmosis plants can cope better with instantaneous energy fluctuations as in the case of installations powered by renewable energy with no energy storage (Epp and Papapetrou, 2005; Kalogirou, 2005; Tzen et al., 2006).

Improvements in membrane and pump technology and developments in energy recovery have currently made reverse osmosis the preferred choice for desalination (Seacord et al., 2005; Stover, 2007; Wilf et al., 2007).

2.2 Reverse osmosis

2.2.1 Osmotic processes

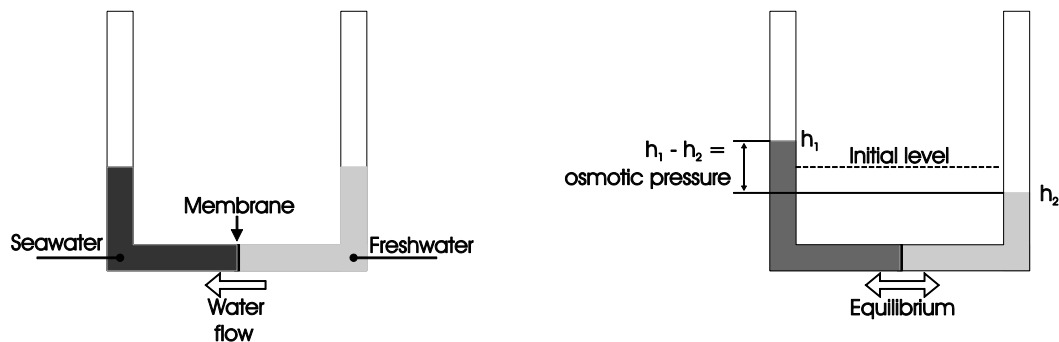


Figure 2.3 Osmosis

A membrane is in essence a selective barrier. When two saline water solutions of different concentration such as freshwater and seawater are separated by a semipermeable membrane (i.e., one that allows the passage of water but opposes that of salt), a flow of water through the membrane will occur naturally from the freshwater (high water concentration) to the seawater (lower water concentration), lowering the concentration of the latter (see Figure 2.3 left). This process is called osmosis and plays a vital role in living cells.

As water flows through the membrane, the volumes of the two solutions change too and a hydrostatic pressure difference develops. The difference reached when the process is in equilibrium is equal to the difference in osmotic pressure between the two solutions; at this point the net flow of water through the semipermeable membrane is zero (Figure 2.3 right).

If enough pressure is applied on the seawater side, the direction of the natural osmosis flow through the membrane can be reversed and water would then flow from the seawater to the freshwater side. This process is called reverse osmosis, and enables the separation of salts from water (Figure 2.4).

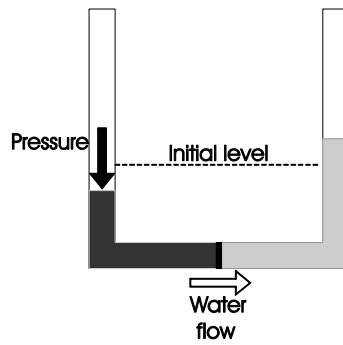


Figure 2.4 Reverse osmosis

When working with seawater, osmotic pressure differences of 25 bar and above are found. This is the minimum pressure that must be applied to the seawater to stop the natural osmotic process (Spiegler and El-Sayed, 1994).

2.2.2 Continuous process

In the example in Figure 2.4, as water flows through the membrane, salts would accumulate on its surface. To avoid this, modern reverse osmosis processes use a cross-flow approach (Figure 2.5) where only a portion of the seawater feed goes through the membrane as freshwater; this constitutes the permeate or product. The rest of the feed flows across the membrane along the feed-brine channel becoming more concentrated, and is therefore commonly referred to as the concentrate, reject or brine; this flow flushes the salts out of the membranes. In essence, the process requires a reverse osmosis membrane and a high-pressure pump to raise the pressure of the seawater to typically 50 bar or higher.

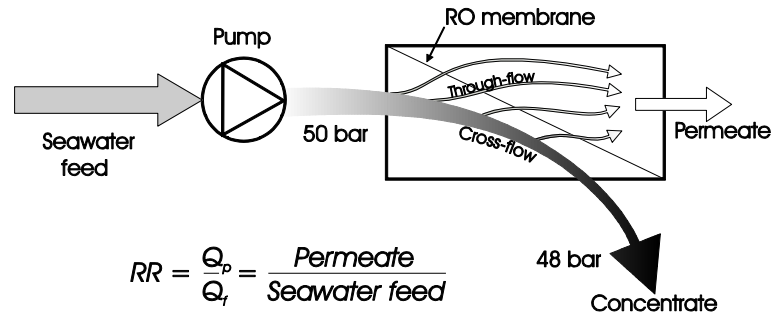


Figure 2.5 Schematic of a reverse osmosis process

The ratio between the permeate (Q_p) and the feed (Q_f) flows is known as the recovery ratio (RR), and is a useful parameter to characterise the operation of a reverse osmosis process. For seawater, overall plant recovery ratios of 30-45% are common.

The selection of an appropriate recovery ratio is a delicate compromise between water production, investment, energy use and lifetime of the hardware, especially the reverse osmosis membranes.

2.2.3 Water transport

An ideal membrane would allow water to flow through freely and completely stop the passage of salts. However, real reverse osmosis membranes are not perfect and present some resistance to the passage water through them. This means that in addition to the thermodynamic minimum energy required for the separation of water and salt in standard seawater (0.7 kWh/m³, see section 2.3.1), additional energy is required in the form of pressure to force water through the membrane. The flow of water is proportional to the net pressure applied above the osmotic pressure. This is shown in Equation 2.1:

$$Q_p = K_w A_m [(P_f - P_p) - (\pi_{avg} - \pi_p)] \quad \text{Equation 2.1}$$

where Q_p is the permeate flow through the membrane, K_w is the water permeability coefficient of the membrane, A_m is the area of the membrane, P_f and P_p are the seawater and permeate pressures, respectively, π_{avg} is the osmotic pressure in the feed-brine channel, and π_p is the osmotic pressure of the permeate. The term in square brackets is known as the net driving pressure (NDP).

Equation 2.1 shows that increasing the seawater pressure would result in higher product water flows and, hence, higher recovery ratios. However, the relationship between the applied pressure and the recovery ratio is not straightforward since increasing the recovery ratio increases the concentration of the brine, and hence its osmotic pressure, affecting also the net driving pressure.

2.2.4 Salt transport

Another imperfection of RO membranes is that they do not completely stop the passage of salt. Nevertheless, data sheets of modern seawater membranes show salt rejection in excess of 99% (Dow, 2009a; GE, 2009; Koch, 2009; Toray, 2009; Toyobo, 2009).

Salt passage is driven by the concentration gradient across the membrane as shown in Equation 2.2:

$$Q_s = K_s A_m (C_{avg} - C_p) \quad \text{Equation 2.2}$$

where Q_s is the flow of salt through the membrane, K_s is the salt permeability coefficient of the membrane, C_{avg} is the average salt concentration in feed-brine channel and C_p is the concentration of the permeate.

The final concentration of salt in the permeate is simply the ratio between the flow of salt and the flow of water through the membrane. Increases in pressure result in higher water flows and therefore lower concentrations.

In the two equations above, the permeability coefficients vary with temperature. As a result, the salt and freshwater flows increase with increasing temperature at a rate of about 3% per °C. However, since the osmotic pressure also increases with temperature, water passage through the membrane levels off above 30 °C (Wilf et al., 2007).

2.2.5 History and technology progress

The development of reverse osmosis started in the 1950s when Reid and Breton (1959) demonstrated the use of compressed cellulose acetate membranes to retard the diffusion of NaCl through the membranes while maintaining the diffusion of water. Building on this, Loeb and Sourirajan's work in the 1950s and 1960s led to the development of the first asymmetric cellulose acetate membrane for reverse osmosis (Buros et al., 1981). This was followed by the development of polyamide composite membranes during the 1970s and 1980s (El-Dessouky and Ettouney, 2002; Wilf et al., 2007). Reverse osmosis was first used to treat brackish water in the late 1960s and subsequently used for seawater in 1970s when also the first commercial-grade reverse osmosis membranes appeared (Buros et al., 1981; Greenlee et al., 2009). Reverse osmosis started competing commercially with thermal desalination in the 1980s (Van der Bruggen and Vandecasteele, 2002).

Since its early stages, reverse osmosis of both brackish and seawater has seen significant advances in the form of greater flux, improved salt rejection, lower energy consumption and reduced costs. Figure 2.6 shows the evolution of flux and salt rejection for seawater membranes. From 1978 to 2004 the flux more than doubled and salt passage in 2004 was about 20% of its value in 1978.

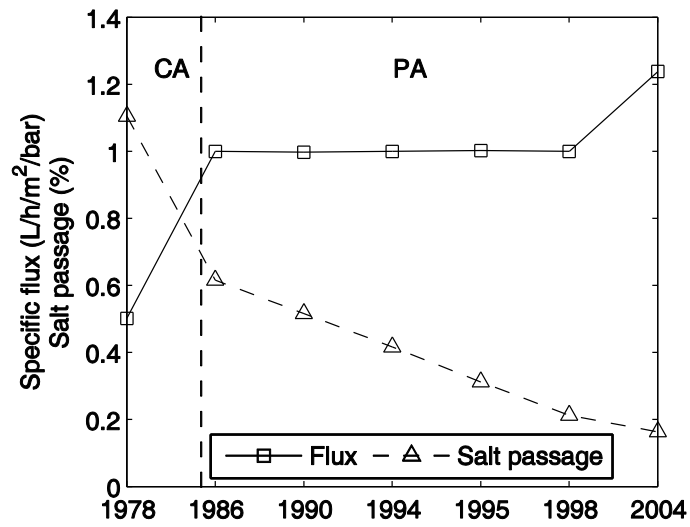


Figure 2.6 Specific flux and salt passage evolution for seawater membranes.
CA, cellulose acetate; PA, polyamide. Data from Wilf et al. (2007)

Large reductions in net driving pressure have also been achieved as presented in Figure 2.7. It is evident in these two figures that polyamide membranes have played a key role in the progress of reverse osmosis.

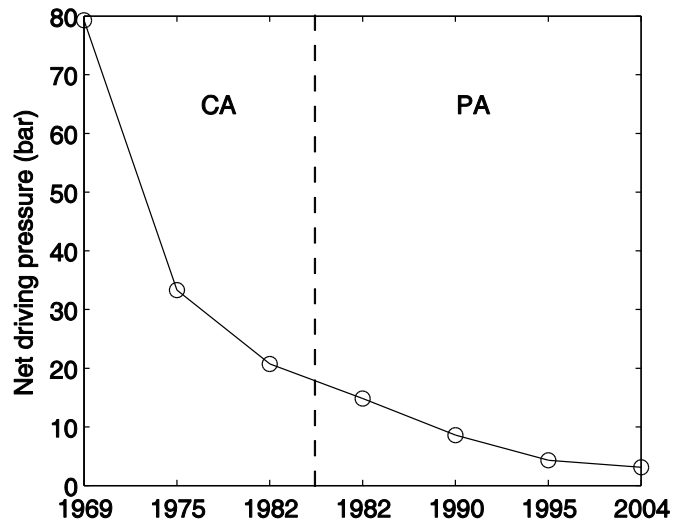


Figure 2.7 Evolution of net driving pressure for brackish water membranes.
CA, cellulose acetate; PA, polyamide. Data from Wilf et al. (2007)

In addition, better engineering of RO membranes has increased their resistance to fouling (fouling is discussed later in section 2.2.9), improving their useful life and reducing the cleaning and replacement costs (Van der Bruggen, 2003).

Altogether, the progress in membrane technology and improvements in other system components such as energy recovery devices, are reflected in the energy consumption of reverse osmosis, where larger volumes of high-quality water can now be produced with less energy (Figure 2.8). For seawater, best practice reverse osmosis today uses about a quarter of the energy consumed in 1980 (MacHarg and Truby, 2004; MacHarg et al., 2008).

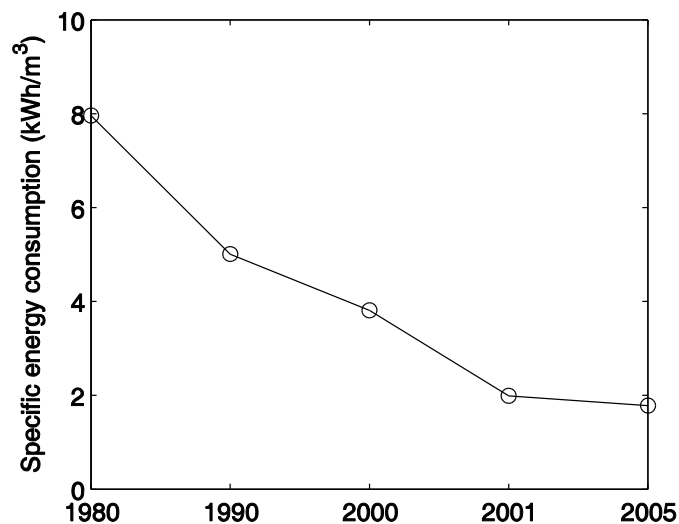


Figure 2.8 Evolution of energy consumption for seawater reverse osmosis.
Data from MacHarg and Truby (2004)

Overall, the rapid progress of RO technology in recent decades has made it the first choice for new installations around the world.

2.2.6 Membrane materials

As mentioned previously, the first reverse osmosis membranes were made of cellulose acetate. Later on, polyamide membranes supported on a porous

polysulfone layer made their appearance. The thickness of these assemblies is about 0.2 mm, with the salt-rejecting polyamide skin being only a few hundred nanometres thick and the support layer between 0.025-0.050 mm. The rest is made up by a polyester fabric to add to the mechanical properties of the membrane (Wilf et al., 2007).

Polyamide composite membranes allow greater water flows than cellulose membranes which translates into lower operating pressures and therefore less energy consumption. Polyamide membranes also present higher salt rejection and are stable over a wider pH range than cellulose acetate membranes. However, their tolerance to chlorine is not as good as that of cellulose acetate membranes, making the latter more suitable for processes where frequent disinfection is required, for example in the pharmaceutical or food industries (Medina San Juan, 2000; El-Dessouky and Ettouney, 2002; Wilf et al., 2007).

2.2.7 Membrane configurations

Four configurations of reverse osmosis membrane are found in the literature: plate and frame, tubular, hollow fibre and spiral wound.

Plate and frame membranes consist basically of a membrane sheet supported on a laminate structure fixed in a frame for rigidity and mechanical resistance. This arrangement results in low area-to-volume ratios, making them bulky. These membranes are usually stacked in industrial applications. The larger clearances between membranes make them less prone to blockages than other arrangements, and they are easy to disassemble for inspection and cleaning (Medina San Juan, 2000).

Tubular membranes represent the next step in increasing the membrane surface without compromising the advantages of plate and frame membranes. Here, one or several tubular membranes are packed inside a porous tube of larger diameter which provides the mechanical resistance to withstand pressure. The water to treat is fed on the inside of the membranes and

collected outside the porous support tube. Tubular membranes pack more area per unit volume than plate and frame membranes but their flow is still very low (Medina San Juan, 2000).

Reverse osmosis desalination used these two types of configurations in its early stages. They are not used so much for desalination anymore but in the food industry and for treatment of waste streams with high fouling potential. These membranes have been phased out from desalination applications due to their low packing density and higher cost in favour of hollow fibre and spiral wound membranes (Sing, 2006; Wilf et al., 2007).

Hollow fibre modules are made up of millions of very thin (about 100 μm) and long (about 2.4 m) extruded tubes (hollow fibres) of membrane material. The salt-rejecting skin is on the external surface of the fibres and water flows radially through the tubes' walls to the hollow inside. Unlike the membrane configurations described above, hollow fibres do not require an additional support structure. Rather, the fibres themselves are strong enough to withstand the pressures required for reverse osmosis. Such strength is the result of a large outside diameter relative to the inside diameter, regardless of their absolute sizes. Inside diameters range from 40 to 80 μm and outside diameters range between 85 and 150 μm (Medina San Juan, 2000; Wilf et al., 2007).

To make the fibres into a module, a bundle of fibres is folded in half and a feed distributor tube (a plastic tube with perforations on its surface) is inserted in the middle of the folded bundle of fibres, extending the length of the whole bundle. Each end of the bundle is then sealed in an epoxy block to hold it in place. One of the epoxy end blocks is subsequently cut perpendicularly to the fibres. This opens one of the ends of the fibres to allow water that permeates through the fibres' walls to flow out of the fibres. The bundle with its end blocks and the feed distributor is placed inside a cylindrical housing. End caps and external connectors are fitted to the arrangement to collect the brine and permeate and to feed seawater to the distributor tube (El-Dessouky and Ettouney, 2002; Wilf et al., 2007).

Due to the small diameter of the fibres, hollow fibre modules pack a very large surface area into a small volume making them less bulky and cheaper than frame and plate or tubular membranes. However, their design does not allow for turbulent seawater flow regimes and as a result hollow fibre membrane modules are only used to treat high-quality waters with low fouling potential (Byrne, 1995; Wilf et al., 2007).

Finally, spiral wound membrane modules are formed by a number of rectangular membrane assemblies attached to and wound around a perforated tube that collects the permeate. The membrane assemblies are formed by two membrane sheets overlaid with a spacer between them (see Figure 2.9 top). Three of the four edges of the sheets are glued together resembling an envelope. The fourth edge of the sheets is attached to the permeate collector tube. Pressurised seawater flows on the external surface of the membrane assembly; water permeates through the membrane sheets to the inside of the envelope and flows towards the collector tube (Medina San Juan, 2000; El-Dessouky and Ettouney, 2002; Wilf et al., 2007). A useful animation about the production of spiral wound elements can be found in the downloads section of the Hydranautics website www.membranes.com (Hydranautics, 2007).

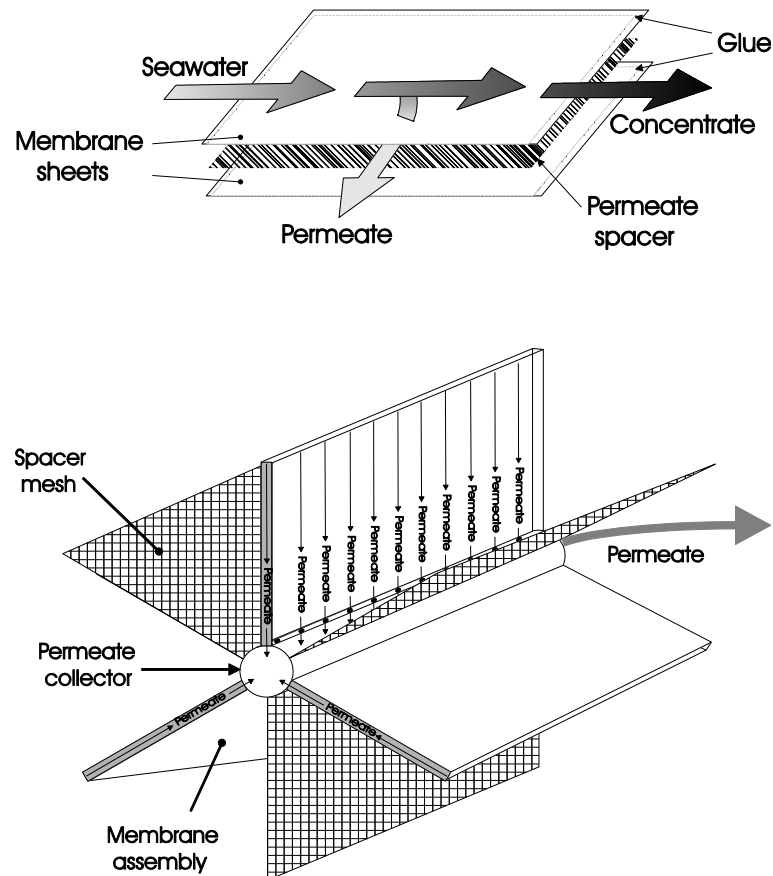


Figure 2.9 Spiral wound module fabrication

To form a module or element, several of these membrane assemblies (envelopes) are attached to the collector tube with a mesh spacer between assemblies as shown in Figure 2.9 (bottom). The whole arrangement is then wound around the collector tube and wrapped in fibreglass. The mesh spacer ensures enough space for seawater to flow between the envelopes, and also increases turbulence to reduce concentration polarisation (see section 2.2.8). These modules are placed inside cylindrical pressure vessels and fitted with end caps and connections to feed seawater to the modules and collect the permeate and the brine. Spiral wound modules are highly standardised in their dimensions and performance and can use the same pressure vessels irrespective of membrane manufacturer.

Spiral wound membranes also pack a large membrane area into a small volume which allows greater permeate flows, reduces the installation footprint and has low costs. Compared to hollow fibre membranes, spiral wound pack less area and produce less water per module. However, spiral wound membranes operate at lower pressures and are less prone to fouling due to the larger clearances between membrane sheets and can handle feeds of poorer quality. Although marginally, spiral wound membranes also have higher salt rejections (less than 1% difference) (Medina San Juan, 2000).

Spiral wound membranes are the most popular configuration at present and they largely dominate the reverse osmosis market.

At this point it is appropriate to note that in the desalination field the term “membrane” is commonly used to refer to both the thin salt-rejecting skin layer as well as to a membrane module such as a spiral wound element.

2.2.8 Concentration polarisation

In reverse osmosis, freshwater permeates through the membrane from the seawater layer adjacent to it. As water molecules move through, salt is left behind and a boundary layer of increased salt concentration develops adjacent to the membrane. This is called concentration polarisation and has a number of negative effects on the desalination process (Medina San Juan, 2000; Wilf et al., 2007):

- Reduction of the net driving pressure due to increased osmotic pressure in the boundary layer and therefore, reduction of water flow through the membrane.
- Greater salt passage through the membrane due to the increased salt concentration gradient across the membrane.

- Increased risk of precipitation and deposition of low-solubility salts on the membrane surface.

Increasing the turbulence of the seawater flow in the feed-brine channels of a membrane element helps reducing concentration polarisation. Minimum brine flow rates and maximum water recovery ratios are specified by membrane manufacturers to ensure proper mixing and flushing of salt and maintain an acceptable brine concentration. Manufacturers also place great effort into engineering feed-brine channels that promote turbulence to reduce the thickness of the boundary layer and reduce the effects of concentration polarisation (Medina San Juan, 2000).

2.2.9 Membrane fouling

Fouling of reverse osmosis membranes is perhaps the main cause of membrane performance loss. Fouling is a very broad subject that includes particulate fouling (suspended and colloidal matter), inorganic fouling (formation of iron and manganese compounds on the membrane surface), biofouling (bacterial growth on the membrane surface), organic fouling (due to dissolved organic matter) and scaling (formation of mineral deposits of sparingly soluble salts) (Schippers, 2007). Due to such great variety, and often combination, of fouling mechanisms, there is no set recipe to deal with fouling and each case must be addressed individually.

The risk of membrane fouling is influenced by the recovery ratio since the foulants' concentration within the membranes increases as freshwater is extracted from the seawater feed.

The deposition of foulants on reverse osmosis membranes results in a range of adverse effects including loss of net driving pressure, loss of permeate flow, increased energy consumption, increased salt passage, reduction of membrane useful life, increased down time for cleaning and increased membrane

replacement and other operation costs (Schipper, 2007). For these reasons the design of suitable feed water pretreatment steps is paramount.

2.2.10 Pretreatment

The pretreatment stages deal with the conditioning of the feed water for reverse osmosis. The aim is to feed reverse osmosis membranes with the best quality water possible to minimise fouling, maintain an acceptable performance and maximise the membranes' useful life. Coagulation, flocculation, disinfection, pH adjustment, addition of scale inhibitors and various filtration techniques such as media, sand, micro-, ultra- and even nanofiltration are used to condition the feed for reverse osmosis processes. Sometimes, sourcing the raw feed from beach wells and underground intake systems can significantly reduce the need for pretreatment stages. The long-term success of a reverse osmosis desalination operation depends largely on the adequate design of the pretreatment train.

2.3 *Energy for desalination*

2.3.1 Energy consumption and CO₂ emissions

Desalination is a very energy-intensive process. The theoretical minimum energy required to separate pure water from standard seawater in a lossless process is 0.7 kWh/m³ (Spiegler and El-Sayed, 1994). This value is independent of the method used. Real seawater desalination processes inevitably incur energy losses and require several times the theoretical minimum.

To put it into perspective, the 7 kWh required to produce one cubic meter of freshwater (high end of RO in Table 2.1) would be enough to pump that same cubic meter of water from sea level to an altitude of about 2000 m. It is then

easy to see that, with current worldwide desalination rates approaching 50 million m^3/d (Figure 2.1), the total energy used by desalination is considerable. Kalogirou (2005) estimated that the world's desalination capacity of 22 million m^3/d in the year 2000 required the equivalent of 203 million tons of oil per year. Extrapolating this to the present, with worldwide desalination more than doubling that in 2000, the industry's yearly energy consumption would be about 400 million tons of oil, which is comparable with the total energy consumption of countries like Germany or India in 2006 (Energy Information Administration, 2009). With such large energy requirements, it is of no surprise then to find desalination often located in regions with easy access to cheap energy, like in the Middle East, where most desalination is found.

Largely powered by fossil energy, desalination is therefore responsible for CO_2 and other emissions. For a rough estimate of this, the CO_2 emissions of Germany and India in 2006 can be looked at: 858 and 1293 million metric tons, respectively (Energy Information Administration, 2009), which represent 2.9 and 4.4% of the world total.

While these are only estimates, what is clear is that the desalination industry consumes large amounts of energy and, consequently, it is responsible for a significant share of CO_2 emissions and is undoubtedly contributing to global warming.

2.3.2 Desalination and renewable energy

To mitigate the effect of the growing desalination industry on the environment, cleaner energy sources, such as renewables, must be used to power desalination. Fortunately, water-scarce regions often have good renewable energy resources. However, in a cost-driven industry, powering from renewable energy the very large desalination plants that produce water in excess of 10 000 m^3/d each, seems a distant goal. Nevertheless, a new seawater RO desalination plant in Perth, Australia is taking steps in this direction by buying

the electricity to power its operation from a local wind farm (The Water Corporation, 2009b). Since both the desalination plant and the wind farm are connected to the local electricity grid, this is not a stand-alone operation, but an effort worth noting nonetheless. At present, another desalination plant is planned for Western Australia's southwest, which will likely follow a similar approach (The Water Corporation, 2009a; The Water Corporation, 2009c).

Synlift systems (www.synliftsystems.de, accessed 20 August 2009) propose a similar approach, also using grid-connected wind turbines coupled to RO desalination systems in sizes of at least 500 m³/d. They propose to use the electricity generated by the turbines to power the RO plant in a sub-grid, and only use the main grid to export any surplus energy or make up for shortfalls. This approach reduces the cost of using the grid (Käufle and Pohl, 2009).

A much harder goal is stand-alone operation. Nevertheless, in recognition of the potential of renewable energies to power desalination in remote applications, many studies have been done and numerous demonstration projects have been built in the past. CRES (1998), Garcia-Rodriguez (2002), Kalogirou (2005) and Epp and Papapetrou (2005) present reviews and good databases of renewable energy desalination projects worldwide. Charcosset (2009) also presents a good review of renewable-energy powered desalination systems using membrane technologies only. Throughout the literature, solar and wind energy are regarded as the most viable renewable options to power desalination at present, particularly at the small scale. Some renewable energy desalination options are presented below.

2.3.2.1 Solar thermal

Of all renewable energies, solar thermal is perhaps the easiest to relate to desalination. This may be due to the resemblance to the natural water cycle or to the association of dry places with high levels of insolation. Traditional solar stills are the prime example, which have attracted and continue to attract many

researchers around the world. Their simplicity and low cost makes them very attractive for remote applications; however, because of their low efficiency (about 4-5 L/d/m² of collector), they are only suitable for very small-scale applications. For example, fields of traditional stills, canal solar stills and also some “large-section” solar stills for seawater desalination were researched and trialled in the state of Baja California Sur in Mexico during the 1970s and 1980s achieving productivities of about 3.5-4 L/d/m² (Bermudez-Contreras et al., 2008).

In the pursuit of higher efficiencies, flat and concentrating solar collectors for seawater desalination can also be used. Solar collectors produce high-temperature heat suitable for thermal desalination processes or to run turbines to produce either mechanical power or electricity for reverse osmosis. For instance, as part of the SMSF (Solar Multistage Flash) project in Mexico in the early 1980s, a 678 m² solar field combining concentrators and flat collectors powered the operation of a 10 m³/d seawater desalination plant through day and night (Bermudez-Contreras et al., 2008). This equates to a productivity of about 15 L/d/m².

Later on in the 1980s, the subsequent and much larger Sonntlan project powered and supplied drinking water to a whole fishing community from solar energy, both thermal and photovoltaic. This included a 20 m³/d MSF desalination plant, a 20 m³/d seawater RO plant, a fish processing plant, ice production facility, deep-freezing produce storage, telecommunications station and electricity for the village (Bermudez-Contreras et al., 2008). In this project, 1540 m² of flat solar collectors supplied heat for the MSF plant, the ice production facility and also for the processing of fish. The operation of the solar powered MSF plant here produced freshwater at about 17 L/d/m².

The use of solar collectors for desalination is significantly more efficient than solar stills but also requires much larger investments and is considerably more complex to run and maintain. This makes their use more suitable for larger-scale applications with dedicated skilled personnel.

2.3.2.2 Photovoltaics

Photovoltaic (PV) solar panels convert solar energy directly into electricity. At present, commercial PV panels are largely based on silicon, either mono-crystalline, poly-crystalline or amorphous. Other materials such as cadmium telluride and copper-indium-gallium diselenide are also used (Markvart, 2000).

PV technology is widely used in locations without easy access to electricity grids for water pumping, lighting and refrigeration, sometimes involving battery storage to ensure continuous operation or to operate at a constant point during daytime hours.

Grid-connected PV systems are also found. Here, any excess power not used locally can be exported to the grid, and similarly any shortfalls from the PV can be made up by drawing power from the grid, eliminating the need for local energy storage.

PV can also be used to run the electric motors driving the pumps in reverse osmosis. An extensive database of PV-RO systems is given by Ghermandi and Messalem (2009). A particularly successful example of this is that of Mr Kunczynski (2003) in La Paz, Mexico, who has been exclusively using photovoltaics to desalinate seawater by reverse osmosis for his estate. Mr Kunczynski has by now produced over 41 thousand cubic meters of desalinated water over nine years of operation and has been granted a patent for his systems (Kunczynski, 2006).

PV-RO works well for small-scale desalination but as the plant size increases, other energy options become more attractive.

2.3.2.3 Wind

Wind energy has been used for centuries to propel sailboats, grind grain, pump water and, more recently, to generate electricity. Modern wind turbines erected on towers several tens of meters tall are capable of generating a few MW of electricity each. Electricity generation from wind energy is today an established technology and, in windy locations, the cost of wind electricity can compete with that of conventional generation (Freris and Infield, 2008).

Wind power can also be used for reverse osmosis, producing either shaft power to drive the pumps directly or electricity to run the pumps' motors. Due to the high variability of the resource, wind-powered desalination is sometimes coupled with flywheels, batteries or some form of backup like diesel generators to maintain the desalination process (CRES, 1998; Rahal, 2001; Miranda and Infield, 2003). Demonstrations of wind-RO seawater systems have been built in various locations including ENERCON's system in the Island of Utsira, Norway (Paulsen and Hensel, 2005), the SDAWES project in the Canary Islands, Spain (Carta et al., 2004) and that in Therasia, Greece built by Vergnet (Fabre, 2003).

Adding PV to wind reverse osmosis systems has also been tried. An example is the system operated by CRES in Lavrio, Greece (Tzen et al., 2008).

2.3.2.4 Wave power

Coupling wave power to desalination is a very convenient combination that offers great potential because the oceans can provide both the raw water and the energy required. This combination has not been researched as extensively as solar and wind desalination but has nonetheless seen significant efforts around the world with very interesting results, some of which have even reached commercialisation. For instance, the DELBUOY (Hicks et al., 1989) saw full scale trials off the coast of Puerto Rico. This device was small-scale (about 1 m³/d) and modular, developed specifically for seawater desalination and designed to be deployed as a farm. It used a buoy to drive a hydraulic

cylinder that fed high-pressure seawater to a reverse osmosis system. Despite showing great promise and units being sold in the late 1980s in Puerto Rico and Belize, the project stopped due a combination of unfortunate circumstances (Hicks, 2004).

Another example with a different approach is that installed in Vizhinjam, India (Sharmila et al., 2004), where an oscillating water column pressurises air to drive a turbine and electricity generator. After some power conditioning steps and using a battery bank, the electricity produced is used to power a conventional reverse osmosis plant producing 600 L/h of freshwater for the local community. As of 2005, this unit was thought to be the only operational wave power desalination system in the world (Davies, 2005).

A third and different approach is Salter's desalination Duck (Cruz and Salter, 2006). Cruz and Salter propose to use the rocking motion of a 12 m Duck to pressurise steam to drive a vapour compression desalination unit located inside the body of the device. Cruz and Salter report that a 1:40 scale model was being built to validate modelling predictions but no newer information regarding practical demonstrations has been found in the literature.

A fourth device is the McCabe Wave Pump, which consists of three hinged barges that are pitched relative to each other by the action of the waves. Large forces are developed between the middle section and the two arms of the device, which are used to pressurise seawater for reverse osmosis. The device has been deployed twice at the Shannon estuary in Ireland (McCormick and Kraemer, 2001).

Other devices include the one proposed by Maratos (2003), the CETO (Carnegie Wave Energy Limited, 2009), the Oyster (Folley and Whittaker, 2009) and the SEADOG pump (Independent Natural Resources Inc., 2009). The latter has recently been licensed to Renew Blue Inc to produce bottled desalinated water (Desalination & Water Reuse, 2009).

Davies (2005) presents a good overview of several wave power devices used for seawater desalination.

2.3.2.5 Renewable energy variability and reverse osmosis

The instantaneous flows of renewable energy in nature are constantly fluctuating. Such patterns have a direct impact on the design and operation of the desalination systems they power.

To deal with such variability, one approach is to use energy storage (batteries) to make up for energy shortages and absorb energy when there is a surplus. For reverse osmosis, this ensures operation at specified flows and pressures. However, batteries are expensive and increase the complexity of the system itself and of its control algorithms. Batteries are also known to be problematic in the field, particularly in the hot climates where desalination is most often required (Riffel and Carvalho, 2009), and they are not easy, nor environment-friendly, to dispose of. In addition, batteries introduce considerable energy losses during the charge-discharge cycle, as shown in the example presented in Figure 2.10. This Sankey diagram corresponds to the energy consumption modelling of a seawater reverse osmosis system powered by photovoltaics, where the round-trip efficiency of the batteries is expected to be less than 50%. In the diagram, the line widths and values represent annual averages of specific energy consumption in kWh/m³; the downwards pointing pink arrows represent losses.

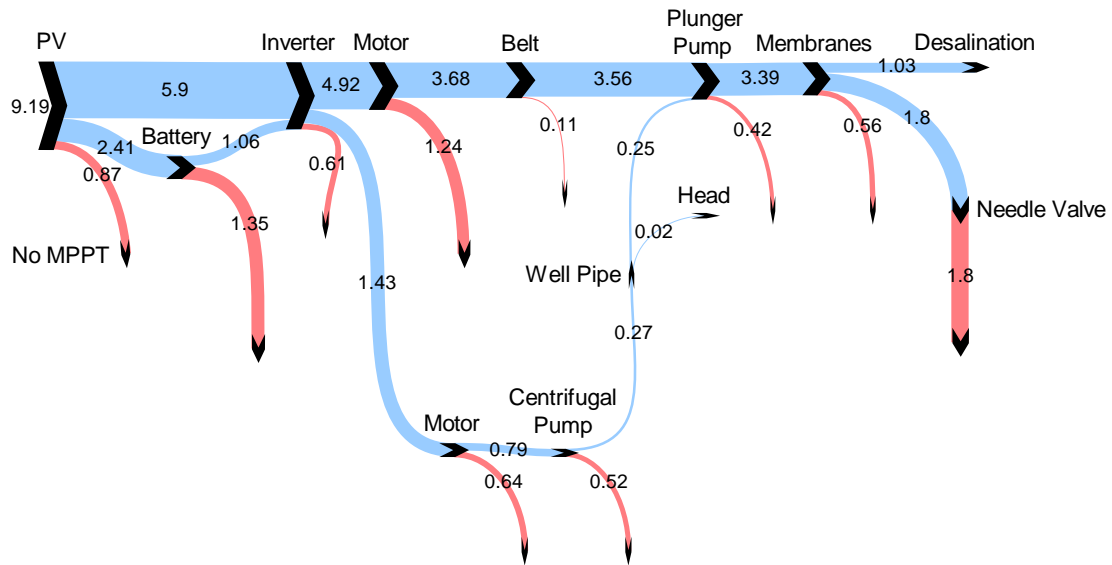


Figure 2.10 Sankey diagram of a PV-RO system using batteries.
The line widths and values represent annual averages of SEC in kWh/m³ (Thomson and Bermudez, 2006)

Alternatively, renewable energy reverse osmosis systems can be designed to operate without batteries. This means that the desalination section would experience variable flows and pressures which:

- Could be detrimental to the RO membranes' useful life. For instance, very low flows in the feed-brine channel increases the risk of fouling.
- Could compromise the efficiency of pumps and motors. For example, the efficiency of a small centrifugal pump would fluctuate considerably with a fluctuating input power.
- Could make the salinity of the product water fall outside acceptable ranges at very low recovery ratios.

On the other hand, the operation of a well-designed system without batteries can have significant advantages as it could:

- Eliminate the losses associated with the batteries' charge-discharge cycle.

- Reduce the system's capital costs.
- Eliminate the problem of disposal of the batteries.
- Improve the reliability of the system by having fewer components
- Reduce the maintenance required.

Thus, the operation of renewable-energy-powered RO systems without batteries is very attractive.

2.4 Energy recovery

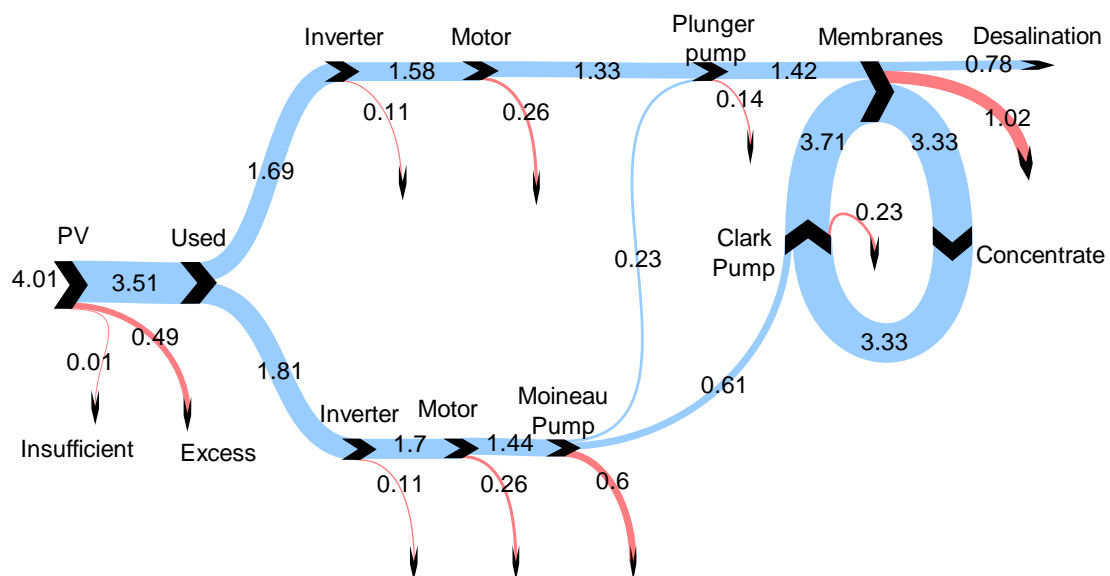


Figure 2.11 Sankey diagram of a seawater PV-RO system with energy recovery.
The line widths and values represent annual averages of SEC in kWh/m³ (Thomson and Bermudez, 2006)

Seawater is typically fed to the reverse osmosis membranes at pressures above 50 bar. With water recovery ratios between 30 and 45% in seawater reverse osmosis, the brine stream carries 55 to 70% of the volume of the seawater feed. Because the pressure drop in the feed-brine channel of the RO

membranes is small, typically no more than 2 bar, the concentrate stream also carries roughly between half and two-thirds of the energy in the seawater feed. Recycling this energy back into the process, as depicted by the loop in the example in Figure 2.11, reduces the energy consumption of the high-pressure pumping stage significantly. For instance, in a very small seawater system desalinating 1 m³/h, it was estimated that the implementation of energy recovery could reduce overall energy consumption by more than 15 000 kWh per annum (Bermudez Contreras and Thomson, 2008). Implementation of energy recovery can also increase water production for a given system, making the whole process more efficient and attractive.

Energy recovery for brackish water RO is less critical because of the higher recovery ratios and lower pressures found in these applications. This means that the amount of energy that can be recovered is much less than in seawater systems and thus energy recovery is rarely used. An exception is the Solarflow system (Dallas et al., 2009), which is a small solar-powered RO unit that operates at low recovery ratios (there are two versions, 16 or 25%). The Solarflow was developed at the Environmental Technology Centre of Murdoch University in Perth, Australia.

2.4.1 Energy recovery economics

In addition to energy efficiency, brine-stream energy recovery can also have a significant influence on the economics of reverse osmosis operations: on the one hand it increases the capital costs, but on the other hand, it reduces energy consumption and therefore, the running costs. The balance depends on factors like the size and type of the application, the amount of energy involved, the cost of the system and the local cost of energy. Furthermore, the long term financial viability of larger seawater RO systems is considered carefully and, as a result, energy recovery is standard practice. Conversely, small systems tend to be bought based on capital costs, and therefore they seldom include energy recovery.

In renewable-energy powered RO systems, the high-cost of the energy produced and the remote locations where these systems are often found demand the maximisation of water production. Therefore, energy recovery in these systems is definitely more critical but this does not guarantee its application.

2.4.2 Classification of brine-stream energy recovery

Historically, energy recovery in large RO plants first employed devices like Pelton wheels and later on Hydraulic Pressure Boosters. In the last decade, a shift towards positive displacement, isobaric chamber devices has been taking place mainly triggered by the success of devices such as the DWEER (dual work exchanger energy recovery) and the PX Pressure Exchanger. These and other devices are categorised in Figure 2.12.

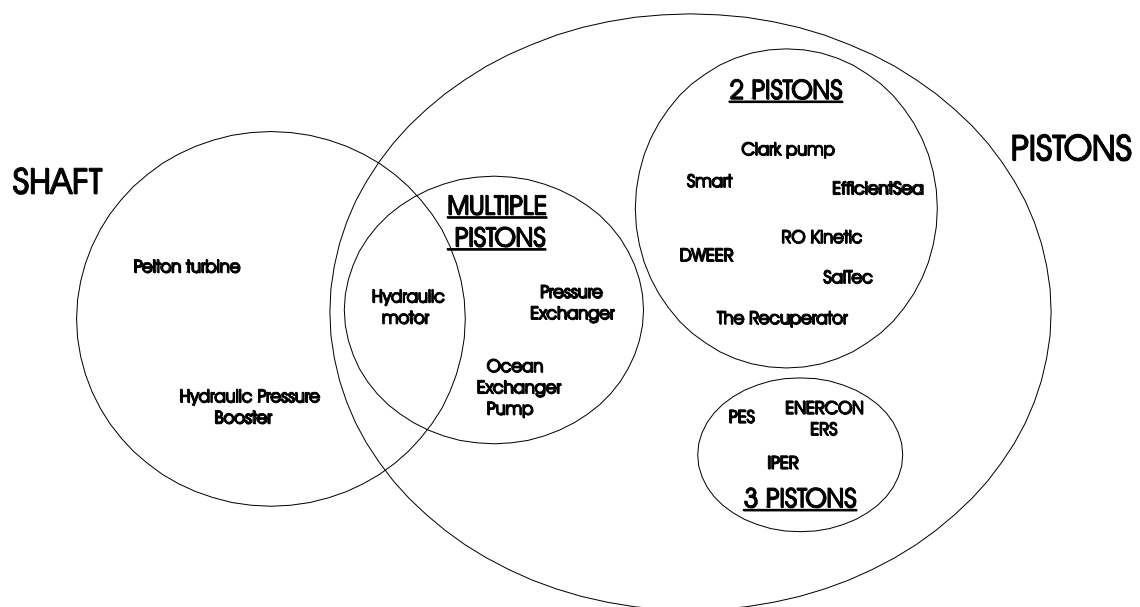


Figure 2.12 Approaches to energy recovery and transfer

The devices in Figure 2.12 mainly use pistons or a rotating shaft to convey energy between the concentrate stream and the feed to the RO membranes. The Pelton wheel and the Hydraulic Pressure Booster use a shaft, while the Clark pump, the IPER (integrated pump and energy recovery) and the DWEER use pistons. The hydraulic motor has both. The PX Pressure Exchanger does not have solid pistons but the interface forming between the concentrate and the seawater in this device works as a physical piston (see section 2.4.6). These are the main devices used commercially for energy recovery and are described next.

2.4.3 Pelton wheel

A Pelton wheel or Pelton turbine consists of a wheel with a number of cups fixed on its perimeter (Figure 2.13). A jet of high-pressure concentrate impacts the cups and makes the wheel rotate. The wheel is coupled to the shaft of the high-pressure pump to assist the motor in pressurising the seawater feed.

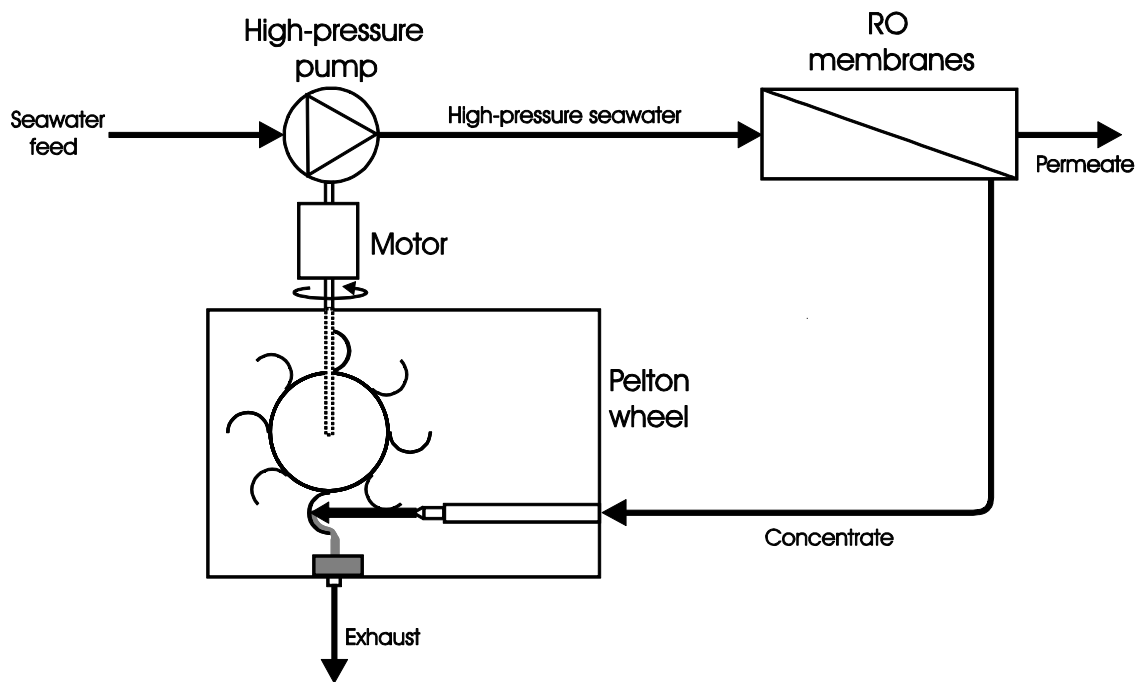


Figure 2.13 System using a Pelton wheel

Pelton wheels are simple, robust and well understood devices. They were introduced as devices for energy recovery in RO in the early 1980s. Despite their high efficiencies in hydroelectricity generation, their use for energy recovery in RO is not as efficient, mainly because of the high speeds of the pump shaft they are coupled to, and also because in an effort to cut costs, the finishing of the cups is not as good as in turbines used for power generation (Doujak and List, 2003).

In addition, the use of Pelton wheels for energy recovery requires two energy conversion steps: first, from hydraulic energy in the concentrate to kinetic energy of the rotating shaft in the Pelton wheel; and second, from the rotating shaft back to hydraulic energy in the high-pressure pump. The overall efficiency of the arrangement is the product of the efficiencies of the Pelton wheel and the high-pressure pump, which is usually centrifugal. As a result, the arrangement only operates at its peak efficiency in a narrow range of pressure and flow. Consequently, their operation point must be carefully chosen to match a

particular operation condition of the RO membranes, reducing the flexibility of the arrangement to accommodate seasonal variations of feed water temperature and salinity as well as water demand.

2.4.4 Hydraulic turbo booster

Oklejas and Oklejas patented the use of the turbocharger for energy recovery in RO applications in 1990 (Oklejas and Oklejas, 1990). Commercial examples are the Hydraulic Pressure Booster manufactured by Fluid Equipment Development Company (www.fedco-usa.com, accessed 24 May 2009) and the Hydraulic Turbocharger manufactured by Pump Engineering (www.pumpengineering.com, accessed 24 May 2009). The turbo booster consists of a turbine and a centrifugal pump impeller connected on the same shaft with no motor. The concentrate stream is directed to the turbine and the impeller is used to raise medium-pressure seawater to high pressure prior to entering the RO membranes (Figure 2.14).

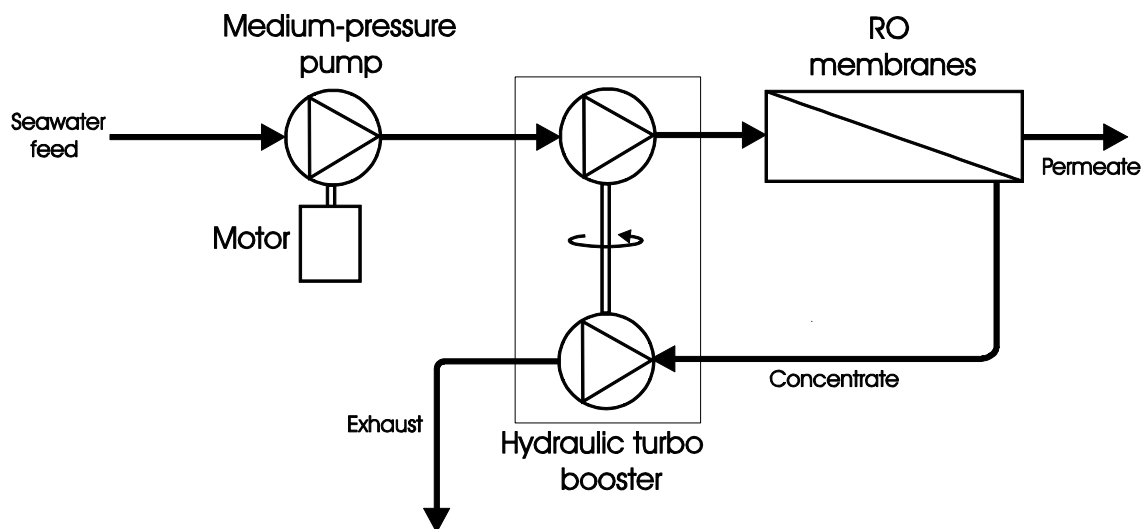


Figure 2.14 System using a hydraulic turbo booster

Since the turbo booster is independent of the motor speed, its own speed can be selected so as to obtain its best efficiency. However, like with Pelton wheels,

the energy recovered is subject to a double efficiency penalty by going through the turbine and the pump impeller, and it only operates at peak efficiency in a narrow range of flows (Stover, 2009).

2.4.5 Dual work exchanger energy recovery (DWEER)

The DWEER is manufactured by Calder (www.calder.ch, accessed 10 June 2009) which was recently acquired by Flowserve. The DWEER is a positive displacement work exchanger device that has two cylinders with a free piston in each (Figure 2.15). The high-pressure concentrate drives the piston in one of the cylinders, pressurising the seawater on the other side of the piston. At the same time, low-pressure seawater pushes the piston in the other cylinder, forcing the exhaust concentrate from the previous stroke out. At the end of the stroke, the roles of both cylinders are reversed by means of a multiport (LinX) valve.

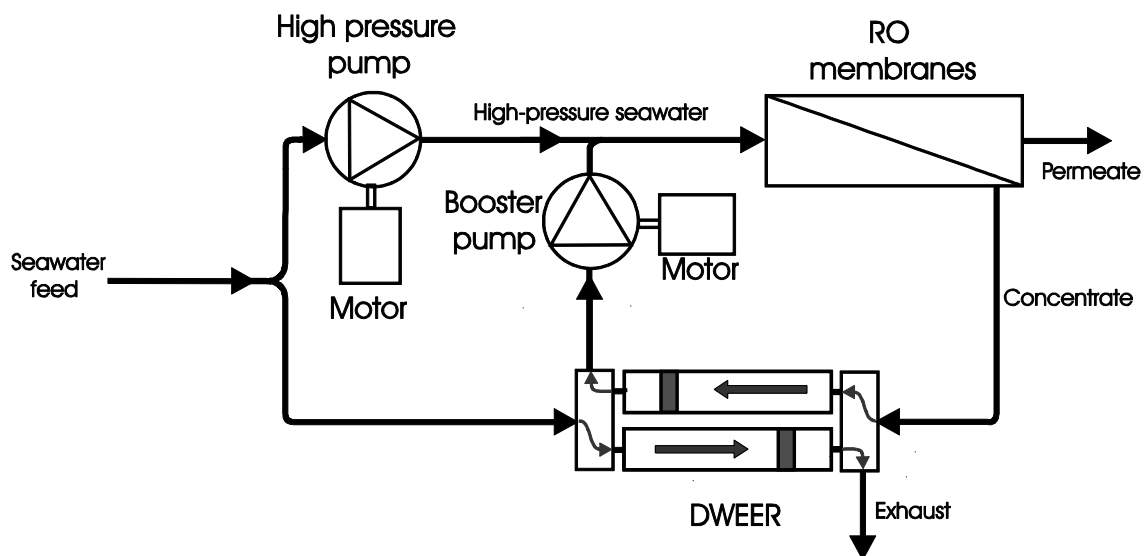


Figure 2.15 System using a DWEER

Although the concept of the DWEER had been around for some time, the development of the LinX valve in the late 1990s brought about faster switching

times and improved the reliability of the device, greatly aiding in the commercialisation of the DWEER (Andrews and Laker, 2001).

2.4.6 PX Pressure Exchanger (PX)

The PX Pressure Exchanger is manufactured by Energy Recovery Inc (www.energyrecovery.com, accessed 13 July 2009). It is also a work exchanger but rather than using two cylinders as does the DWEER, the PX has twelve chambers around the circumference of a ceramic rotor (Figure 2.16), which stretch axially along the length of the device.

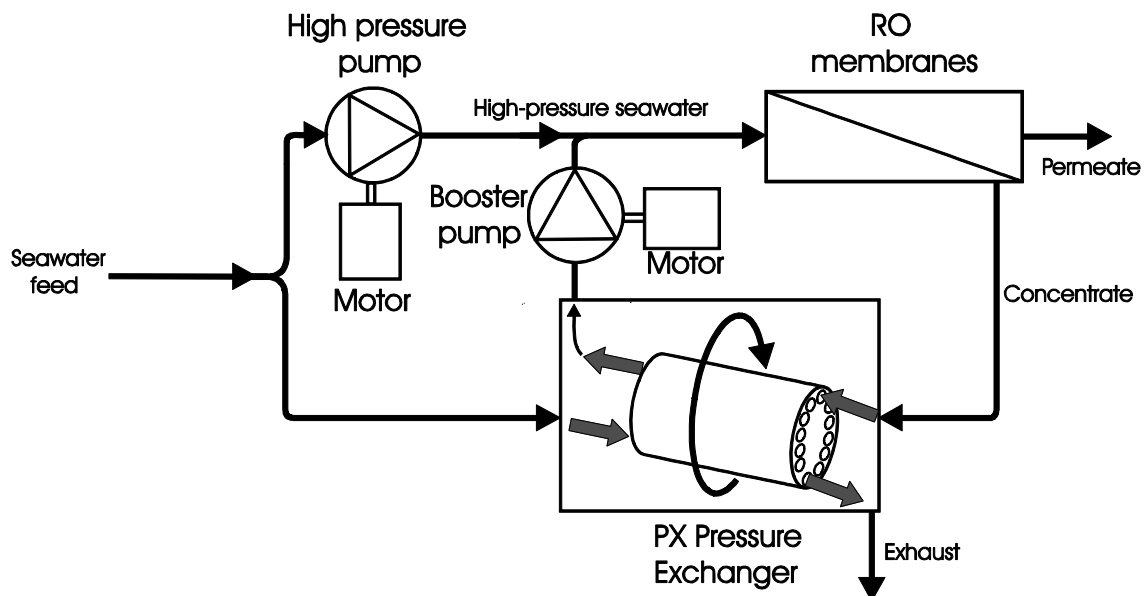


Figure 2.16 System using a PX

On the right-hand side of the PX in Figure 2.16, high-pressure concentrate enters the chambers in the top half of the rotor, pressurising seawater. At the same time, low-pressure seawater enters the chambers in the bottom half of the rotor, pushing out exhaust concentrate. The flows entering the shaped chambers cause the rotor to spin, and thus, the chambers filled with seawater in the bottom half are subsequently exposed to high-pressure concentrate in

the top half and vice versa. Their alternate exposure to low-pressure seawater and high-pressure concentrate as a result of the rotation effectively acts like a switching valve.

Unlike the DWEER, the PX does not have solid pistons inside the chambers. Instead, the interface that forms between the concentrate and the seawater acts like a physical piston. This, however, allows some mixing between the streams, but mixing is kept within acceptable ranges by reducing the contact time in the device (high rotational speed). An animation of the operation principle of the PX can be found in the “Products” section of the company’s website www.energyrecovery.com (Energy recovery Inc, 2007).

2.4.7 Booster pump

Both the DWEER and the PX are isobaric chamber devices and as such, a booster pump is required in their systems as seen in Figure 2.15 and Figure 2.16. This pump makes up for the pressure losses in the RO membranes, the pipe work and in the energy recovery devices themselves so as to match the pressure of the seawater from the high-pressure pump.

2.4.8 High-pressure pump

The high-pressure pump in systems using DWEERs or PXs for energy recovery only pressurises a flow of seawater equal to the permeate (product water). This represents a significant size reduction of the high-pressure pump compared to systems using Pelton wheels or HPBs, where the main pump handles the whole of the feed.

DWEERs and PXs use the energy they recover to pressurise the rest of the feed (equal to the concentrate flow). This can be achieved at very high efficiencies (95% or higher) because DWEERs and PXs transfer the energy

directly between streams without intermediate conversion stages, unlike Pelton wheels and HPBs.

2.4.9 Integrated pump and energy recovery (IPER)

The IPER is manufactured by VARI-RO (www.vari-ro.com, accessed 10 June 2009) and consists of three pistons used to pressurise seawater. The pistons are driven jointly by the concentrate from the RO membranes and an oil hydraulics drive. Computer-controlled valves are used to operate the flows, which open and close at zero flow to minimise surges (Childs and Dabiri, 1999). The IPER has been used in solar powered desalination studies using photovoltaics as well as various solar thermal technologies (Childs et al., 1999).

2.4.10 Energy recovery for small-scale seawater reverse osmosis

Recognising the importance of energy recovery for the economic success of seawater RO, energy recovery in large installations is common practice. However, most small-scale seawater RO systems do not have any form of energy recovery. Instead, they have needle valves that dissipate the energy in the concentrate and provide the necessary backpressure for the process (see Figure 2.10). This keeps capital costs down, but such systems are very energy wasteful and expensive to run.

The lack of suitable energy recovery devices for small-scale, land-based applications is largely responsible for the neglect of energy recovery practices at this level. Scaling down devices that are successful at the large scale does not work because clearances, tolerances and losses become more significant in smaller devices. For instance, Gwillim (1996) looked at Pelton wheels for a seawater RO system of 3 m³/day but the idea was considered impractical due to the high manufacturing costs and the high windage losses expected in the small Pelton wheel required. This favours a positive displacement approach.

Positive displacement devices offer good efficiencies for small-scale applications. However, devices like the DWEER and the PX are not manufactured in the required sizes. Kunczynski (2003) and Subiela et al. (2009) have had some experience with a small version of the PX (PX-15) that is now discontinued because it was susceptible to fouling. Perhaps the tolerances required in a smaller device were too narrow. This highlights the challenge of the high-precision required in the manufacturing of small-scale devices, which must be made of corrosion-resistant materials to handle seawater (e.g., ceramics, certain grades of stainless steel, engineering plastics). The matter can get even more complicated by the need to use accurate valve gear to achieve precise reciprocation timings and ensure smooth flows at high-pressure.

2.4.11 Pumps with built-in energy recovery

In 1980, Bowie Keefer patented a hand-operated piston pump for reverse osmosis with built-in energy recovery behind the piston to aid in the pumping (Keefer, 1980). In this patent, Keefer also presents an embodiment where the energy recovery pump could be operated by the reciprocating action of a water-pumping wind turbine. This patent has been used in the production of desalination units that go in lifeboats.

Later on in 1984, Keefer patented a multi-piston (at least three), reciprocating pump driven by a crank, with built-in energy recovery in between the crankshaft and the pistons (Keefer, 1984). These energy recovery pumps were demonstrated desalinating seawater, some operating from solar PV, achieving very good energy efficiencies (Keefer et al., 1985).

2.4.12 Hydraulic motor

Hydraulic motors are positive displacement devices that convert pressure energy usually from pressurised oil into rotary motion and are widely used in industry. Where the use of oil represents health and safety, environmental or product contamination concerns, water-driven hydraulic motors are used instead. Danfoss (www.danfoss.com, accessed 27 April 2009) manufacture a range of water-hydraulics axial-piston motors and pumps for various industrial applications including seawater reverse osmosis. The hydraulic motor can be used for concentrate-stream energy recovery coupling it to the electric motor of the high-pressure pump similar to the Pelton wheel arrangement shown in Figure 2.13.

In the 1990s, Dulas Ltd demonstrated the use of a Danfoss hydraulic motor for energy recovery in a small reverse osmosis application (Gwillim, 1996). Originally, Danfoss motors were not built to handle seawater and suffered from corrosion problems (Thomson, 2003). Danfoss have since developed a range of hydraulic motors specifically for energy recovery in seawater RO that overcomes these issues. These are the ones currently used by Kunczynski (2008) in his long-term demonstrations of PV-powered seawater RO. As part of their seawater reverse osmosis range, Danfoss now market an integrated unit for pumping and energy recovery at fixed recovery ratio, which incorporates an axial-piston pump and an axial-piston motor assembled on a double-shafted electric motor (Danfoss, 2009). Danfoss have also shown prototypes of this unit where the angle of the swash plate can be modified to adjust the recovery ratio (Orchard and Pauly, 2008).

2.4.13 Device selection

The one remaining energy recovery device of relevance is the Clark pump; it was introduced in Chapter 1 and is described in more detail in Chapter 3. The Clark pump will be referred to in the discussions of this section.

One way to select an energy recovery device is using its water-to-water energy transfer efficiency. However, ready access to this information is not always available and there are also other important factors that must be considered.

For example, device manufacturers tend to quote the best achievable efficiency omitting efficiencies at part-load, and presenting comparisons between devices in conditions where their own device performs better. To enable a fair comparison, devices should be assessed on a level ground with common system boundaries and equal operation ranges where they are set to achieve objective performance targets using the same inputs. Furthermore, a fair comparison must include all other components required in the system, which complicates matters further as the choice of components can be overwhelming.

At this point, it is important to make a distinction between device and system efficiency, which are closely related but are by no means synonyms. For instance, a particular device may not be the most efficient, but the components and system configuration it requires could well result in a system with very good overall efficiencies and vice versa. Needless to say, if a configuration is found that takes advantage of the efficiency of its components, the potential for reduction of overall energy consumption is greatly improved.

Researchers at Fraunhofer ISE in Germany (Went et al., 2009) have developed an analysis tool to perform comparisons of energy recovery options for small-scale seawater RO systems. They simulated the performance of seawater RO systems with various energy recovery approaches, assuming realistic efficiency values for all other system components. Their findings, presented in Figure 2.17, suggest that for all energy recovery approaches, there is a water recovery ratio that minimises the overall system energy consumption. In the figure, energy conversion refers to devices that use a shaft like the hydraulic motor; pressure exchanger refers to isobaric chamber devices like the PX Pressure Exchanger and the DWEER; and pressure intensifier refers to devices that use pistons with different effective areas like the Clark pump.

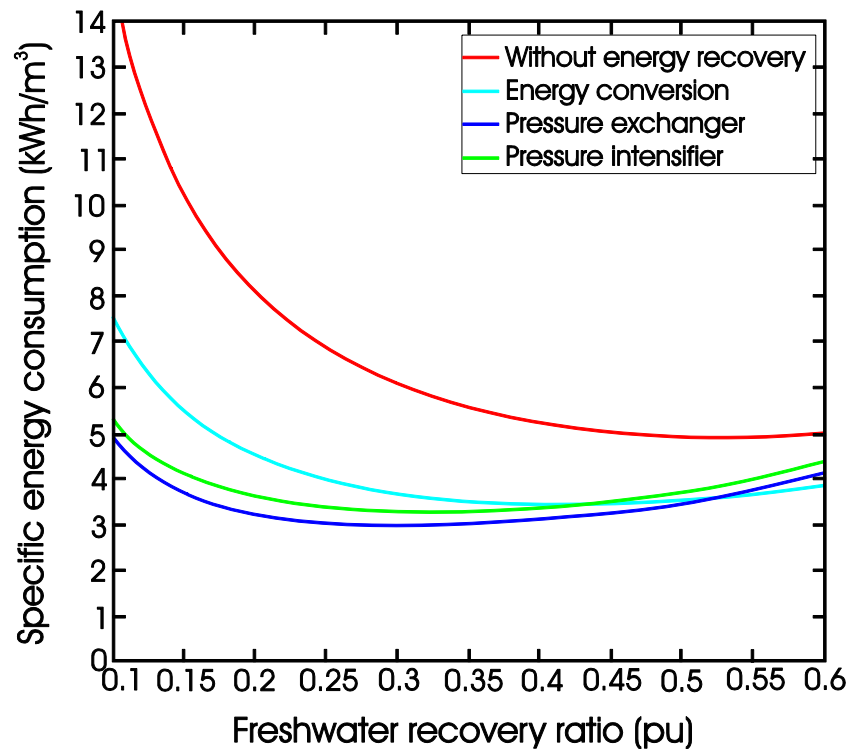


Figure 2.17 Energy consumption for various energy recovery approaches.
After Went et al. (2009)

In this figure, pressure exchanger devices present the lowest specific energy consumption over a wide range of recovery ratios, closely followed by pressure intensifiers. The minimum in the curves for these two types of devices are found at recovery ratios between 30 and 35% and their values stay low over a wide range of recovery ratios. Systems using an energy conversion approach like the hydraulic motor, present slightly higher specific energies at their minimum point, which is found at recovery ratios close to 45%. However, at lower water recovery ratios, energy conversion devices deviate faster from the minimum than pressure exchanger devices and pressure intensifiers. These findings tie up well with the experience of Thomson (2003) using the Clark pump, and with that of Kunczynski (2008) using hydraulic motors, who operates his systems at recovery ratios of around 40%.

Meanwhile, since pressure exchanger devices are not manufactured in the required sizes for small RO applications, the best energy efficiencies in small-

scale systems are obtainable with pressure intensifiers like the Clark pump, followed by hydraulic motors like Danfoss's.

In addition to energy efficiency, there are three other important factors to consider. One is the requirement of chemicals to prevent membrane fouling. Working at low recovery ratios has been suggested as a means to reduce the fouling potential of seawater and brine to avoid the use of chemicals altogether (Keefer et al., 1985; Paulsen and Hensel, 2005); Dow Filmtec recommend the use of a scale inhibitor when operating at recoveries above 35% (Dow, 2005). Therefore, pressure intensifiers could have the edge here since their SEC is better at lower recovery ratios compared to hydraulic motors. However, Kunczynski (2008), who operates his PV-powered systems at higher recovery ratios without the use of chemicals, observes that daily flush of the membranes with permeate water for a few minutes before overnight shutdown maintains the RO membranes in a healthy state.

A second factor is the operation regime of the system. For instance, a RO system directly coupled to a PV array with no battery storage would have to cope with the fluctuations of the solar energy, resulting in variations of flow and pressure driving it away from its best efficiency point. Such a system would benefit from the use of pressure intensifiers, which maintain good efficiencies in a broad range of recovery ratios. A system with a hydraulic motor is not expected to cope as well with input energy fluctuations, deviating faster from its best efficiency. However, this presumably would not be so much of an issue if batteries are used, since the RO part could then operate at a nearly constant point. Again, this is the approach followed by Kunczynski. However, despite its advantages, the use of batteries also represents additional complications that deserve careful consideration as mentioned in section 2.3.2.5.

A third, and very important, factor is the cost of the water produced. In addition to the cost of the energy recovery device itself, the selection of a particular device implies the use of specific components in the system, which also has an influence on capital costs and the cost of the water produced. Unfortunately,

there is not enough information readily available with these systems to enable a comparison.

While the discussions above do not point to a best device or approach for energy recovery in general, a pressure intensifier like the Clark pump looks more attractive for renewable-energy-powered reverse osmosis systems without energy storage as it could offer better system efficiencies over a wide range of operation.

The following chapter describes the Clark pump in more detail and reviews the experience with it at Loughborough University's CREST.

Chapter 3 The Clark pump

3.1 Concept

The Clark pump is manufactured by Spectra Watermakers (www.spectrawatermakers.com, accessed 17 July 2009). It consists of two in-line cylinders with a piston in each and a rod linking the pistons as shown in Figure 3.1 (top). The presence of the connecting rod reduces the effective area of the inner side of the pistons (chambers 2 and 3 in Figure 3.1 bottom), defining a volumetric ratio between the four chambers. The pistons and rod reciprocate inside the cylinders as a solid assembly. Photographs of the Clark pump can be found in Spectra Watermakers website.

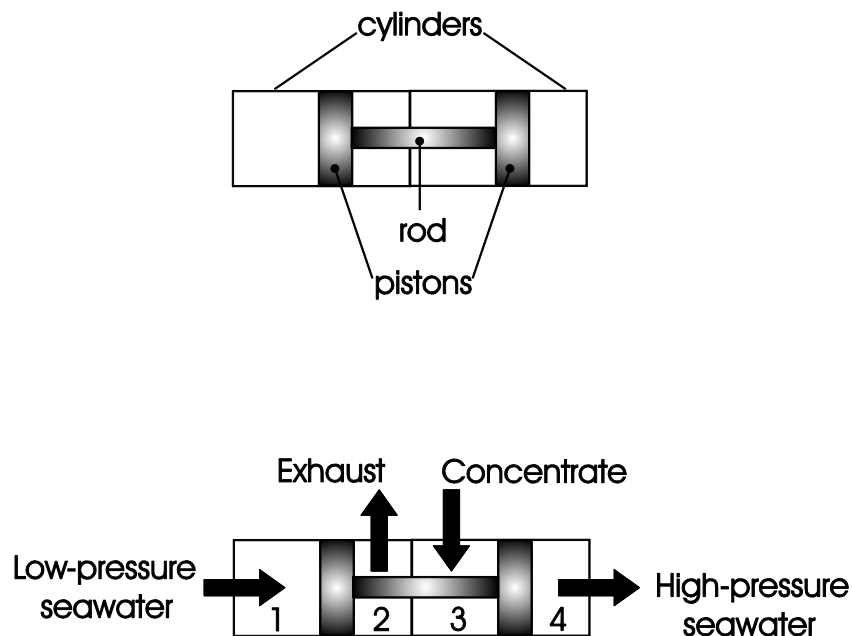


Figure 3.1 Schematics of a Clark pump.
Top: basic components; bottom: example with flows and chamber numbers

Clark Permar patented the Clark pump (Permar, 1995) and teamed up with Spectra Watermakers Inc to develop it, to whom he then licensed the technology for desalinators onboard small yachts. The Clark pump had its first applications in the late 1990s in small systems producing up to 1.8 m³/d of freshwater in continuous operation (Smith, 2000).

The concept of using two pistons and a rod for fluid pumping, however, is not new. For instance, patents by Wilson (1983) and Pinkerton (1979) also use this idea, but the practical implementation was only possible once Clark Permar devised suitable reciprocation mechanisms and proved the concept.

3.2 Mechanics

During one stroke of the Clark pump, the pistons-rod assembly in Figure 3.1 (bottom) is driven to the right by the low-pressure seawater flowing into chamber 1 and the high-pressure concentrate flowing into chamber 3. The combination of these forces, made possible by the connecting rod, intensifies the pressure of seawater in chamber 4 above the pressure of the concentrate. At the same time, the exhaust concentrate from the previous stroke is driven out of chamber 2. The operation of the Clark pump is symmetrical and at the end of the stroke the reciprocation valve gear (not shown in the figure) swaps the flows round and seawater then flows to chamber 4 and the pistons-rod assembly would move to the left. An animation of the operation of the Clark pump can be found in the “Technology” section of Spectra’s website www.spectrawatermakers.com (Spectra Watermakers, 2009).

3.3 Basic system configuration

The basic configuration of a system using a Clark pump is presented in Figure 3.2, and shows that only one motorised low-pressure pump is required to achieve the high pressures required for seawater reverse osmosis. Here, the

low-pressure pump feeds seawater to the Clark pump at around 5 bar, which in turn raises the pressure of the seawater to the level required to achieve the design recovery ratio, typically 50 bar or higher. This is achieved by virtue of the energy that the Clark pump recovers from the concentrate. The simplicity of this configuration makes it very attractive.

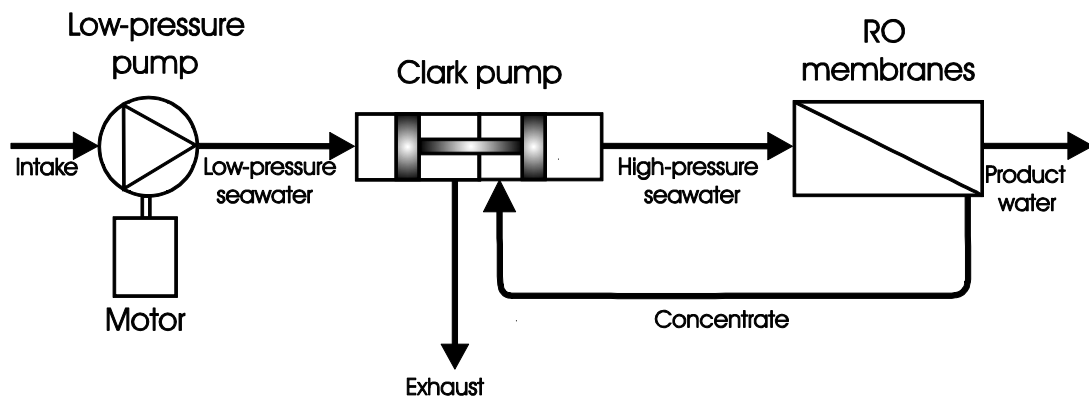


Figure 3.2 Basic configuration of a system with a Clark pump

Because of the positive displacement nature of the Clark pump, the flow difference between the high-pressure seawater and the concentrate is equal to product flow in the RO membranes. This fixes the recovery ratio of the system by design, which is 10% for the standard model.

Since the motorised pump is the only source of motive power in this configuration, the overall system efficiency is heavily dependent on the efficiency of this component. Unfortunately, the efficiencies of small low-pressure pumps are low. Nonetheless, it is possible to obtain good specific energies with this configuration as shown below.

Spectra Watermakers reported performance data for a system configured as in Figure 3.2 (Smith, 2000). Their data indicate a specific energy consumption of 3.18 kWh/m^3 at 25°C for $35\,000 \text{ mg/L}$ seawater and 10% recovery ratio. Furthermore, the data reported allow the exploration of the energy flows within

their system. This is depicted in the Sankey diagram of energy flows presented in Figure 3.3. In the diagram, the line widths and values represent specific energies in kWh/m³.

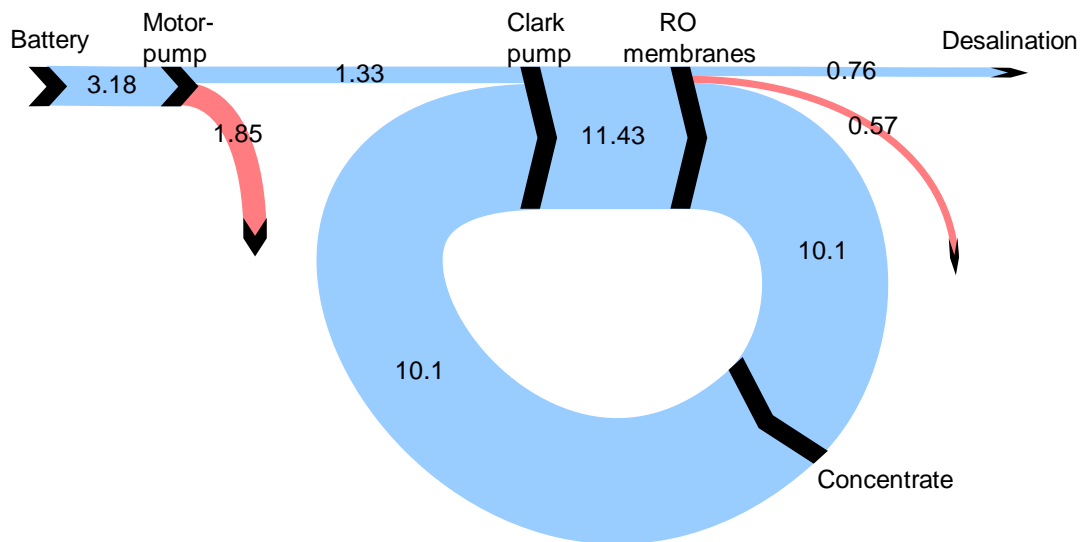


Figure 3.3 Energy flows in Spectra Watermakers' system.
Values in kWh/m³. Derived from data in Smith (2000)

The 3.18 kWh/m³ on the far left corresponds to the electric energy supplied by a battery to operate the system. Part of this energy (1.33 kWh/m³) is used by a motorised diaphragm pump to raise the seawater to a modest pressure, about 4 bar in this example. However, the low efficiency of this unit, about 42%, results in more than half of the electric energy being lost here. This corresponds to the 1.85 kWh/m³ in the downwards pointing arrow. All pink arrows pointing down in this and subsequent Sankey diagrams represent losses.

Next in the diagram is the Clark pump, which uses the energy it recovers from the concentrate (10.1 kWh/m³) to further raise the pressure of the seawater to the level required to obtain a 10% water recovery ratio; this is about 38 bar in this example and corresponds to the 11.43 kWh/m³ coming out of the Clark pump.

In the RO membranes, 0.76 kWh/m^3 are used for the actual desalination process. This represents the minimum energy set by thermodynamics to achieve the separation of salts and water. Most of the energy entering the membranes (10.1 kWh/m^3) ends up in the concentrate, which in turn flows to the Clark pump where it is returned to the membranes, closing the energy recovery loop. The energy in the concentrate is very large in relation to other flows in the system because of the low water recovery ratio defined by the Clark pump (only 10%).

The data reported by Spectra do not allow the separation of the losses in the membranes from those in the Clark pump. In Figure 3.3, their combined losses, 0.57 kWh/m^3 , have been placed in the RO membranes.

3.4 Injection configuration

Around the time the Clark pump made it to the market, researchers at CREST in the UK were looking for an energy recovery device to use in their investigations on small-scale seawater reverse osmosis desalination powered by wind and solar energy without energy storage (Miranda, 2003; Thomson, 2003). To cope with the fluctuating and intermittent nature of these renewables, they required an energy recovery device that would maintain high efficiency levels over a wide range of flows and pressures. The Clark pump, which they tested and modelled extensively, delivered these characteristics.

However, the configuration in Figure 3.2 presents a limitation: the fixed recovery ratio and the maximum allowed feed flow rate to a single Clark pump set a limit to the amount of permeate that can be produced per Clark pump. With a finite energy generator like a PV array, this means that to operate the RO system at its full capacity for most of the time, the PV array must be oversized, which is inefficient and expensive. Alternatively, to keep capital costs down, the RO system could be designed to produce its full capacity at peak PV

power. This would make better use of the PV array but would underutilise the RO system most of the time.

To improve the utilisation of both the PV array and the RO system, CREST researchers used the injection configuration in Figure 3.4 (Thomson, 2003). This configuration enables a variable recovery ratio as well as higher permeate flow rates per Clark pump and allows better utilisation of the PV array by means of an additional pump in the system combined with the use of variable speed motors. This configuration was demonstrated at CREST desalinating seawater using a PV array without batteries (Thomson and Infield, 2005).

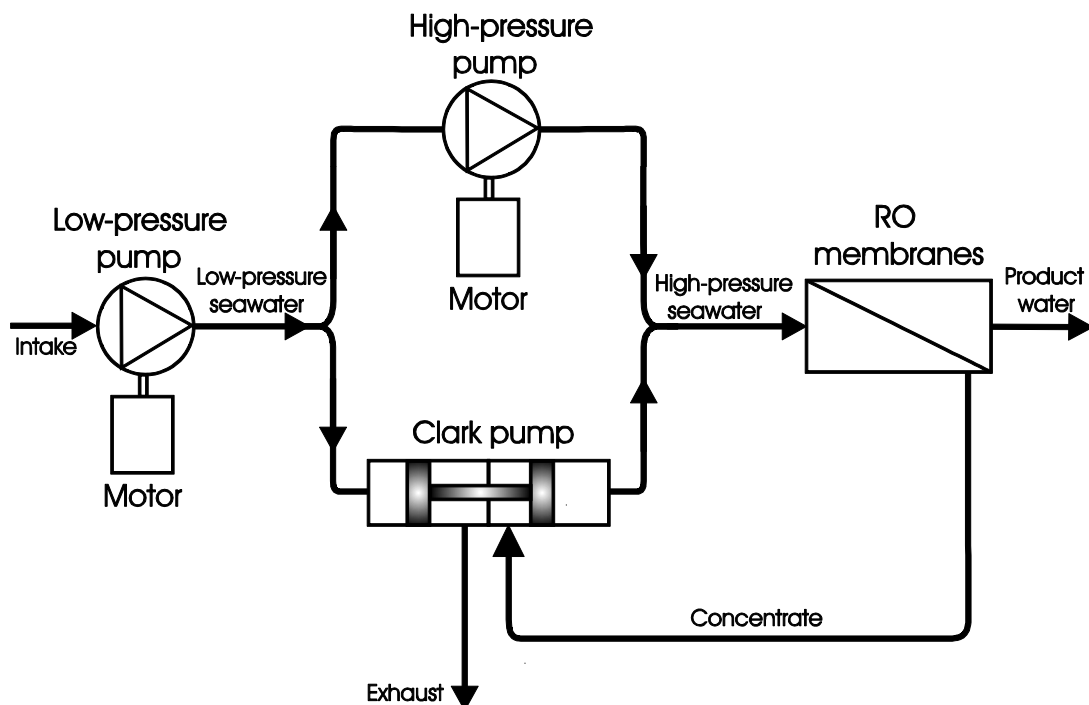


Figure 3.4 Injection system configuration of the Clark pump

In spite of the excellent results achieved with this configuration, two observations from the experience with this system are (Thomson, 2003):

- The overall complexity of the configuration because of the additional pump and motor. Furthermore, splitting one already small motor into two even smaller ones could lead to considerable efficiency losses.

- The fact that while the high-pressure pump achieved efficiencies of around 80%, the low-pressure pump operated sometimes at efficiencies as low as 40%.

Chapter 4 The challenge and initial investigations

4.1 State of the art summary

Previous chapters have shown that energy recovery is often overlooked in small seawater RO plants. This is largely because of the very few energy recovery devices commercially available for small systems. For the high pressures and low flows found in these systems, positive displacement devices offer the best efficiencies (Barlow et al., 1993; Gwillim, 1996; Thomson, 2003). The Clark pump (and similar devices) and the hydraulic motor are the two main options in the market.

The Clark pump itself is highly energy efficient; with its basic system configuration, good specific energy consumptions can be achieved. However, this configuration is limited by the amount of freshwater that can be produced per Clark pump. Moreover, the overall efficiency of the configuration is constrained by the efficiency of the low-pressure pump.

The injection configuration of the Clark pump can increase the amount of freshwater produced per Clark pump and also introduces some flexibility in the operation of the system. On the other hand, this configuration is more complex, and still needs a low-pressure pump.

The hydraulic motor is a very reliable device. However, its rotary approach to energy recovery requires several energy conversion steps, which make it less efficient than the direct, linear approach of the Clark pump. In addition, research suggests that a system using a hydraulic motor for energy recovery would operate at its best efficiency in a narrower range than an intensifier like the Clark pump (see section 2.4.13). A discussion with Mr. Tony Markham from the Water Hydraulics Company (www.waterhydraulics.co.uk, accessed 24 September 2008) further encouraged the use of the linear approach.

4.2 Motorised pump efficiency observation

Considerable specific energy consumption reductions could be achieved if pumps with better efficiencies could be used in the Clark pump configurations. For example, Figure 4.1 shows that increasing the efficiency of the motorised pump from the 42% of the Spectra Watermakers system presented in Figure 3.3 up to 60% would reduce the overall specific energy consumption by almost one third, i.e., from 3.18 kWh/m³ down to 2.22 kWh/m³. These two points are represented by the circle markers at the extremes of the curve in Figure 4.1. The trend of the curve joining these two points was estimated calculating the specific energy consumption for the same system at intermediate motor-pump efficiencies.

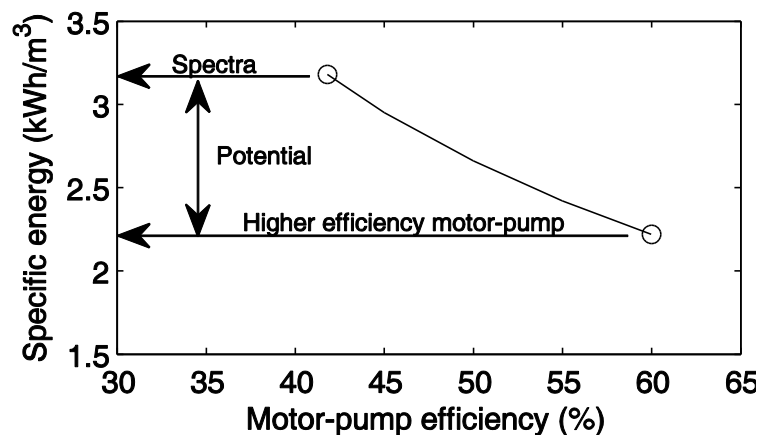


Figure 4.1 Potential for specific energy reduction

Efficiency increases like that illustrated in Figure 4.1 can be achieved and maintained over wide ranges if high-pressure pumps are used. For instance, plunger and axial-piston pumps are capable of efficiencies around 80% (pump only) over wide ranges, but this assumes their operation at high pressure. Operating such pumps at low pressures would be significantly less efficient. Thus, to take advantage of their higher efficiencies, a different system configuration that operates at high pressure would be required. Since the Clark pump configurations require a low-pressure pump, this would also require a different approach to energy recovery.

4.3 Thesis objectives

The summary above highlights that, at the small scale, there is still room for innovative energy recovery devices and provides the following specific objectives:

- To design a positive displacement, linear-motion energy recovery device.
- To use a simple system configuration, preferably with only one motorised pump.
- To use a system configuration that exploits the high efficiency of high-pressure pumps such as a plunger or axial-piston pump.
- To design a system configuration that operates efficiently over wide ranges of flow and power.

4.4 Many possibilities

In using pistons and cylinders in a linear fashion to handle fluids, many arrangements are possible. Examples of these are found in many patents of devices to pump fluids for a variety of applications (Garretson, 1950; Arp and Varnum, 1970; Shaddock, 1972; Taylor, 1974; Pinkerton, 1979; Wilson, 1983). With this in mind, a brainstorming session resulted in a number of possible device geometries to explore. These are presented in Figure 4.2.

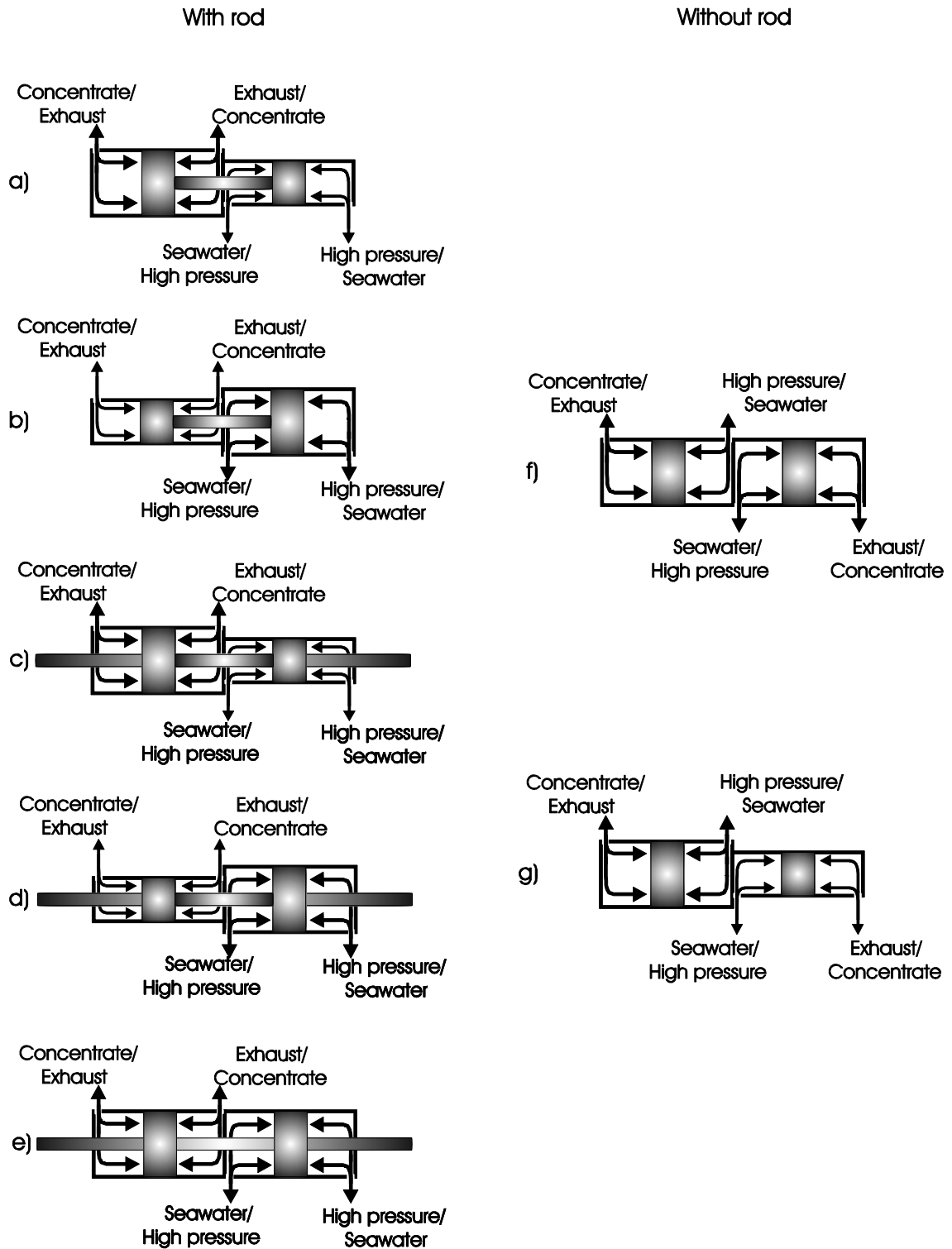


Figure 4.2 Spectrum of geometries

The layouts in Figure 4.2 are categorised into those with a rod connecting the pistons (left column) and devices without a rod (right column). In the five layouts

with a rod connecting the pistons, Figure 4.2 a) through to e), the concentrate and exhaust would alternate in the chambers of the cylinder on the left-hand side. At the same time, the seawater feed to the device and the pressurised seawater would alternate in the chambers of the cylinder on the right-hand side.

In the layouts without a rod, Figure 4.2 f) and g), the concentrate and high-pressure seawater must be in one cylinder during one stroke while the seawater feed and the exhaust occupy the other cylinder. During the second stroke, the pairs of flows would swap into the other cylinders.

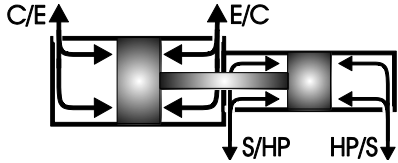
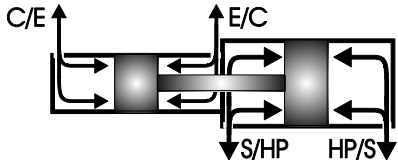
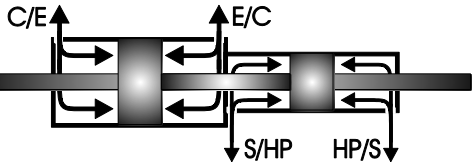
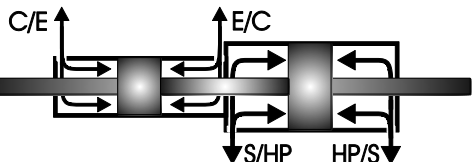
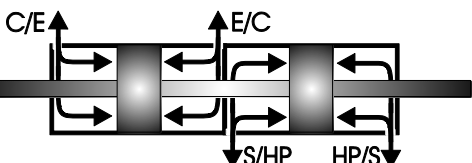
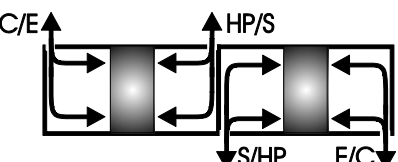
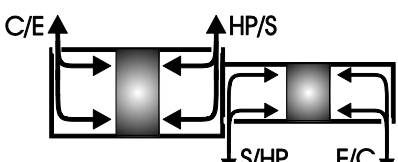
4.5 Initial selection

Before a detailed analysis, the proposed layouts were screened to ensure they could deliver the characteristics required:

- First, to achieve a simple system configuration, the devices should be capable of pressure intensification. Otherwise an additional (booster) pump would be required.
- Second, each flow in the device must be symmetric during both strokes so as to maintain a constant operating point of the system.

The assessment of the layouts in terms of these criteria is presented in Table 4.1. After this screening, only devices c), d) and e) are still of interest.

Table 4.1 Capabilities of the device layouts

C, concentrate; E, exhaust; S, seawater input; HP, high-pressure seawater	Pressure intensification	Symmetric flows
<p>a)</p> 	✓	
<p>b)</p> 	✓	
<p>c)</p> 	✓	✓
<p>d)</p> 	✓	✓
<p>e)</p> 	✓	✓
<p>f)</p> 		✓
<p>g)</p> 		

4.6 Generalised configuration

The three devices selected – c), d) or e) – are very similar. The only distinction between them is the relative size of their pistons, which suggests that they can be analysed on a common basis. For this, a generalised system configuration is presented in Figure 4.3, which includes all possible system components: a low-pressure pump, a high-pressure pump, RO membranes and an energy recovery device. The latter could be any of the three selected devices. Based on this system configuration, a mathematical model was derived to study the devices. This is presented in the following chapter.

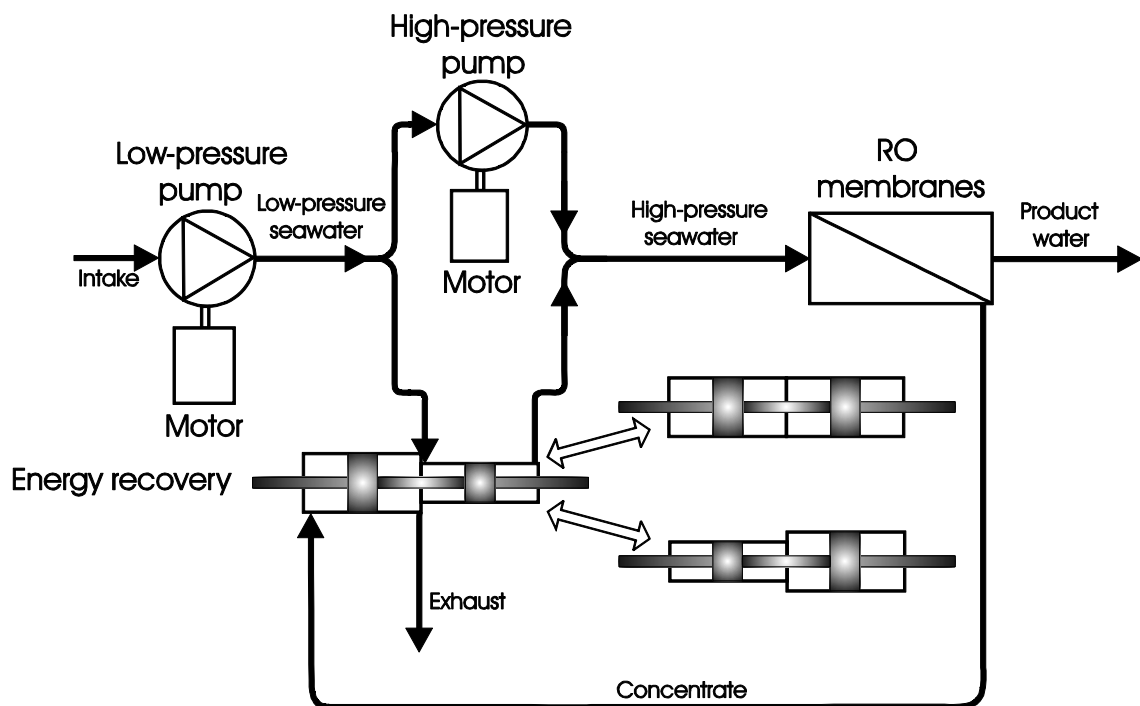


Figure 4.3 Generalised system configuration

Chapter 5 Generalised analysis of pressure intensifiers for energy recovery

5.1 Pistons

The intensifiers resulting from the investigations in the previous chapter rely on their pistons to convey energy from the high-pressure concentrate to low-pressure seawater. The rod connecting the pistons makes possible the energy transfer from one cylinder to the other. Both pistons move at the same speed, and so flows are proportional to effective piston area after allowing for the area of the rod.

5.2 Piston area ratio

The ratio of the areas of either side of each piston, r_a (Equation 5.1), can be used to characterise the various devices.

$$r_a = \frac{A}{B} \quad \text{Equation 5.1}$$

In this equation, A is the area on the seawater side of the pistons, both high pressure and low pressure, whereas B is the area on the concentrate sides, both high pressure and low pressure (exhaust). The location of these areas and the ratio between them is shown for the three intensifiers in Figure 5.1.

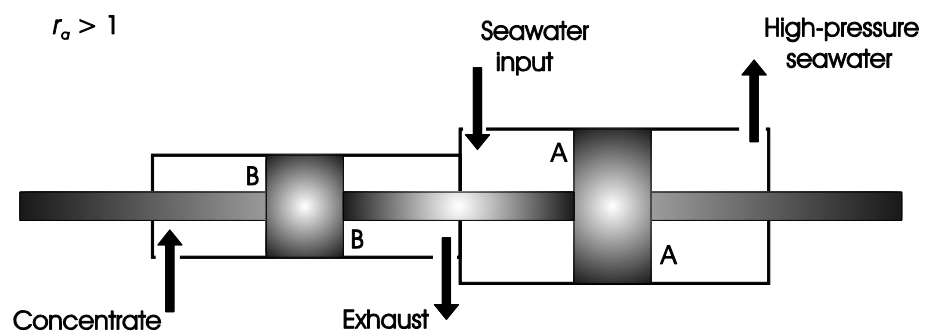
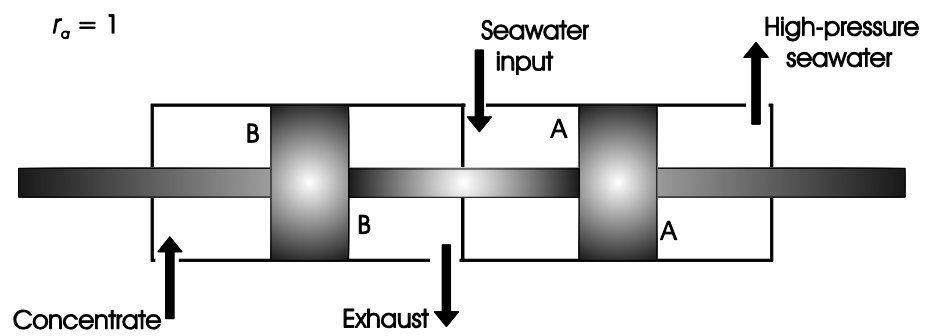
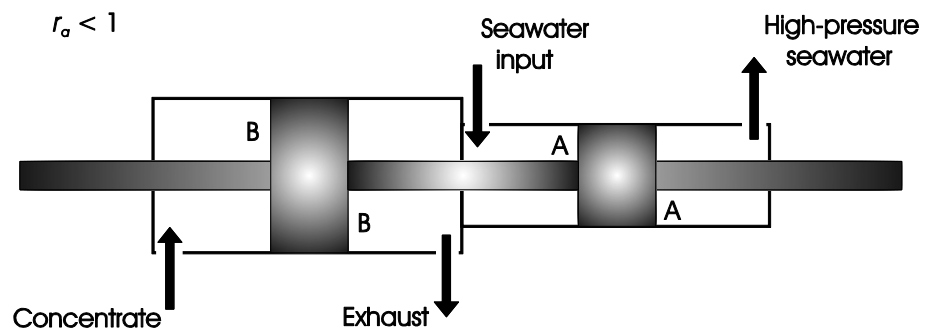


Figure 5.1 Flows and piston areas in the three intensifiers

5.3 Area ratio of the Clark pump

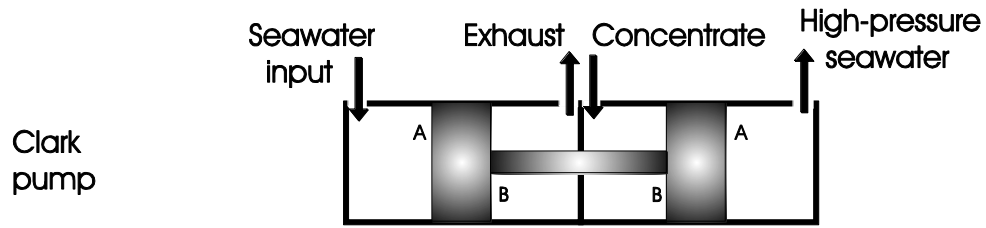


Figure 5.2 Piston areas in a Clark pump

Despite its different chamber layout, the piston area ratio of a Clark pump can also be estimated using Equation 5.1. The Clark pump uses two pistons of the same size but the presence of the connecting rod causes a difference in the effective areas of either side of the pistons. In consequence, in a Clark pump, areas *A* or *B* correspond to different sides of the same piston, unlike any of the layouts in Figure 5.1. This is illustrated in Figure 5.2, where it is clear that area *A* is greater than area *B*, and therefore the piston area ratio of a Clark pump is $r_a > 1$. Therefore, all subsequent discussions about devices with area ratio $r_a > 1$ are also applicable to the Clark pump.

5.4 Device equations

5.4.1 Energy recovery

An ideal case is analysed here, where no leaks or friction losses are present. This maintains the underlying principles and simplifies the equations presented.

Given the positive displacement nature and geometry of pressure intensifiers, the pistons' area ratio defines the ratio between flow rates (Equation 5.2).

$$r_a = \frac{A}{B} = \frac{Q_t}{Q_c} = \frac{Q_i}{Q_e} \quad \text{Equation 5.2}$$

where Q is the flow and the suffix t corresponds to the high pressure, c to concentrate, i to inlet and e to exhaust. For reference, a List of symbols and abbreviations can be found on page xii.

Equation 5.2 can be illustrated using the example of a device with $r_a < 1$ in Figure 5.3. Letter P refers to pressure.

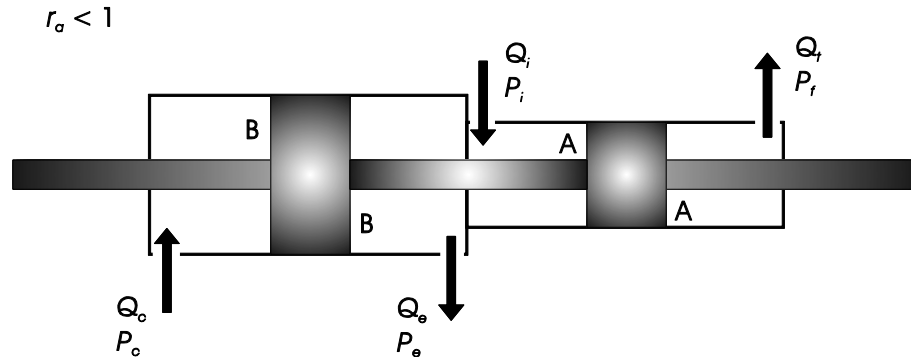


Figure 5.3 Flow rates and pressures in a device with $r_a < 1$

The pistons' area ratio r_a also defines the relationship between the pressures in the various chambers of the device. To find this relationship, a balance of forces is used. The balance of forces (F) is given by:

$$\Sigma F = P_c B + P_i A - P_f A - P_e B = 0 \quad \text{Equation 5.3}$$

This can be rearranged to:

$$\frac{A}{B} = \frac{P_c - P_e}{P_f - P_i} = r_a \quad \text{Equation 5.4}$$

Whilst a device with $r_a < 1$ has been used in this section to illustrate the equations, it is important to stress that they are equally applicable to all three devices.

5.4.2 RO membranes

The expression that relates the permeate flow with the properties of the seawater and the properties of the membrane is given in Equation 2.1 and is repeated here:

$$Q_p = K_w A_m [(P_f - P_p) - (\pi_{avg} - \pi_p)] \quad \text{Equation 5.5}$$

This equation shows that the product flow of the RO membranes Q_p is proportional to the water permeability of the membranes K_w , the area of the membranes A_m and the net driving pressure, which is the term in square brackets. In the equation, an average osmotic pressure value π_{avg} is used to take into account the concentration increase of the seawater as it progresses along the membranes and freshwater is being extracted.

5.5 System equations

Figure 5.4 repeats the generalised system layout presented in Figure 4.3 but with the addition of identifying flow rates and pressures, which are used in the following equations.

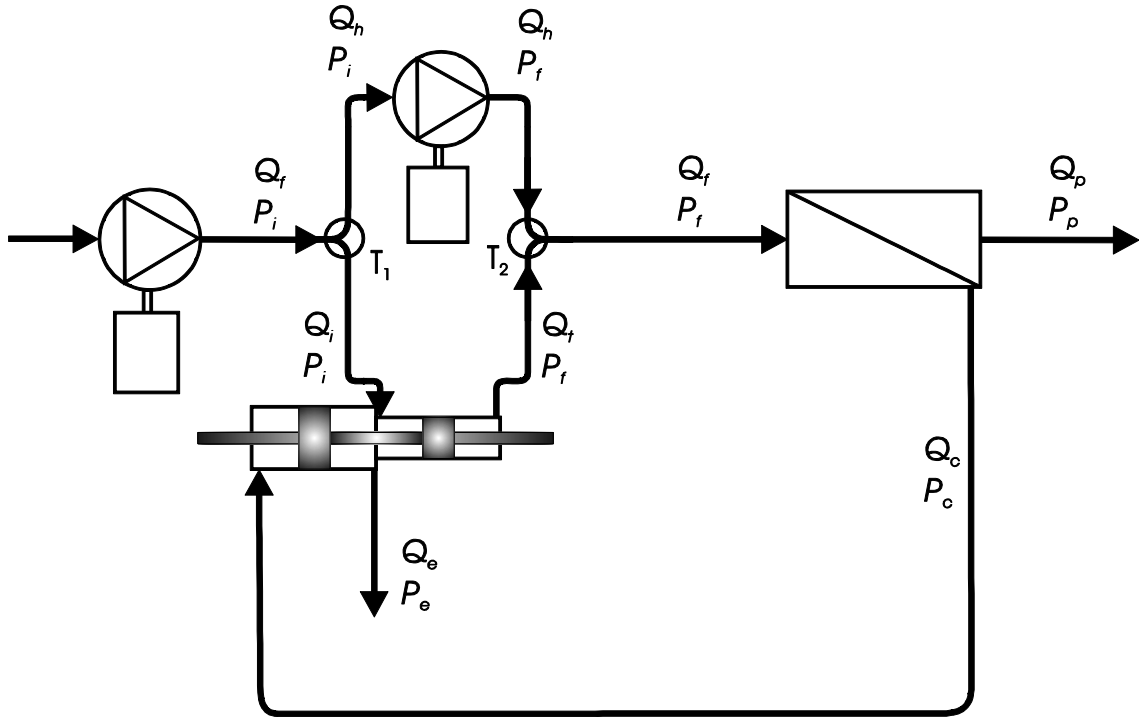


Figure 5.4 Flows and pressures

5.5.1 Flow balances

A flow balance equation can be drawn for every component in Figure 5.4. The most relevant are presented below.

RO membranes:

$$Q_f = Q_p + Q_c \quad \text{Equation 5.6}$$

Or, in terms of the recovery ratio, RR :

$$RR = \frac{Q_p}{Q_f} \rightarrow 1 = RR + \frac{Q_c}{Q_f} \quad \text{Equation 5.7}$$

High-pressure tee (T_2 in Figure 5.4):

$$Q_f = Q_h + Q_t \quad \text{Equation 5.8}$$

5.5.2 Pressure differences

A pressure difference is associated with every component in the system. These are defined here as the difference between the outlet and inlet pressures. The most important are presented below.

RO membranes:

$$\Delta P_{RO} = P_c - P_f \quad \text{Equation 5.9}$$

Energy recovery device:

$$\Delta P_{ER}^{f-c} = P_f - P_c \quad \text{Equation 5.10}$$

Finally, in the loop comprising the RO membranes and the energy recovery device, the total pressure change must be zero. In other words, the energy recovery device must make up for the pressure loss in the membranes. Thus:

$$\Delta P_{RO} + \Delta P_{ER}^{f-c} = 0 \quad \text{Equation 5.11}$$

5.6 Analysis

In order to determine the operation point of the system in Figure 5.4, all system and device equations must be solved simultaneously. While it is not possible to do this analytically, the following sections combine equations to explore separately the effect of the piston area ratio r_a on the water product flow rate, the recovery ratio and the membranes' feed pressure.

5.6.1 Permeate flow rate

To find the permeate flow rate Q_p , a combination of Equation 5.2, Equation 5.6 and Equation 5.8 results in:

$$Q_p = Q_h - (1 - r_a)Q_c \quad \text{Equation 5.12}$$

This equation shows that the high-pressure pump flow rate Q_h , can be used to vary the permeate flow rate Q_p . In this equation, Q_h and Q_p have a one-to-one relationship (gradient = 1), with the term containing the area ratio r_a separating the three curves shown in Figure 5.5.

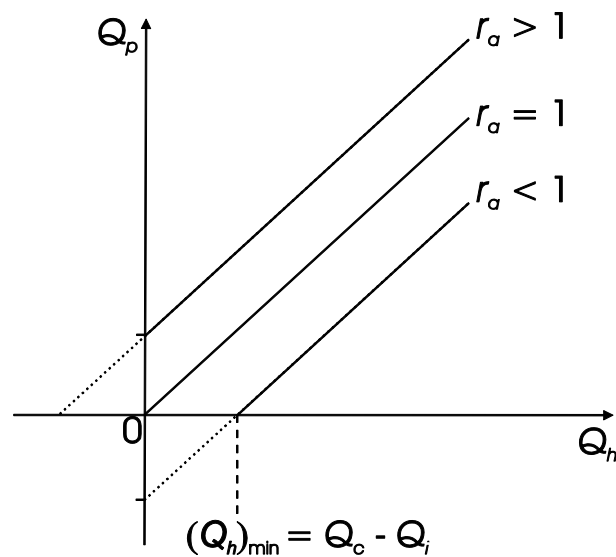


Figure 5.5 Permeate and high-pressure pump flow rates

Equation 5.12 also indicates how much seawater the high-pressure pump must pressurise (Q_h) compared to the permeate flow rate (Q_p) as summarised in Table 5.1.

Table 5.1 High-pressure pump flow rate

r_a	Comparison
< 1	$Q_h > Q_p$
$= 1$	$Q_h = Q_p$
> 1	$Q_h < Q_p$

For a system with $r_a = 1$, the high-pressure pump will pressurise a flow rate equal to the permeate Q_p , which is shown as a line starting at the origin in Figure 5.5. This figure also shows that with $r_a < 1$ there is a minimum flow rate $(Q_h)_{min}$ that must be supplied by the high-pressure pump in order to get a positive permeate flow. This means that the high-pressure pump must make up for the flow difference between the concentrate and the seawater fed to the energy recovery device as well as pressurise all of the permeate flow, thus making this pump an essential component at $r_a < 1$.

In the case of $r_a > 1$, there is no minimum flow required from the high-pressure pump. Indeed, the high-pressure pump may be omitted completely and the system would still produce freshwater as seen in the basic implementation of the Clark pump (Figure 3.2), which has an area ratio $r_a > 1$. This is due to the seawater flow to the energy recovery device being greater than the concentrate flow. However, the optional use of a high-pressure pump (Figure 3.4) introduces some flexibility in the system as will be shown in the analysis of the recovery ratio below.

5.6.2 Recovery ratio

The recovery ratio RR can be found by combining and rearranging Equation 5.12 and Equation 5.7 as in Equation 5.13. This expression is plotted in Figure 5.6.

$$RR = 1 - \frac{1}{r_a} \left(1 - \frac{Q_h}{Q_f} \right) \quad \text{Equation 5.13}$$

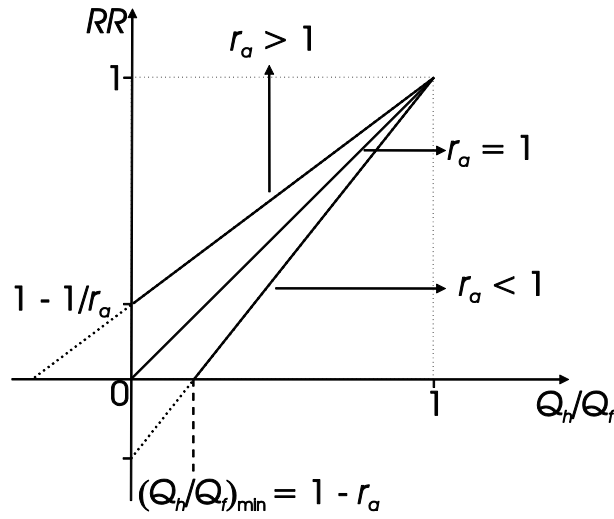


Figure 5.6 Freshwater recovery ratio

The recovery ratio can be modified by varying the Q_h/Q_f ratio, as shown in Figure 5.6. This can be achieved by adjusting the speed of the pumps.

The minimum flow $(Q_h)_{min}$ shown in Figure 5.5 and discussed in the previous section is also apparent in the curve for $r_a < 1$ in Figure 5.6. Here, a similar value $(Q_h/Q_f)_{min}$ is found, where the recovery ratio of systems with $r_a < 1$ equals zero. In such systems, permeate flows, and hence recovery ratios, greater than zero are only found above this minimum.

Figure 5.6 also reinforces the point that an installation with a device with $r_a > 1$ can still desalinate water ($RR > 0$) without a high-pressure pump ($Q_h/Q_f = 0$), but in this case the water recovery ratio is fixed by the geometry of the device.

5.6.3 Membranes' feed pressure

The pressure of the feed to the membranes P_f can be found by combining and rearranging Equation 5.9 and Equation 5.4 to give:

$$P_f = \frac{\Delta P_{RO} + r_a P_i - P_e}{r_a - 1} \quad \text{Equation 5.14}$$

With an atmospheric discharge of the exhaust ($P_e = 0$) Equation 5.14 reduces to:

$$P_f = \frac{\Delta P_{RO} + r_a P_i}{r_a - 1} \quad \text{Equation 5.15}$$

This means that for a fixed inlet pressure (P_i), and with r_a fixed by design, the pressure drop in the membranes (ΔP_{RO}) dictates their feed pressure (P_f).

5.6.3.1 Area ratio $r_a > 1$

For a device with $r_a > 1$, the membranes' feed pressure P_f decreases with increasing pressure drop as shown in Figure 5.7.

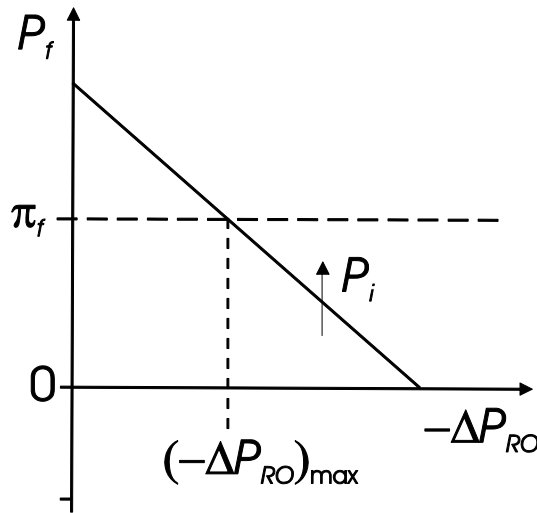


Figure 5.7 Effect of pressure drop for $r_a > 1$

In this figure, one can also see that there is a pressure drop $(-\Delta P_{RO})_{\max}$ that corresponds to the osmotic pressure of the seawater feed (π_f). This sets a maximum pressure drop beyond which the system will not produce any freshwater.

Varying the input pressure (P_i) causes the curve in Figure 5.7 to move vertically: an increase in P_i will move the curve upwards (increase feed pressure) and vice versa. For instance, keeping the inlet seawater to the energy recovery device at atmospheric pressure, e.g., just flooding its inlet port, results in the curve starting at the origin (intercept = 0 when $P_i = 0$). This means that in a system with a device with area ratio $r_a > 1$, P_f would not rise unless there is positive pressure behind the energy recovery device ($P_i > 0$), thus indicating the need for a low-pressure pump to feed seawater to it.

5.6.3.2 Area ratio $r_a < 1$

When the area ratio is less than unity, opposite trends are found as illustrated in Figure 5.8. Here, the membranes' feed pressure P_f increases with pressure drop and there is now a minimum pressure drop required for the system to

desalinate any water. Furthermore, decreasing the inlet pressure P_i now moves the curve up, and therefore it should be possible to achieve positive membranes feed pressures $P_f > 0$ at inlet pressure $P_i = 0$.

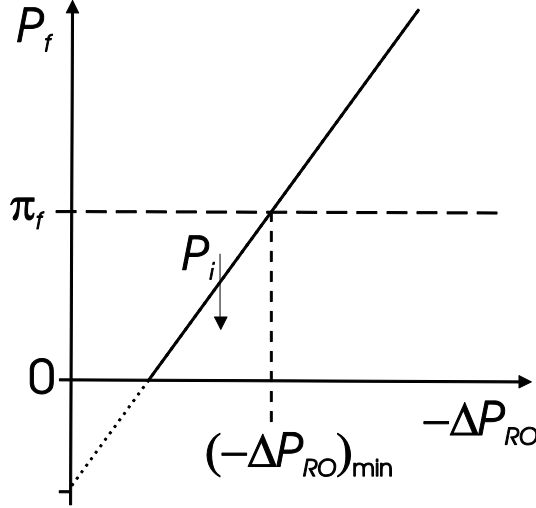


Figure 5.8 Effect of pressure drop for $r_a < 1$

5.6.3.3 Area ratio $r_a = 1$

For devices with $r_a = 1$, Equation 5.15 reduces to $P_f = 0/0$ and cannot be used to find the membranes feed pressure. Instead, going back to the more general device equations presented in previous sections, and considering that for $r_a = 1$ the flow of the high-pressure pump Q_h equals the permeate flow Q_p , a rearrangement of Equation 5.5 gives:

$$P_f = \frac{Q_h}{K_w A_m} + (\pi_{avg} - \pi_p) + P_p \quad \text{Equation 5.16}$$

Since at $r_a = 1$ all four flows in the energy recovery device are the same, this equation shows that the membranes feed pressure will rise above the osmotic pressure (i.e. desalinate water) only when the high-pressure pump is applied ($Q_h > 0$) and that the membranes feed pressure is independent of the pressure drop. It must be noted that for $r_a = 1$, the low-pressure pump will pressurise the seawater entering the system to the required level to make up for any pressure

drop in the RO membranes. It is then evident that a system with $r_a = 1$ requires both a high-pressure pump and a low-pressure pump to operate.

5.6.4 Device comparison

A summary of the main points in the discussions of the above analysis is presented in Table 5.2, and highlights the main differences and similarities between the devices.

Table 5.2 Comparison of the pressure intensifiers

	$r_a < 1$	$r_a = 1$	$r_a > 1$
Positive displacement	✓	✓	✓
Requires a high-pressure pump	✓	✓	
Requires a low-pressure feed pump		✓	✓
Possibility of varying RR through the high-pressure pump	✓	✓	✓
Possibility of varying RR through the low-pressure pump		✓	✓
Fixed RR with only one motorised pump			✓
Auto-adjusts pressure to maintain a fixed RR			✓
Pressure intensification achieved by piston area differential	✓		
Pressure intensification by energy transfer from input seawater		✓	✓
Pressure drop in the membranes determines their feed pressure	✓		✓
Requires a minimum pressure drop in the membranes	✓		
Has a maximum allowed pressure drop to desalinate water			✓
Self-regulating back pressure (no throttling valve required)	✓	✓	✓

5.7 Area ratio of the new device

The analysis above suggested that at $r_a < 1$ the energy recovery device would be capable of working at atmospheric inlet pressure ($P_i = 0$) while devices with $r_a \geq 1$ require positive pressure at the inlet.

To explore this in more detail, rearranging Equation 5.14 provides an expression for the inlet pressure P_i as a function of r_a (Equation 5.17), which is plotted in Figure 5.9. In this figure, an atmospheric discharge of the exhaust ($P_e = 0$) and perfect membranes ($\Delta P_{RO} = 0$) are considered.

$$P_i = \frac{P_f(r_a - 1) - \Delta P_{RO} + P_e}{r_a}$$

Equation 5.17

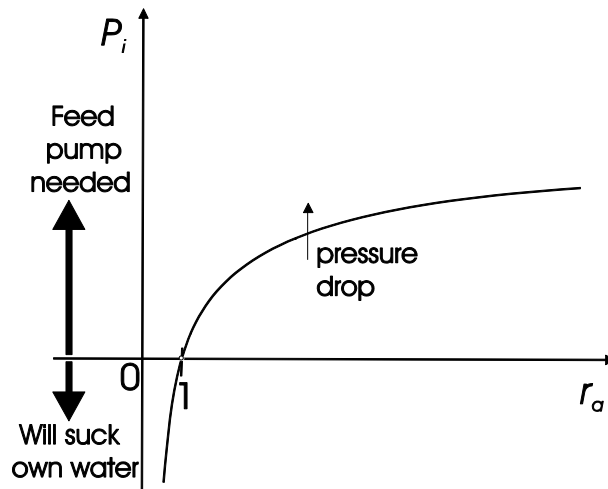


Figure 5.9 Inlet pressure versus area ratio for $\Delta P_{RO} = 0$

It is evident in the figure that devices with $r_a > 1$ require positive pressure behind them, i.e., a feed pump. The figure also shows that just flooding the inlet port should be enough for devices with $r_a = 1$. However, working with real membranes with a measurable pressure drop moves the curve upwards, resulting in devices with $r_a = 1$ also requiring a feed pump in practice.

Nevertheless, even when working with real membranes, negative inlet pressures are still possible for devices with $r_a < 1$. This makes such devices worth investigating further as it appears that they would be capable of sucking their own seawater in, making the low-pressure feed pump redundant. The elimination of this pump would result in a simplified system configuration with only one high-pressure motorised pump as illustrated in Figure 5.10. This would also address the poor efficiencies of the low-pressure pump observed in the systems using Clark pumps reviewed in previous chapters.

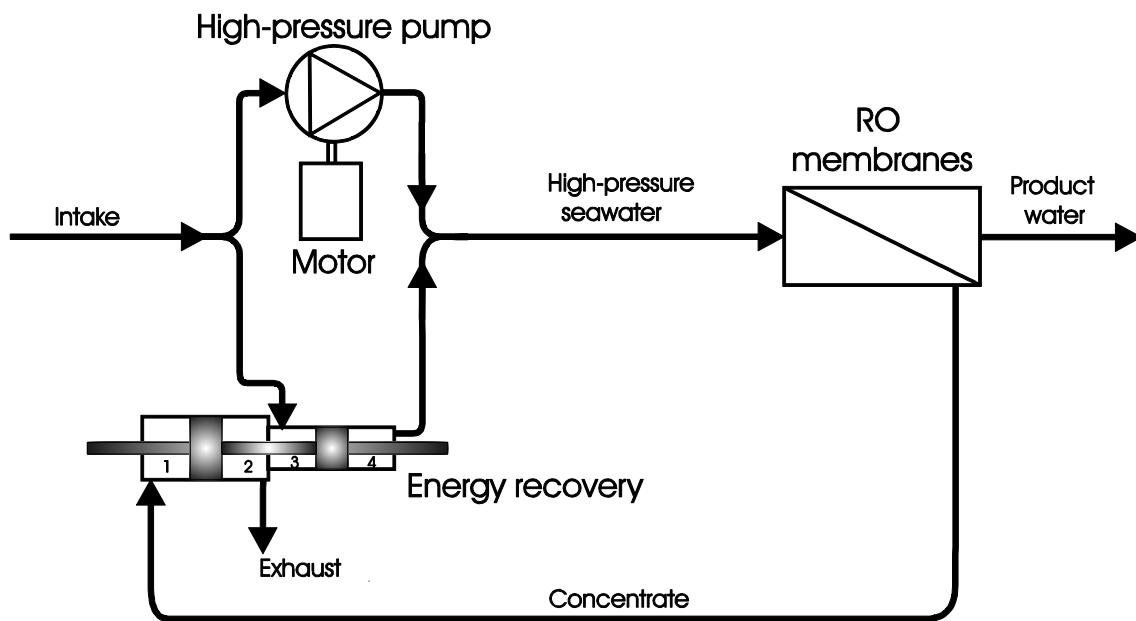


Figure 5.10 New system configuration

5.8 System operation description

For the example in Figure 5.10, seawater flows in from the left through a common intake, which is split between the energy recovery device and the high-pressure pump. They operate in parallel, each pressurising a portion of the flow; their high-pressure outputs are combined prior to entering the RO membranes. After these, the concentrate flows into the energy recovery device.

In the energy recovery device, the concentrate is the energy input; it flows into chamber 1, displacing the pistons and rod to the right. Most of the energy in the

concentrate is used to pressurise the seawater in chamber 4; the rest of the energy is used to draw seawater into chamber 3, and to push the exhaust from the previous stroke out of chamber 2.

At the end of the stroke, a reciprocation arrangement (not shown in the figure) would swap over the connections, directing the concentrate to chamber 2 and allowing the new exhaust to flow out of chamber 1 so that the pistons and rod reverse direction. The reciprocation arrangement would also swap over the roles of chambers 3 and 4.

After the findings of the theoretical analysis presented in this chapter, computer simulations were used to study devices with $r_a < 1$ within a system in more detail. This is the subject of the following chapter. If realised in practice, this energy recovery device and system configuration would be remarkable achievements since their implementation has not been found reported elsewhere.

Chapter 6 System modelling and performance predictions

6.1 Simulink model

In the analysis of the previous chapter, it was stated that an iterative approach is required to solve the system and device equations simultaneously given the interdependencies of all system components. MATLAB-Simulink has been used for this purpose. Its graphical approach simplifies the programming of the system model and makes the relationships between components easier to identify and portray.

Thus, a Simulink model of a system using an energy recovery device with $r_a < 1$ was built following the modelling philosophy of Murray Thomson and Marcos Miranda (Miranda, 2003; Thomson, 2003). The high-level structure of the model is presented in Figure 6.1.

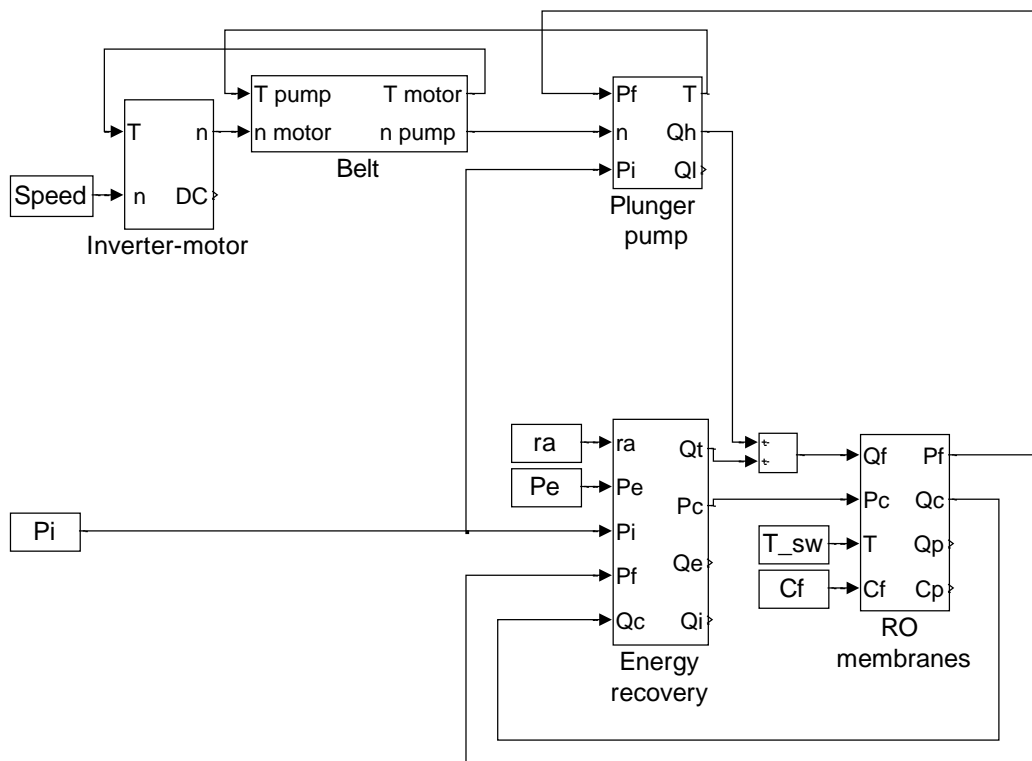


Figure 6.1 Simulink high-level structure of the system model

For simplicity, the losses in the belt and energy recovery device are not modelled. Testing of the Clark pump (Thomson, 2003), which operates on similar principles to the proposed device, showed efficiencies of up to 97%. This suggests that efficiencies in excess of 90% for a commercial product of the proposed energy recovery device could be expected, and therefore the small losses in the device would not change the modelling results significantly.

6.2 Effect of piston area ratio

The model presented above requires some input constants. These include the exhaust discharge pressure (P_e), the seawater temperature (T_{sw}), the inlet pressure for the energy recovery device (P_i) and the salinity of the seawater feed (C_f). Their values are presented in Table 6.1.

Table 6.1 Model constants

Model input	Description	Value
P_e	Exhaust pressure	0 bar
T_{sw}	Seawater temperature	25 °C
P_i	Inlet pressure	-0.5 bar
C_f	Seawater salinity	32 000 mg/L

The model was run over a range of piston area ratios for several motor speeds. The influence of the piston area ratio on key operational variables is presented in Figure 6.2. Typical ranges of these variables for 4 inch by 40 inch (i.e., 0.1 m in diameter by 1 m in length) seawater membranes are presented in Table 6.2. These correspond to the dashed lines in Figure 6.2.

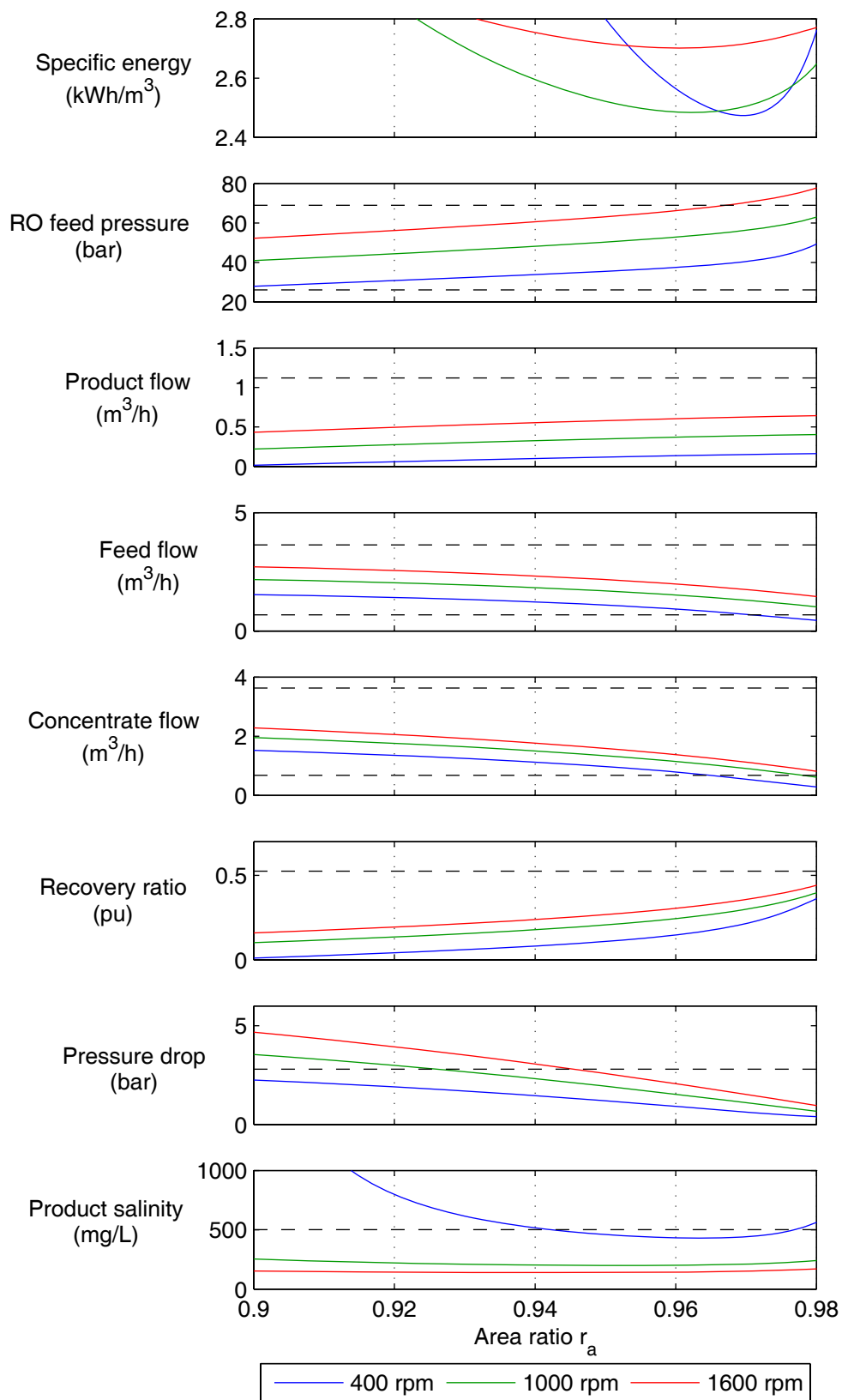


Figure 6.2 Effect of the area ratio at various motor speeds

Table 6.2 Typical values

Parameter	Typical value		Reason
RO feed pressure	Maximum	69 bar	Rating of the pressure vessels (Phoenix Vessels Ltd, 2000)
	Minimum	26 bar	Overcome the osmotic pressure of the feed
Product flow (per element)	Maximum	0.28 m ³ /h	Limit flux to minimise fouling (Dow, 2005)
	Minimum	--	--
RO feed flow (per element)	Maximum	3.63 m ³ /h	Limit pressure drop (Dow-ROSA, 2005)
	Minimum	0.7 m ³ /h	Ensure turbulent regime in the feed-brine channel to reduce concentration polarisation (Dow-ROSA, 2005)
Concentrate flow (per element)	Maximum	3.63 m ³ /h	Limit pressure drop (Dow-ROSA, 2005)
	Minimum	0.7 m ³ /h	Ensure turbulent regime in the feed-brine channel to reduce concentration polarisation (Dow-ROSA, 2005)
Recovery ratio (per element)	Maximum	15-17 %	Reduce risk of precipitation of sparingly soluble salts; reduce concentration polarisation; maintain sufficient net driving pressure in the membranes. (Dow Filmtec, 1998; Koch-ROPRO, 2000; Dow, 2009b)
	Minimum	--	--
Pressure drop (per element)	Maximum	0.7 bar	Avoid membrane damage (e.g., telescoping) (Koch, 2000)
	Minimum	--	--
Product salinity	Maximum	500 mg/L	Ensure acceptable water taste (See section 2.1.4)
	Minimum	--	--

6.3 Selection

The specification of a piston area ratio was based on specific energy consumption.

Looking at the graph of specific energy in Figure 6.2 (top), the curves present minima between $r_a = 0.96$ and $r_a = 0.97$ for all three motor speeds. While at

$r_a = 0.96$ all parameters are within the recommended ranges in Table 6.2, at $r_a = 0.97$ the membranes' feed pressure is above the recommended maximum at 1600 rpm, and the concentrate flow is below the lower threshold at 400 rpm. Thus, $r_a = 0.96$ was chosen for the energy recovery device.

6.4 Performance predictions

6.4.1 Area ratio $r_a = 0.96$

Having chosen the area ratio, the model was then run over a wide range of input power (nearly 1:8 minimum-to-maximum ratio) to explore the performance of the device in a system. The results are presented in Figure 6.3, which includes the same key parameters that were presented in Figure 6.2 but now as a function of electrical input power. As before, the dashed lines represent the recommended limits presented in Table 6.2.

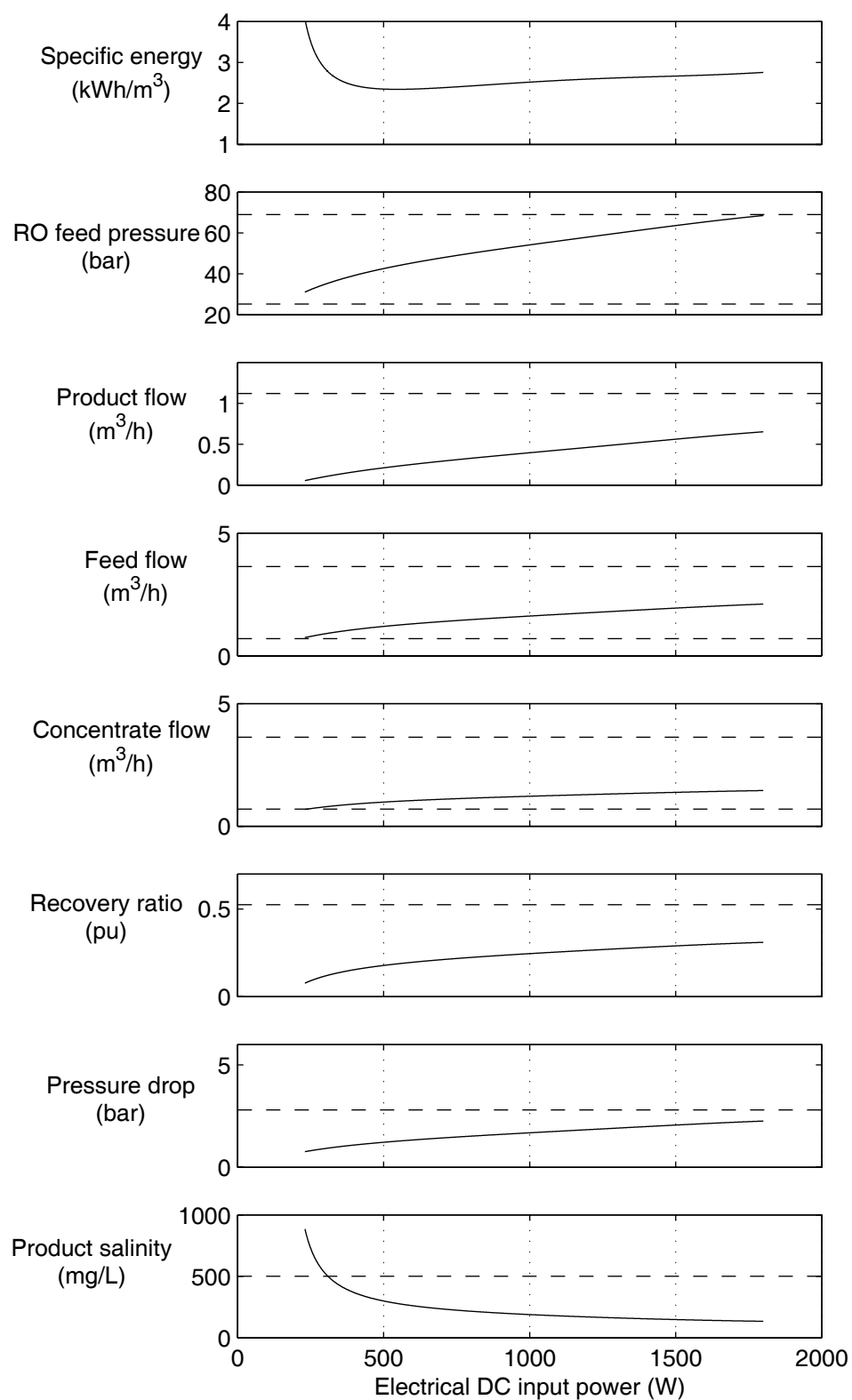


Figure 6.3 Operation with $r_a = 0.96$

Most parameters in this figure are within the recommended ranges. The only exception is the product salinity, which reaches values above its maximum recommended value (500 mg/L) but only at very low powers. At such levels, the membranes only produce a small water flow, while the salt passage is not affected as much, thus increasing the salinity of the product. To deal with this, the user could choose to either discard the portion of the product that falls outside of set quality ranges or, since this only happens at low product flow rates, allow it to mix with the rest of the product in a tank, where the overall concentration will not be overly affected.

The results in Figure 6.3 also show that the expected specific energy consumption of the system is very good, with a minimum just under 2.4 kWh/m³, and more importantly, that it remains below 3 kWh/m³ over a very wide power range. Again, it is only at very low powers that the efficiency drops, which is in turn due to the poorer efficiencies of the inverter and motor at low speeds as well as those of the membranes at pressures just above the osmotic pressure of the seawater, i.e, very low recovery ratios and high feed volumes.

6.4.2 Energy flows at $r_a = 0.96$

The curves in Figure 6.3 indicate a very good performance throughout the input power range. Table 6.3 shows the model results for one point of the simulations presented above (1196 W of input power, about midrange in Figure 6.3). This corresponds to a specific energy of 2.59 kWh/m³. Figure 6.4 illustrates the breakdown of the energy flows that make up this value.

Table 6.3 Model predictions with $r_a = 0.96$ at 1196 W of input power

SEC (kWh/m ³)	P_f (bar)	Q_p (m ³ /h)	Q_f (m ³ /h)	Q_c (m ³ /h)	RR (%)	ΔP_{RO} (bar)	C_p (mg/L)
2.59	58	0.46	1.75	1.29	26	1.8	170

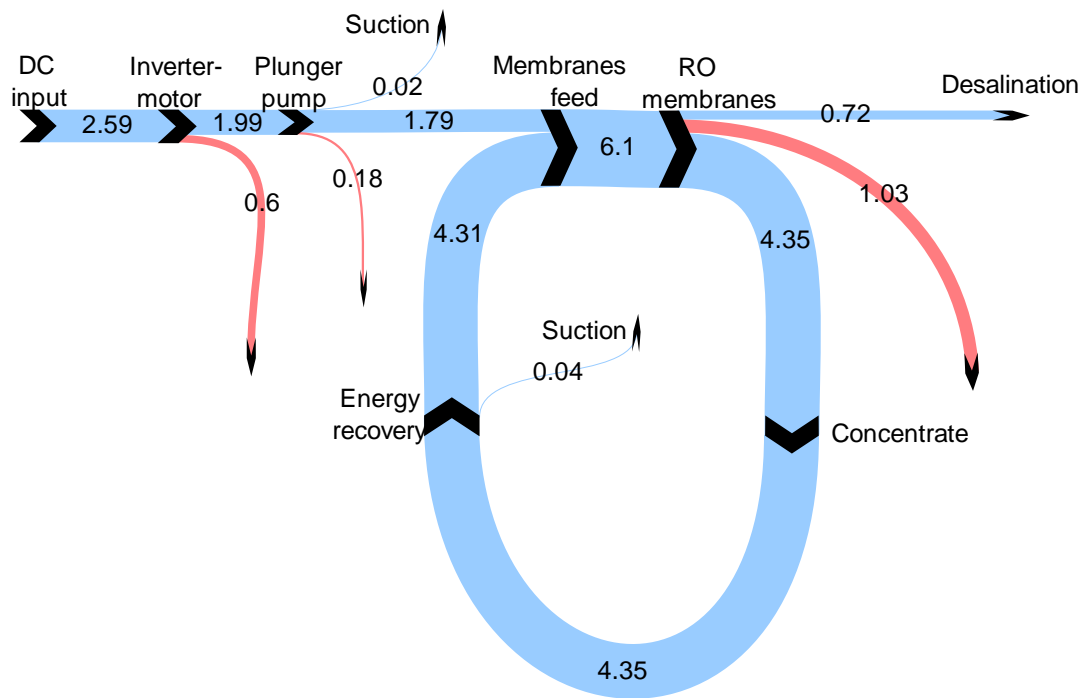


Figure 6.4 Specific energy flows at 1196 W input power.
Values in kWh/m³

Starting from the left in the Sankey diagram, 2.59 kWh/m³ of electric energy flow from the DC input to the inverter-motor. The pink arrow pointing down represents losses. The 1.99 kWh/m³ is the shaft power transferred from the motor to the high-pressure plunger pump.

In the plunger pump, most of the energy is used to pressurise seawater that goes to the membranes' feed (1.79 kWh/m³). The upward-pointing arrow labelled "Suction" corresponds to the useful work done by the pump to suck in seawater (0.02 kWh/m³) in the absence of a low-pressure pump. It is evident that this is only a very small fraction.

At the membranes feed, the energy in the high-pressure output of the plunger pump and the energy recovered from the concentrate are combined and then flow into the RO membranes. Some of this energy (0.72 kWh/m³) is used for the actual desalination process but more than two-thirds of the membranes' input ends up in the concentrate stream and flows into the energy recovery unit. The

pink arrow corresponds to viscous losses in the membranes (pressure drop in the feed-brine channel and through-flow losses).

In the energy recovery device, most of the concentrate energy is used to pressurise seawater in parallel with the high-pressure pump (see Figure 5.10). As mentioned above, the seawater pressurised in the energy recovery unit combines with the plunger pump output at the membranes' feed closing the energy recovery loop. As with the high-pressure pump, the energy recovery device also draws its own seawater in, which is represented by the upwards "Suction" arrow.

6.4.3 Comparison to the basic Clark pump

In order to compare with the Sankey diagram of the basic Clark pump configuration presented earlier in section 3.3, the model was adjusted to run at a recovery ratio of 10% and at the feed water salinity used by Spectra Watermakers.

Additionally, the Simulink model of the motor used in the simulations so far corresponds to a 3 kW motor. To obtain the 10% recovery ratio required for the comparison, the motor had to operate at about 290 W and was very inefficient due to its very low loading. Comparing the results obtained with this motor to those obtained with the Clark pump system, which has a motor-pump unit optimised for the application, would yield a biased outcome. Thus, for the purpose of this comparison only, it was necessary to change the motor in the model for a smaller one better suited for the job. With the new motor, the inverter-motor-pump efficiency together is of 59% and the corresponding Sankey diagram is presented in Figure 6.5.

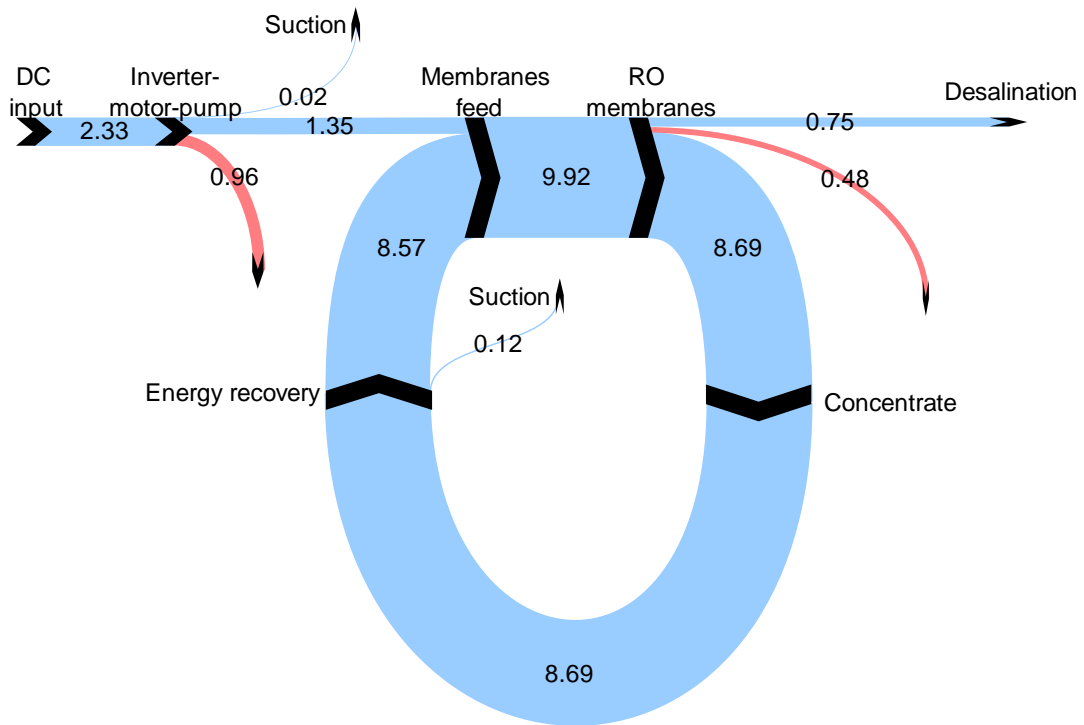


Figure 6.5 Simulation results of operation at 10% recovery ratio.
Values in kWh/m³

Comparing Figure 6.5 with the earlier Figure 3.3 (page 57), it is clear that both systems have very good energy recovery. Nevertheless, the input in Figure 6.5 is considerably smaller. This confirms that the proposed energy recovery device and system configuration make possible the use of a more efficient pump with the corresponding reduction of overall energy consumption (see section 4.2).

6.4.4 Area ratio $r_a = 0.90$

For practical reasons that will be explained later in section 7.2, it was necessary to compromise on the area ratio of the energy recovery device and use 0.90 instead of 0.96 as originally specified. Consequently, new simulations were performed to investigate the effects that this would have on the performance of the device. The results are presented in Figure 6.6 (red curve). This figure also includes the results obtained previously with $r_a = 0.96$ for reference (blue curve). As before, the dashed lines in the figure correspond to the recommended values in Table 6.2.

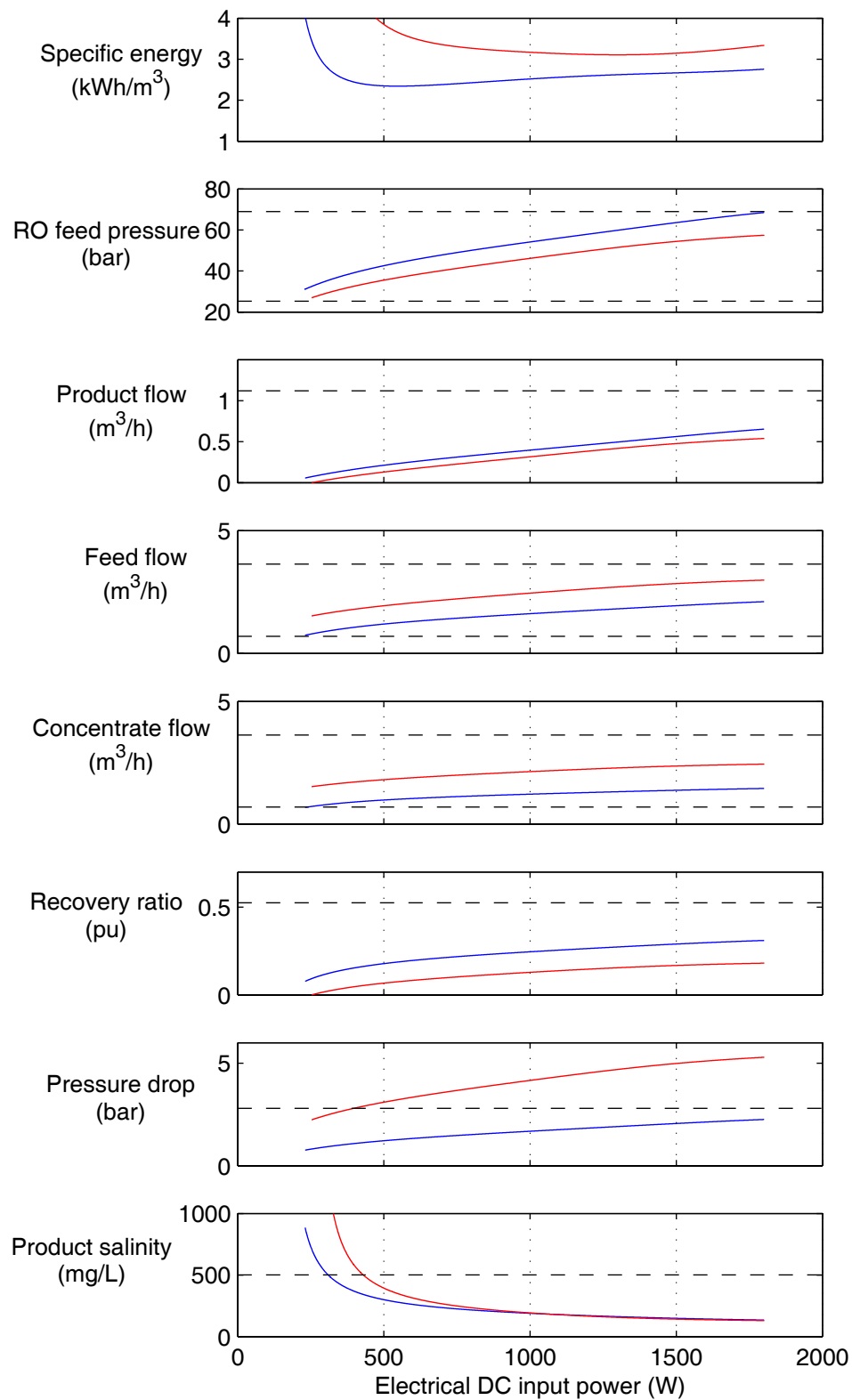


Figure 6.6 Operation with $r_a = 0.90$ (red) and $r_a = 0.96$ (blue)

It is clear that the system could also operate usefully with an area ratio of $r_a = 0.90$. However, it is also evident in the figure (top graph) that going from $r_a = 0.96$ to $r_a = 0.90$ resulted in a considerable increase in specific energy consumption. In addition, this has also caused a considerable increase in the pressure drop, which now falls above the recommended maximum value. This is a consequence of the increased feed flow. The relationship between area ratio and feed flow is explained below.

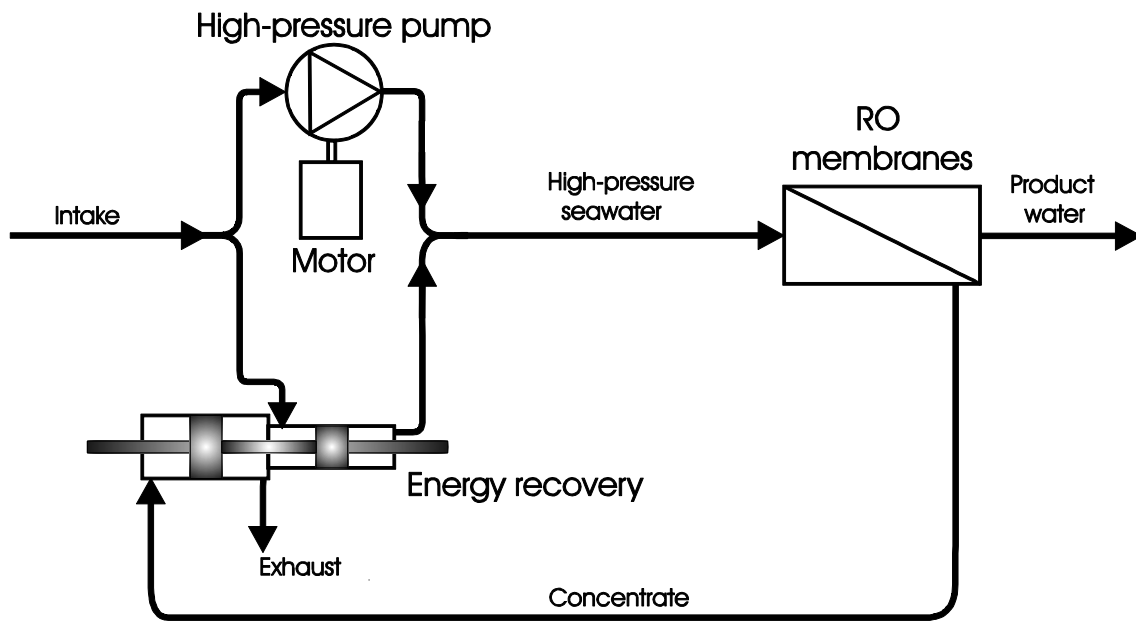


Figure 6.7 The proposed device and system configuration

In the proposed system (Figure 6.7), a reduction in the area ratio of the energy recovery device from 0.96 to 0.90 means that the concentrate flow would be greater in relation to the seawater flow pressurised in the device. To understand its effects, this can be seen as an increase in the area of the piston in the bigger cylinder that handles the concentrate and exhaust, which results in an increased concentrate flow. To maintain the same seawater pressure, the force on the small piston must remain the same and therefore, the concentrate pressure is lowered as a result of the increased concentrate piston area. The reduced pressure also reduces the water production and results in an increase in the total RO membranes feed flow. The additional flow comes from the high-

pressure pump which for the same power can now pump more water at the reduced pressure. The increased feed flow results in higher pressure drops in the membranes and the reduced product flows cause higher specific energy consumption. All these trends are observed in Figure 6.6.

6.4.5 Energy flows at $r_a = 0.90$

The model predictions for the same input power as before (1196 W) for the area ratio $r_a = 0.90$ are presented in Table 6.4. This table also includes the predictions at $r_a = 0.96$ shown previously.

Table 6.4 Model predictions with $r_a = 0.90$ and $r_a = 0.96$ at 1196 W of input power

r_a (pu)	SEC (kWh/m ³)	P_f (bar)	Q_p (m ³ /h)	Q_f (m ³ /h)	Q_c (m ³ /h)	RR (%)	ΔP_{RO} (bar)	C_p (mg/L)
0.90	3.11	50	0.38	2.62	2.24	15	4.5	166
0.96	2.59	58	0.46	1.75	1.29	26	1.8	170

The table shows that for the same power, the system with $r_a = 0.90$ operates at lower pressure and produces less water. However, the pressure drop is significantly higher because of the increased feed and concentrate flows. Overall, this results in an energy consumption of 3.11 kWh/m³, which represents a 20% increase over the consumption of the system with $r_a = 0.96$ discussed earlier. Figure 6.8 illustrates the energy flows within the system at $r_a = 0.90$ and 1196 W of electrical input power.

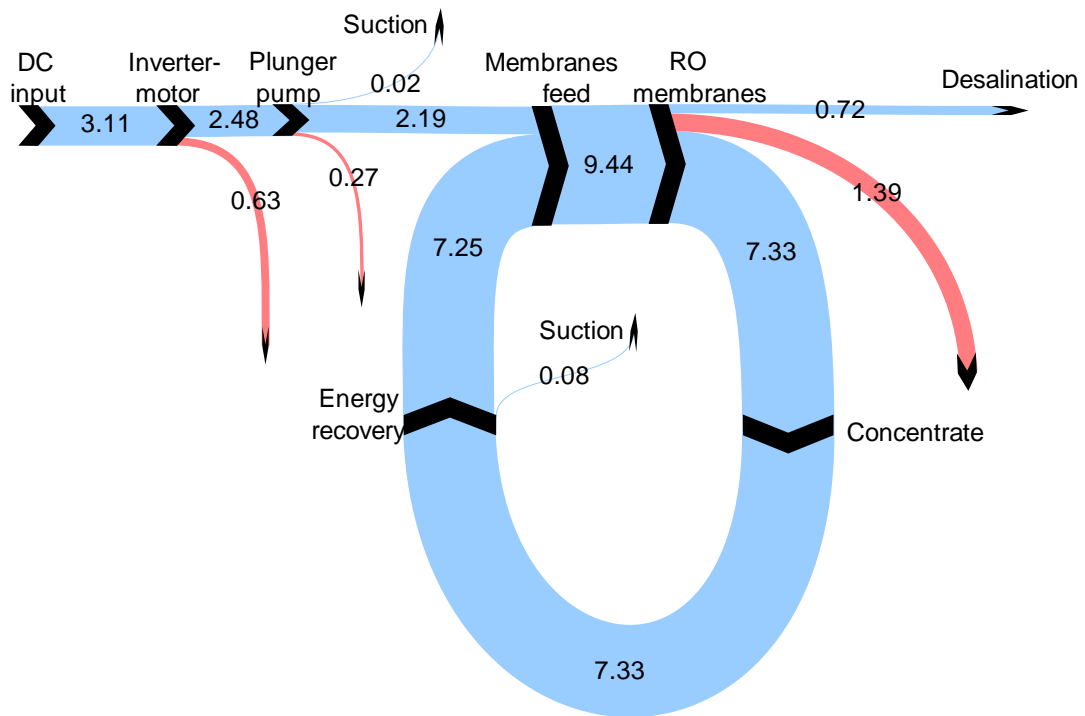


Figure 6.8 Energy flows at $r_a = 0.90$ and 1196 W.
Values in kWh/m³

Comparing the Sankey diagram in Figure 6.8 with the diagram corresponding to $r_a = 0.96$ presented in Figure 6.4 (page 92), similar patterns are found. However, it is evident that the reduction in area ratio resulted in a considerable increase of the energy flows in the energy recovery loop as well as in an increase in membrane losses. Both these results are because of the larger feed and concentrate flows, which now carry more energy and increased the pressure drop in the membranes as well as the losses in the motor and high-pressure pump.

In conclusion, while it is expected that a device with area ratio $r_a = 0.90$ would not operate as efficiently as one with $r_a = 0.96$, it has been shown that it could operate usefully over a wide range of input power and that reasonable results could be expected if a prototype was built. The following chapter describes the practical implementation of the proposed energy recovery device.

Chapter 7 Prototype implementation

The analysis in Chapter 5 and the simulations in Chapter 6 both give good indications that a pressure intensifier with area ratio $r_a < 1$ has the potential to reduce the overall energy consumption of a system and therefore is worthwhile building. This chapter describes the practical implementation of the intensifier concept in a first prototype.

7.1 New chamber arrangement

Once the area ratio had been specified at $r_a = 0.96$, more thought was given to practical considerations and two practical issues were identified with the design in Figure 4.2 c) (page 64):

- First, the asymmetric design would likely make the prototype more expensive to build.
- Second, having the rod protruding from the ends of the device could result in external leaks.

This suggested that a different arrangement of the chambers in the device could be beneficial and it was realised that the concept could be implemented with the chamber layout presented in Figure 7.1 (bottom). This new arrangement is symmetrical and eliminates the protruding rod.

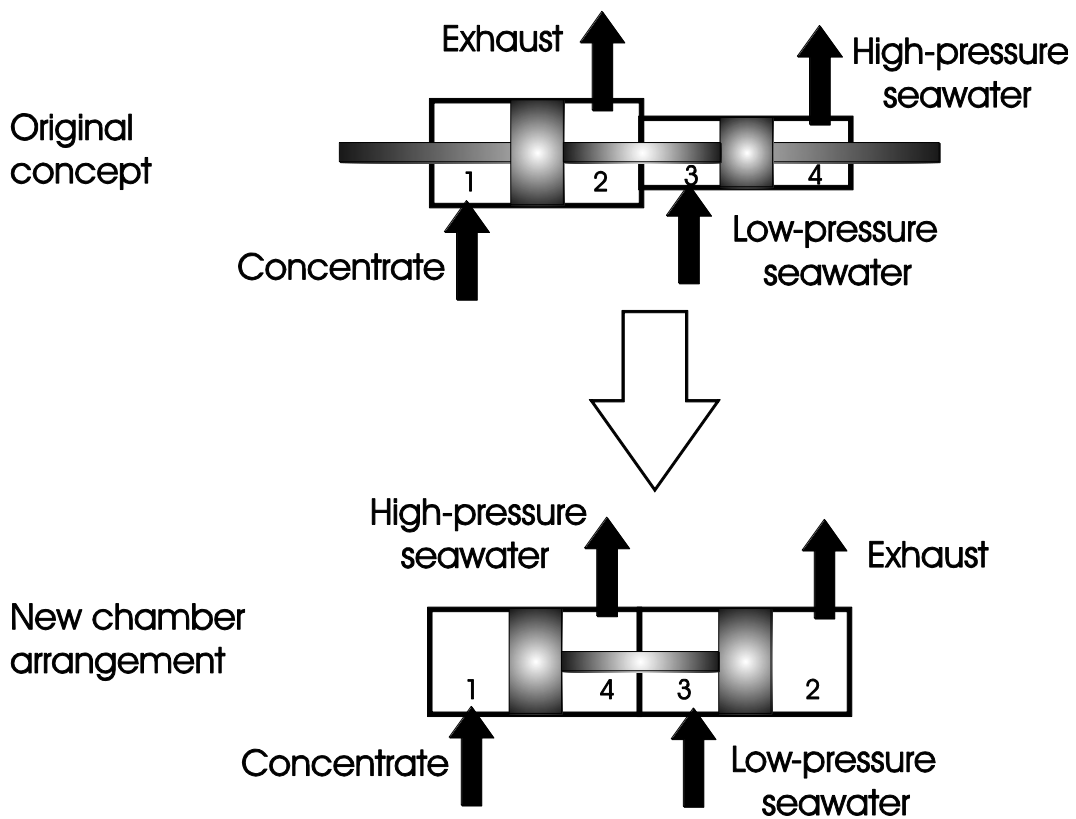


Figure 7.1 New chamber arrangement

With this layout, the flows in the small cylinder of the original layout (chambers 3 and 4 in Figure 7.1 (top)) would occupy the smaller middle chambers in the new arrangement (Figure 7.1 bottom), while the flows originally in the big cylinder (chambers 1 and 2) would now be in the two larger outer chambers of the new layout.

It is important to realise that, while the new arrangement presented in Figure 7.1 resembles very much a Clark pump, the layout of the flows in the two devices are not the same (see Figure 7.2). In consequence, the operation modes of the two concepts are fundamentally different. Nevertheless, the mechanical similarity of the hardware indicated that the new concept could be implemented using the housing of CREST's existing Clark pump by reversing the roles of the two pairs of chambers. This approach was followed.

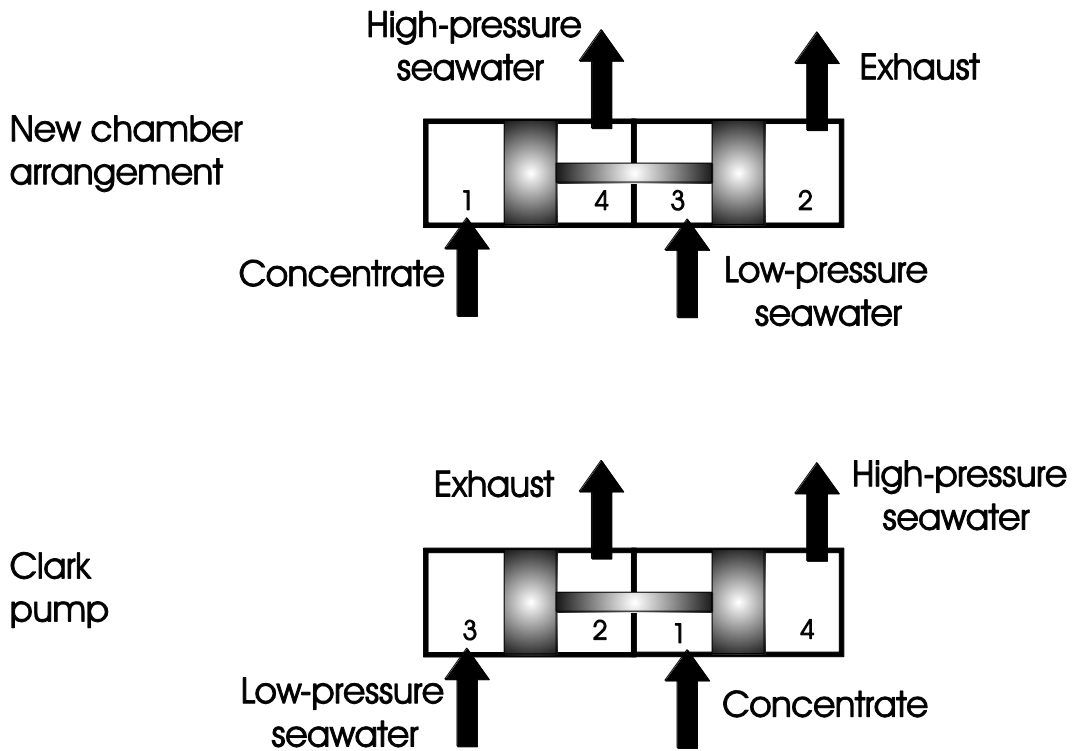


Figure 7.2 Comparison of the new arrangement and the Clark pump

7.2 New area ratio

The use of the Clark pump housing had the advantage of allowing all the work to be completed in-house, but it also meant that the area ratio was predefined at $r_a = 0.90$, instead of the $r_a = 0.96$ originally sought. As discussed in section 6.4.4, a device with $r_a = 0.90$ is also feasible and would suffice to prove the new energy recovery concept but its performance is not expected to be as efficient as that of a device with an area ratio of 0.96.

7.3 Internal flows in the standard Clark pump

To assess the extent to which the hardware of the Clark pump could be used in the implementation of the new concept, the detailed operation of the pump was investigated. Figure 7.3 presents a schematic of a Clark pump.

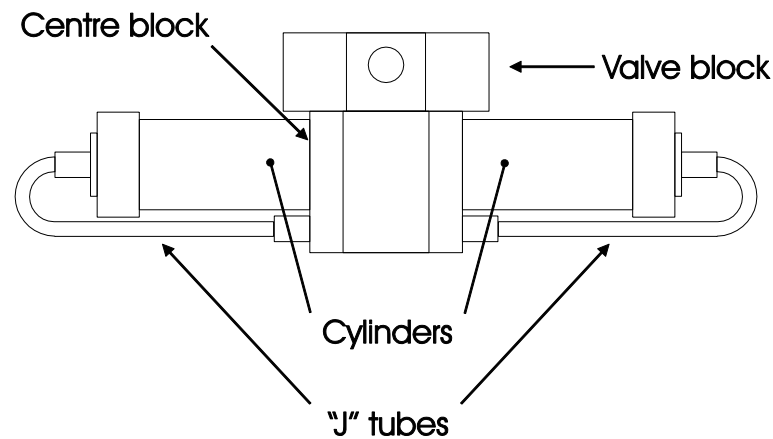


Figure 7.3 Schematic of a Clark pump

Externally, the Clark pump consists of an assembly of a valve block, a centre block, the cylinders that contain the pistons and the “J” tubes. A spool valve to direct the concentrate is located in the valve block and an arrangement of check valves that direct the seawater is located at the bottom of the centre block. The “J” tubes connect the check valves with the cylinders.

The internal flows in a Clark pump are presented in Figure 7.4. The figure shows a frontal view of the Clark pump similar to Figure 7.3, but with the valve and centre block separated to illustrate the flows between the two blocks; in a real pump the two blocks are attached to each other. Figure 7.4 also shows the spool valve, the pilot valve that actuates it, the check valves and the ports on the contacting surfaces between the valve block and centre block. In the figure, these surfaces would be perpendicular to the plane of the page (and hence not possible to see them) but are depicted parallel to the page for clarity. All flows are colour coded according to the legend.

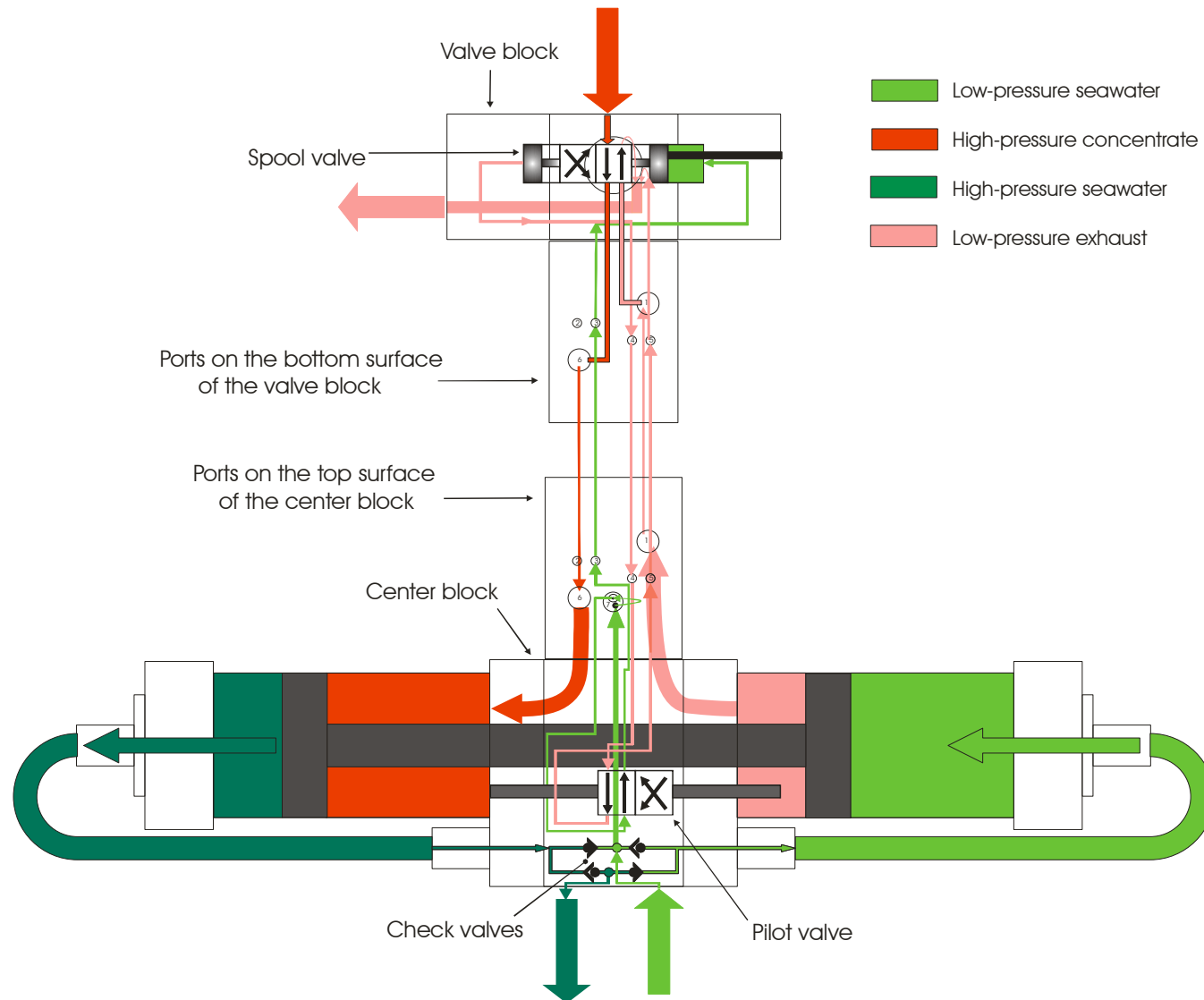


Figure 7.4 Reciprocation valve gear and internal flows in a Clark pump

In the figure, the concentrate flows into the Clark pump at the top (red arrow). It then goes through the spool valve, out of the valve block, into the centre block and finally into the inner (rod-side) chamber of the left cylinder where it pushes the piston to the left.

At the same time, low-pressure seawater flows into the Clark pump at the bottom (pale green arrow). After the check valves, the seawater flows through the “J” tube on the right and into the outer chamber of the right cylinder pushing this piston and hence moving the whole rod-pistons assembly to the left. A very small portion of the seawater is used to actuate the spool valve. This small flow is taken before the check valves. The pilot valve in the centre block alternates this flow to either side of the spool valve.

The joint action of the concentrate and the low-pressure seawater pressurise the seawater in the chamber adjacent to the concentrate (dark green) above the pressure of the concentrate. This goes through the “J” tube as well as the check valves to finally flow out of the pump.

The exhaust concentrate from the previous stroke (pink colour) flows out of the inner chamber of the right cylinder through the centre block, into the valve block and the spool valve where it is directed out of the pump.

Towards the end of the stroke, the piston on the right-hand cylinder pushes a pin that drives the pilot valve, re-routing the control flow. This flow kept the spool valve pushed to the left during the stroke and now pushes it to the right, swapping over the exhaust and the concentrate in the middle chambers of the pump and now pressurising the seawater in the chamber on the far right. This affects the check valves, which now direct the low-pressure seawater to the outer chamber of the left cylinder and the pistons-rod assembly starts moving to the right to start a new stroke repeating the process.

Once the detailed operation of the Clark pump was understood, the work proceeded to modify it to give it the capabilities of the new energy recovery concept.

7.4 Modifying the Clark pump

7.4.1 Main flows

In order to use the hardware of the Clark pump, the first step was to redirect the flows to the appropriate chambers. In a standard Clark pump, the concentrate and the exhaust alternate between the middle chambers; in the new arrangement these flows occupy the outer chambers (see Figure 7.2). Similarly, the seawater, both low and high pressure, occupies the outer chambers in a Clark pump while in the new arrangement it occupies the middle chambers.

At first sight, simply reconnecting the four flows would suffice to reverse the roles of the two pairs of chambers. However, this would not work because, in the absence of a low-pressure pump, the concentrate would flow around the check valves and out of the pump without doing any useful work (the pistons would not move). In addition, the high-pressure seawater chamber of the re-plumbed arrangement would be connected to the spool valve and cause it to change over continuously with no movement of the pistons. As a result, the cylinders housing the pistons could be used but new connections were required to direct the flows to the appropriate chambers.

7.4.2 Valve gear

A second issue with using the Clark pump housing was how to make the pistons and rod reverse direction at the end of the stroke if new connections were used. As mentioned previously, in the Clark pump, the spool valve swaps round the flows in the middle two chambers at the end of each stroke (Figure 7.5) while an arrangement of check valves alternates the other two flows between the outer chambers. This reciprocation valve gear relies on specific pressures corresponding to particular ports in the Clark pump. Having new

connections for the main flows meant that an alternative means of reciprocation would be required.

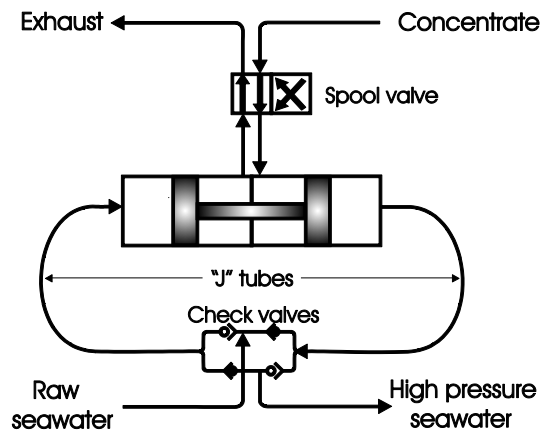


Figure 7.5 Reciprocation valve gear in the Clark pump

Electronic valves would be suitable for this purpose and were initially considered but they are very expensive. This led to consideration of also using the Clark pump's valve gear in addition to the pistons' housing.

7.4.3 Practical modifications

In order to use a Clark pump's housing and valve gear for the implementation of the new energy recovery concept, the valve gear needed to be reconfigured as per Figure 7.6 (left). Comparing this with the layout of a Clark pump in Figure 7.6 (right), it is evident that the flows must be reconnected internally after the spool and check valves but before the cylinders. Since the valve gear is located within the pump blocks, this would mean that the reciprocation valve gear had to be effectively isolated from the cylinders while still keeping it within their respective blocks. On the other hand, this would also mean that the external port connections could be maintained as in the standard Clark pump.

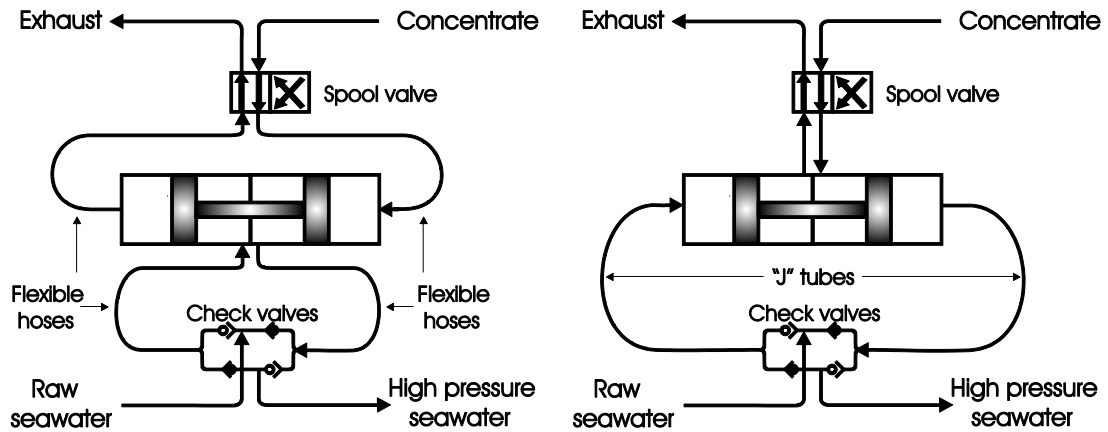


Figure 7.6 Reciprocation valve gear reconfiguration.
Left: modified Clark pump; right: standard Clark pump

Fortunately, the valve and centre blocks could be and were detached (Spectra Watermakers, 2005) and the stainless steel “J” tubes removed. Then, flexible high-pressure hoses were used to realise the new connections between the valve block and the outer chambers of the cylinders as well as between the check valves and the middle chambers as per Figure 7.6 (left). Engineering plastic blocks were machined and fixed to the valve block and to the main body of the pump to take the fittings for the new connections; these are the white blocks in the photographs in Figure 7.7.



Figure 7.7 Separation of the valve block

The modified Clark pump had now the main flows redirected to the appropriate chambers.

7.4.4 Control flows

While it was required to redirect the main flows in the modified Clark pump, it was also required to keep the connections of the control flows that operate the spool valve in the valve block as they were in the original Clark pump. Because of the separation of the valve block to redirect the main flows, nylon tubes were used to reconnect the small control flows between the valve block and the centre block. These connections were also done by means of the plastic blocks used before for the redirection of the main flows. A photograph of the modified Clark pump is presented in Figure 7.8. The stainless braided hoses carry the main flows and the white plastic tubes carry the control flows.

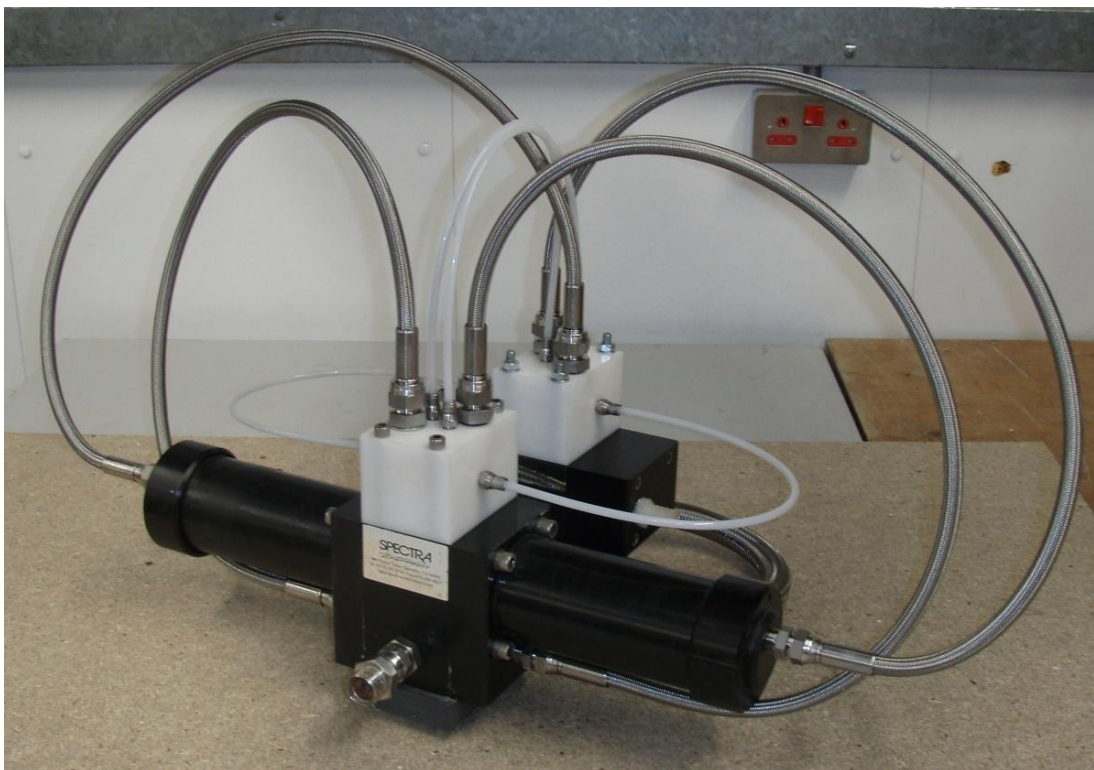


Figure 7.8 The modified Clark pump

As mentioned before, in the standard Clark pump the control flow driving the spool valve is taken from the main seawater input, which is at about 5 bar. This pressure is supplied by the low-pressure pump (Figure 3.2). However, with the elimination of the low-pressure pump, the seawater feed was then at negative pressure in the modified Clark pump and could not operate the spool valve. A new way of operating it was required.

One option was to take a small flow from the concentrate to operate the spool valve. To implement this, a pressure reducer would have to be used given that the pressure of the concentrate is very high and the spool valve was not intended to operate with such high pressure and could be damaged. Another option was the use of mains water, which is supplied at low pressure (3-5 bar). The latter was chosen. However, using an external flow of mains water to drive the valve in the modified Clark pump required an additional connection as well as sealing some of the internal ducts in the body of the pump that previously carried the control flow. The new connection was also added in the plastic block fitted to the main body of the pump.

7.5 Preliminary tests

Preliminary runs to test the modified Clark pump were carried out using tap water at low pressure and an arrangement of needle valves to simulate the RO membranes (Figure 7.9). In this arrangement, the valve V_p simulates the pressure difference across the membrane, while valve V_c simulates the pressure drop in the feed-brine channel. This valve arrangement enabled control over the simulated concentrate and permeate flows.

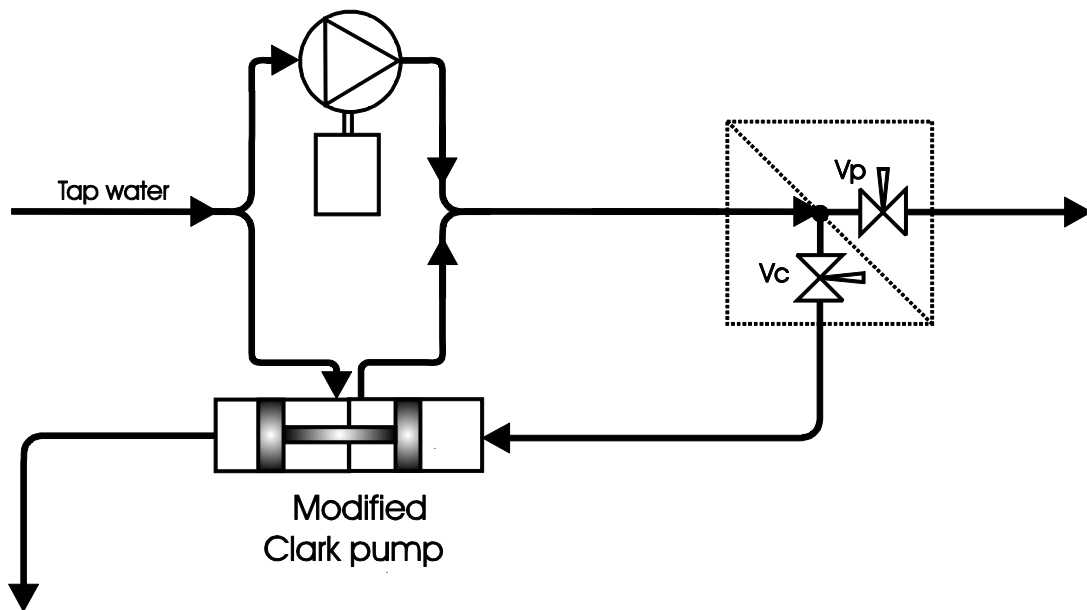


Figure 7.9 Arrangement for preliminary testing

During the first batch of preliminary tests no pressure intensification was achieved and erratic flows were observed. Detailed study of the instantaneous flows in and out of the various chambers indicated that the pistons were not attached to the rod. In the conventional operation of the standard Clark pump the pressures are always such that the pistons are pushed together, naturally staying in contact with the rod despite not being fixed to it.

In the modified Clark pump this was no longer the case and the pistons and rod were moving independently. This was a consequence of the high pressure now being in an inner chamber, where the pressurised water could get between the rod and the high-pressure piston (Figure 7.10), acting on them in opposite directions. With this separation, the effective area on both sides of the high-pressure piston was the same and so were the pressures, i.e., no pressure intensification took place.

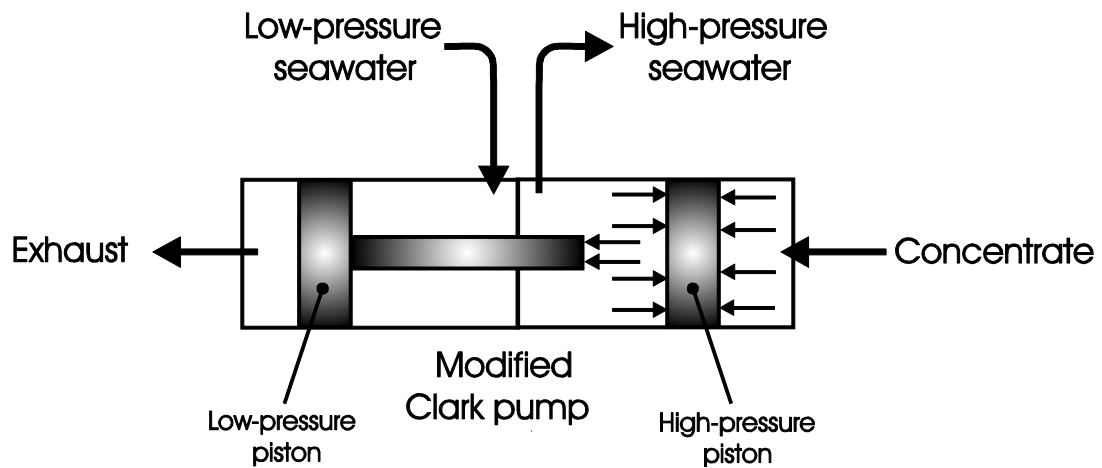


Figure 7.10 Independent movement of the rod and high-pressure piston

To solve the problem, a new rod was manufactured and the pistons were fixed onto it as shown in Figure 7.11. With the new assembly, the modified Clark pump was capable of pressure intensification and the erratic flows disappeared. The modified Clark pump was then connected to real RO membranes and was tested as described in the following chapter.

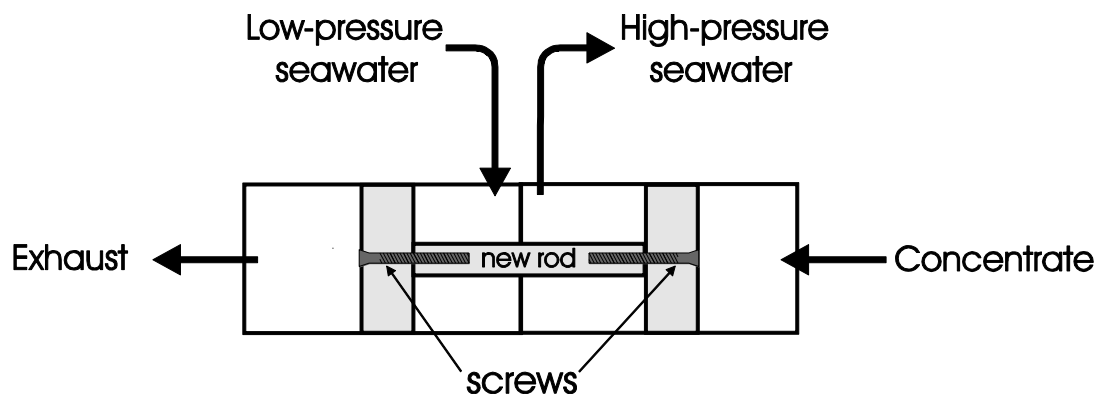


Figure 7.11 Attaching the pistons and new rod

7.6 The pressure exchanger-intensifier

In 2007, contact was established with Dr Matt Folley from Queen's University Belfast, who was also working at the time on the simulation of a very similar

idea for an energy recovery device for wave-powered seawater reverse osmosis (Folley et al., 2008). Folley et al. refer to their energy recovery device concept as a “pressure exchanger-intensifier” (PEI), which is essentially the same as the modified Clark pump in a very similar system configuration.

In their approach, Folley et al. propose the use of pressurised seawater from a wave energy converter directly in reverse osmosis. This is more efficient than generating electricity to run a motor to drive the high-pressure pump of a RO system, but eliminates the possibility of using batteries so as to operate at a constant point. For this reason Folley et al. looked at the PEI with the objective of accommodating the wide power fluctuations observed in wave power devices. In contrast, the work presented in this thesis has studied the concept with the objective of improving the system’s efficiency.

Folley et al. point out that the device fixes the ratio between the pressures of the RO membranes’ feed and the concentrate. This was also shown earlier in the Chapter 5 (Equation 5.4). Folley et al. also mention that the device fixes the pressure drop across the RO membranes. The results in the system modelling presented previously in Chapter 6 (Figure 6.3) suggest something slightly different, because the pressure drop across the RO membranes actually varies. However, these variations are very small compared with those expected from a system using a basic Clark pump.

Folley et al. observe that the use of the PEI results in a nearly constant concentrate flow. This is also evident in Figure 6.3 and follows from the variable recovery ratio of the configuration, which contrasts with the operation of a basic Clark pump where the recovery ratio is fixed. Folley et al. also observe that the nearly constant concentrate flow is particularly beneficial for the membranes at low feed pressures because it ensures a healthy flow in the membranes. This feature represents an advantage when working with reverse osmosis systems with fluctuating power inputs.

Finally, the work presented by Folley et al. was based primarily on computer simulations. The work in this thesis has also shown simulation results and, in

addition, it also includes the practical testing of the concept. The outcomes of the testing are presented in the next chapter.

Chapter 8 Testing and results

8.1 General arrangement

The modified Clark pump was tested in the closed loop configuration shown in Figure 8.1 (reciprocation valve gear not shown). Here, the system was fed from a tank which was replenished by both the product water and the depressurised concentrate (exhaust). It must be noted that this configuration was only used for testing. In a normal system, the product would flow to a separate storage tank for distribution and use, while the exhaust would be disposed of.

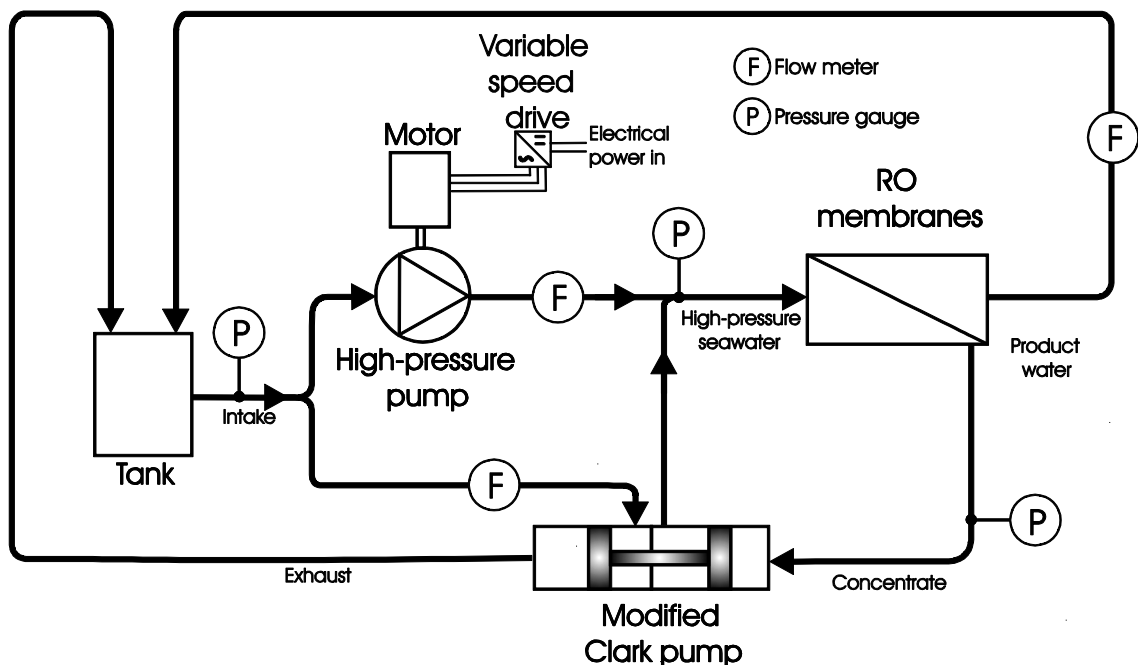


Figure 8.1 Prototype test arrangement

A photograph of the reverse osmosis rig used for testing is presented in Figure 8.2. The modified Clark pump can be seen in the middle of the rig just under the four blue pressure vessels that house the RO membranes. The high-pressure plunger pump is located at the bottom of the rig (blue with a red oil cap), immediately to the right of its electric motor (gray and black). The vertical blue

container in the left of the photograph houses a cartridge filter to prevent impurities in the tank from reaching the pumps.

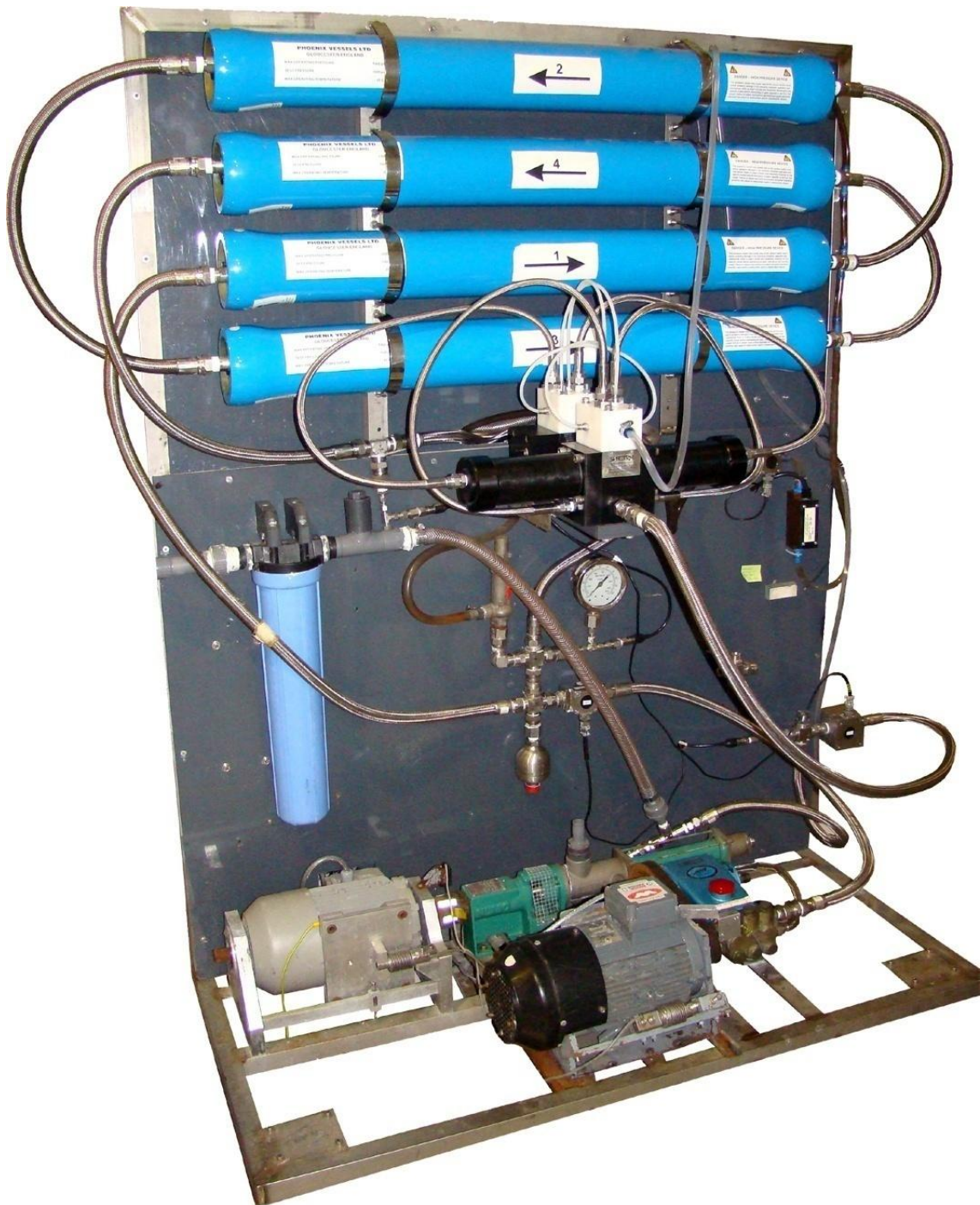


Figure 8.2 The test rig

8.2 Successful operation

During testing, the prototype system in Figure 8.2 desalinated seawater successfully, where:

- The modified Clark pump served effectively to recover energy from the concentrate stream.
- Most of the energy recovered was used to pressurise seawater above the pressure of the concentrate, contributing to the membranes high-pressure feed flow.
- The modified Clark pump sucked the seawater in from a tank and through a cartridge filter without the need of a low-pressure pump.
- The high-pressure pump was the only input of motive power in the system.
- The modifications of the reciprocation valve gear were successful and the new pistons-rod assembly reversed direction at the end of each stroke.

Thus, the tests demonstrated the energy recovery concept, which is the main objective of the work presented in this thesis. The following sections look in detail into the performance of the modified Clark pump and the system in general.

8.3 Test setup details

The hardware used in the test rig is described in Table 8.1. All these components were already part of CREST's RO test rig before this thesis work commenced and were reconfigured to achieve the layout required for use with the modified Clark pump.

Table 8.1 Test rig hardware

Item	Model	Maximum ratings	Quantity	Notes
High-pressure pump	CAT 317	150 bar 15 L/min	1	Plunger pump
Variable speed electric motor	Brook Hansen WD100LB	3 kW 3-phase	1	Variable speed
Variable frequency inverter	FKI-22220	2.2 kW	1	--
RO membranes	Koch TFC 1820 HF	--	4	4 inch by 40 inch, in series.

For the testing, the rig was powered from mains AC electricity, which was rectified to DC and then converted to variable frequency AC power in the inverter. In a field operation, a renewable energy generator such as a PV array could be connected directly to the DC input of the inverter.

The test rig also has three oval gear flow meters from Titan Enterprises (www.flowmeters.co.uk, accessed 25 August 2009) and three pressure gauges from Druck (www.druck.com, accessed 25 August 2009), located as indicated in Figure 8.1. A data acquisition system logged these parameters.

A straight NaCl solution was used for the tests. Its concentration at the pumps intake was close to 32 000 mg/L. The temperature of the NaCl solution was around 25 °C throughout the testing.

The variable frequency inverter was used to control the speed of the motor driving the high-pressure pump. The speed and torque of the motor and the electrical power input to the inverter were also logged.

Eight tests were performed to cover a range of motor speeds. The system was first brought to full speed operation where it was allowed to stabilise. The data were logged and then averaged during one full minute of stable operation.

For the subsequent tests, the motor speed was reduced in steps of about 11%, repeating the data logging and averaging at each speed.

The range of motor speeds covered corresponds to a range of electrical DC input power stretching between 286 W and 1196 W, which represents a minimum-to-maximum input power ratio of just above 4.

8.4 Results

The averaged data for key parameters during all tests are given for reference in the Appendix A . The analysis presented next uses those data.

8.4.1 Product flow

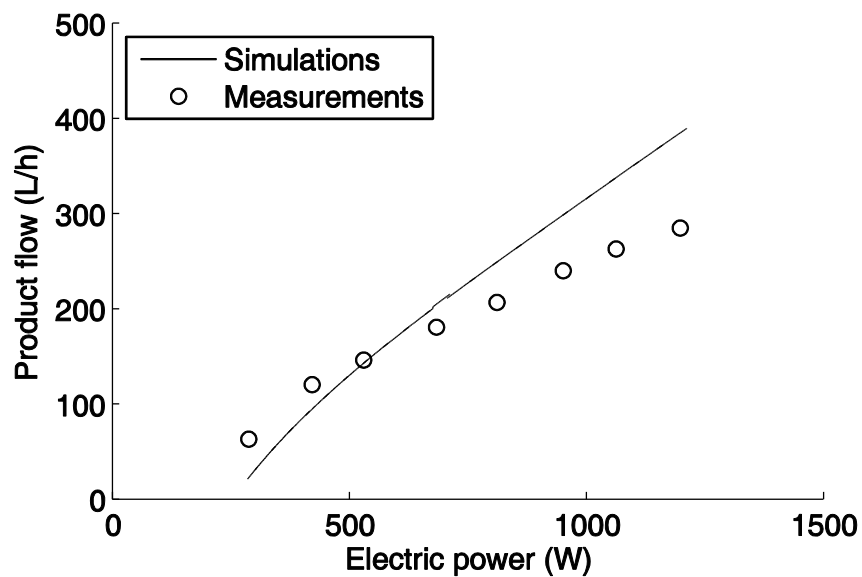


Figure 8.3 Product flow

The system desalinated seawater successfully over a wide range of input power. The measured product flows for the eight tests are presented in Figure 8.3 as the circle markers, and range from 64 to 286 L/h. Simulation results are also included in the figure (continuous line).

In Figure 8.3, the product flows are almost linear with input power which suggests that a roughly flat specific energy consumption could be expected throughout the operation range. Indeed, this is confirmed in Figure 8.4, where specific energy consumptions between 3.5 and 4.5 kWh/m³ are observed. These specific energies are not outstanding but they are very respectable for such a small system and even more so for a first prototype where everything can potentially be improved.

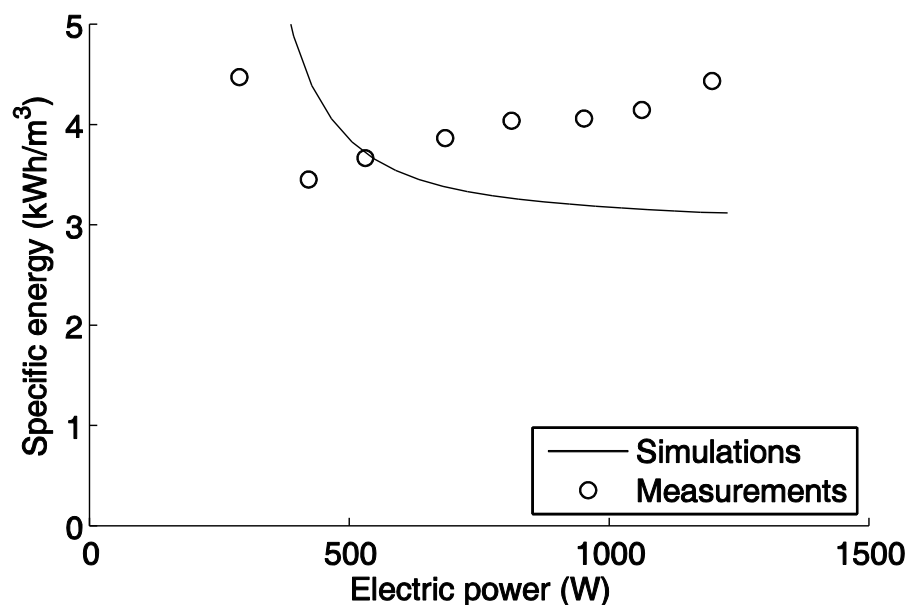


Figure 8.4 Specific energy

It is evident in these two figures that there are some discrepancies between the measurements and the simulations, where for the most part the product flow measurements are below the modelling results, giving higher measured specific energies. Since the RO membranes are already six years old and have not

been maintained, fouling seems a likely explanation for their low product flows and the high specific energies observed. To investigate this, the membranes' water production is looked at more closely in the next section.

8.4.2 RO membranes performance

To study the membranes' performance the product flow can be plotted against the feed pressure. An almost linear correlation between these two parameters is expected as illustrated by the continuous line in Figure 8.5, which corresponds to modelling results. The measured flows follow this trend quite closely up until 38 bar. At higher pressures their trend changes and the membranes actually produce more water than expected for the pressure levels reached. This is in opposition to what would be expected for fouled membranes, and this finding suggests that the membranes have degraded and are now allowing more water through. If this were the case, the salt passage in membranes would also be expected to rise, yielding a product of higher salinity.

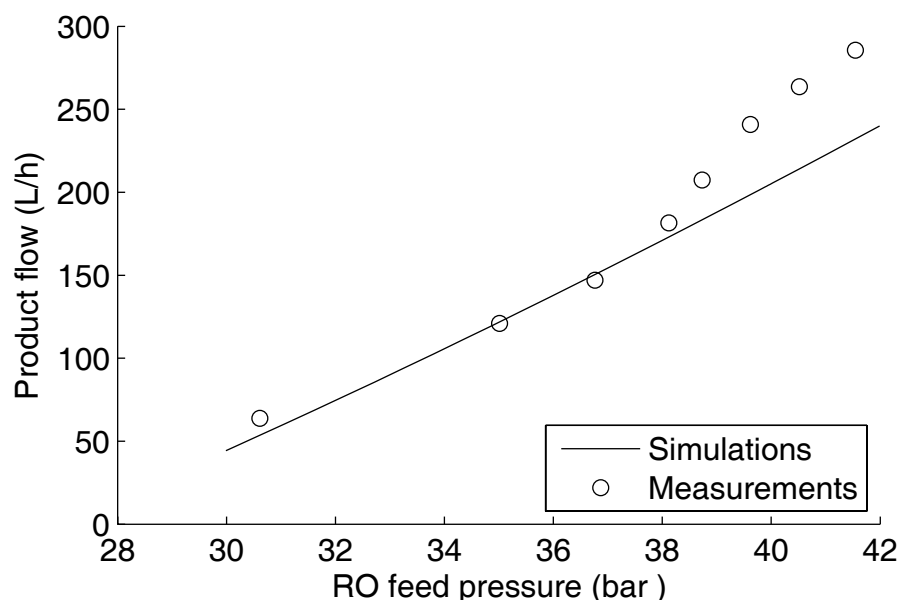


Figure 8.5 Effect of feed pressure on product flow

During the first of the tests (full motor speed, 1196 W), the salinity of a sample of the permeate was determined with a conductivity meter in the laboratory as 741 mg/L. This is considerably higher than the 166 mg/L predicted by the model for the same power and supports the above suggestion regarding membrane degradation.

However, the low product flow observations from Figure 8.3 still remain unexplained. This now suggests that during testing, the membranes' feed pressure was not rising to expected levels, which would cause low product flows and must be investigated.

8.4.3 Membranes feed pressure

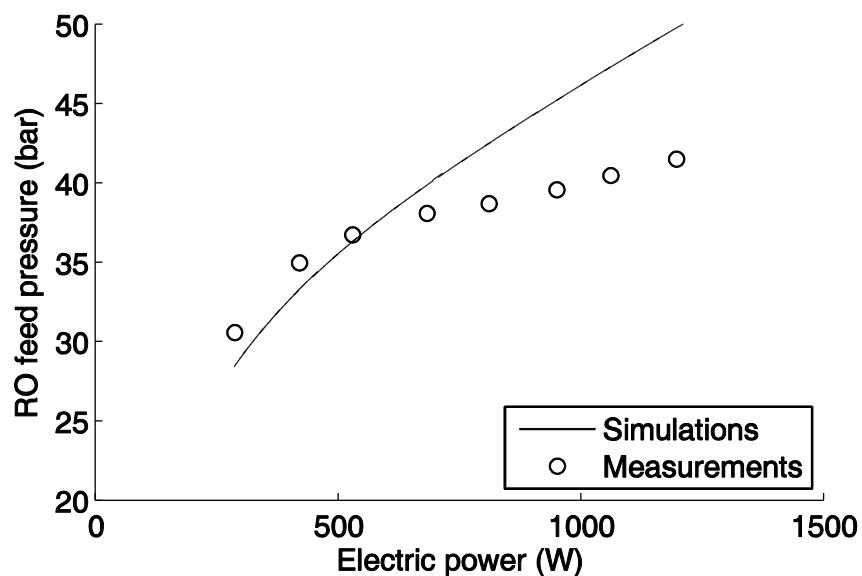


Figure 8.6 RO membranes feed pressure

During testing, the membranes' feed pressure reached values between 30.6 and 41.5 bar, which are presented in Figure 8.6 alongside the model predictions. In this figure, the measured data profile appears somewhat flatter, especially at higher powers. The pattern of the discrepancies between product

flow measurements and simulations observed in Figure 8.3 is very similar to the pattern found with the feed pressures in Figure 8.6, which confirms that the low product flows are primarily caused by low feed pressures.

However, the low pressures must now be explained. A likely reason is a low feed flow to the RO membranes. This was investigated.

8.4.4 Flows in the modified Clark pump

A low membranes' feed flow could be due to either the plunger pump flow or the modified Clark pump flow (see Figure 8.1). However, the plunger pump has a very reliable operation record; the recently modified Clark pump, on the other hand, is a more likely cause of the discrepancies.

After approaching this issue from various angles and studying the effects of several variables, the most revealing was the ratio between the seawater inlet flow and the exhaust flow in the modified Clark pump. This is shown in Figure 8.7, where values very close to the area ratio dictated by the geometry of the device $r_a = 0.9$ were expected for all tests. This is the case for the two lower pressures, where ratios of 0.89 and 0.88, respectively, are found. Beyond 35 bar the ratios drop rapidly.

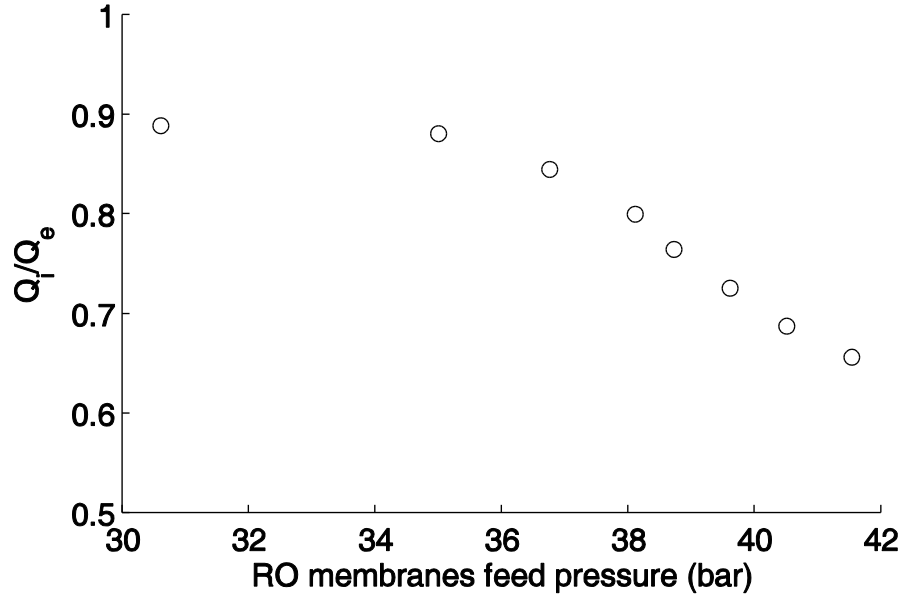


Figure 8.7 Inlet-to-exhaust flow ratio in the modified Clark pump

The decreasing flow ratios in Figure 8.7 indicate that, in order to maintain the flow balance, the suction chamber of the modified Clark pump was receiving a flow input in addition to that coming from the tank and registered by the flow meter. This could result from internal leakage between the middle two chambers of the pump. A combination of two facts could be responsible for such leakage: first, the new rod linking the pistons (see section 7.5) is slightly thinner and not as smoothly finished as the original rod; and second, the large pressure difference between these two middle chambers of the pump (in excess of 40 bar at full motor speed). Furthermore, if the new rod-pistons assembly is not perfectly centred within the pump as a result of fixing the pistons to the rod, this would also affect the seals between the middle two chambers, adding on to the possibility of a leak between them.

To explore this possibility, a leakage flow was calculated from the measurements and plotted against the pressure difference across the two middle chambers. The leakage flow (Q_{leak}) was calculated as the difference between the seawater inlet flow expected from the area ratio of the modified Clark pump ($Q_{i\text{ calculated}}$) and the actual measurements of that same flow (Q_i).

For this, the three logged flows (plunger pump flow, Q_h ; product flow, Q_p ; modified Clark pump inlet flow, Q_i) were used as follows:

1. Feed flow Q_f : $Q_h + Q_i = Q_f$ Equation 8.1

2. Exhaust flow Q_e : $Q_f - Q_p = Q_e$ Equation 8.2

3. Calculated inlet flow $Q_{i \text{ calculated}}$: $r_a Q_e = Q_{i \text{ calculated}}$ Equation 8.3

4. Leakage flow Q_{leak} : $Q_{i \text{ calculated}} - Q_i = Q_{leak}$ Equation 8.4

Leakage flows are presented in Figure 8.8 and shows a profile that is reasonably matched by the quadratic trend line added from the second point on.

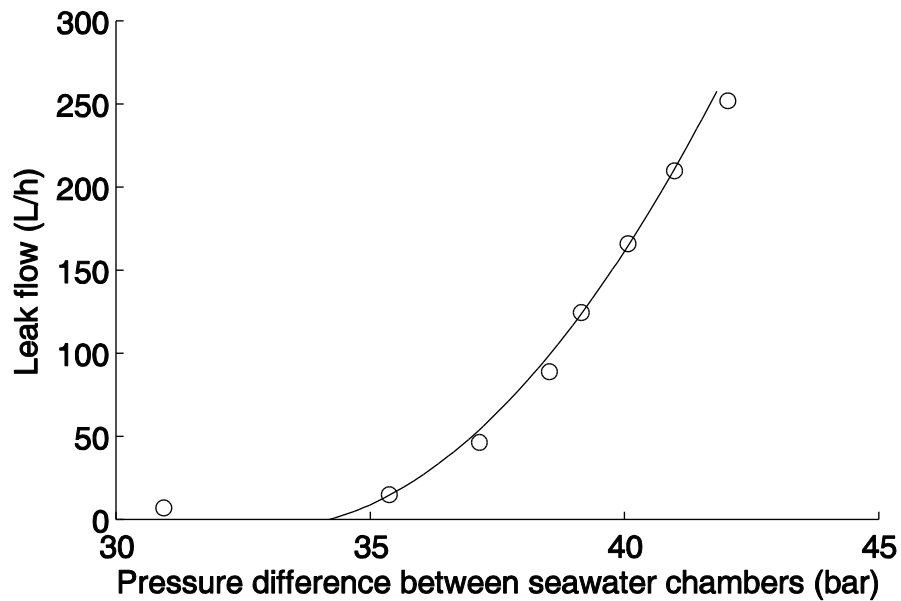


Figure 8.8 Pressure-driven leak

This figure supports the explanation of a pressure-driven leak between the middle chambers, which would lead to a reduction of the membranes' feed flow, causing low pressures and ultimately the low product flows measured. Given the magnitude of the leakage, a considerable amount of energy is being lost in this way.

8.4.5 Energy balance

To estimate the significance of the leakage losses, a specific energy balance around the modified Clark pump can be drawn using its flows and pressures. In the first test (1196 W of DC input power), 4.01 kWh/m³ enter the pump in the concentrate of which 2.66 kWh/m³ (66%) leave the pump in the pressurised seawater and 0.03 kWh/m³ (1%) are used to suck the seawater in. The leak flow and pressure difference between the middle chambers equate to a loss of 1.03 kWh/m³ (26%), which shows that the leak is a major inefficiency of the pump and must be a high priority to address in future prototypes.

After considering the leak losses, there is still 7% of the energy that remains unaccounted for. This corresponds to the friction losses in the pump. As mentioned in section 7.5, the rod and pistons in the original Clark pump were not joined together but nevertheless they reciprocated as a single unit. This loose arrangement allowed each piston some flexibility to compensate for any eccentricities of the forces applied (e.g., the rod not perfectly centred in the pistons) and also to compensate for any unevenness on the contacting surfaces either between the pistons and the rod, or between the pistons and the cylindrical housing. With the modifications of the Clark pump, the pistons were tightly screwed onto the new rod and this rigid arrangement is likely to present more friction during reciprocation, as it removes the flexibility inherent to the original arrangement causing additional energy losses.

To place the losses discussed above in the context of the whole system, the specific energy flows measured from the test rig at full motor speed (1196 W of electrical input power) are presented in the Sankey diagram in Figure 8.9. This diagram may be compared with the simulated performance presented in Figure 6.8 (page 98). The most conspicuous difference is the large loss in the modified Clark pump resulting from the internal leakage and friction.

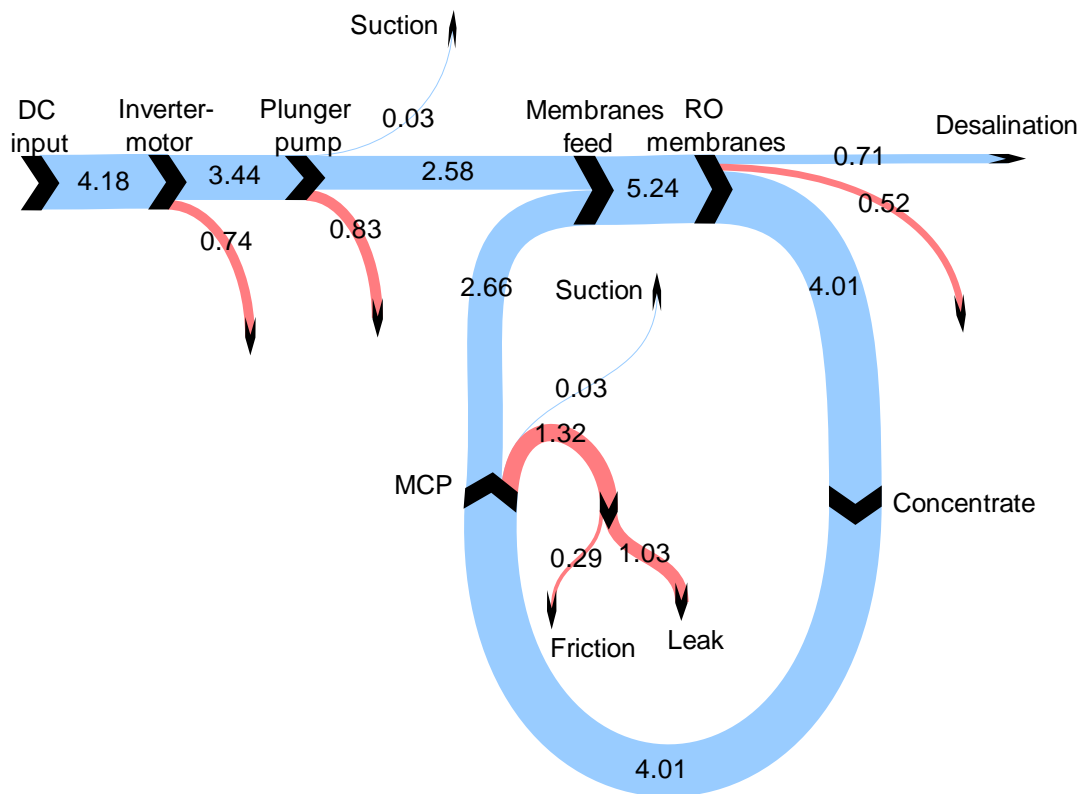


Figure 8.9 Specific energy flows during the test at 1196 W.
Values in kWh/m³

As a knock-on effect, the leakage and friction have also caused the smaller energy flows through the modified Clark pump and RO membranes, including the reduced membrane losses. These reductions arise from the lower water flows at also lower pressures in this section of the system as explained earlier.

8.4.6 Uneven operation

It was also noticed during testing that the operation of the modified Clark pump was not as smooth as with the original configuration. Pressure spikes were observed at the end of each stroke, and even during each stroke, the pressures and flows were not constant. Disruptions to the reciprocation timing brought about by the modifications could be responsible for this. These issues must be investigated to ensure the smooth operation of subsequent prototypes.

8.5 Revised modelling

In order to check the consistency of the explanations given in the results analysis above, the model presented in Chapter 6 was modified to incorporate them. This was done as follows:

- Internal leakage in the modified Clark pump. The data in Figure 8.8 were used to determine a leakage flow profile. These flows were then subtracted from the ideal seawater flow as calculated in the original model.
- RO membranes degradation. The effect of membrane degradation was incorporated as an increase in water production and salt passage in the membrane model.
- Friction. Since the friction losses are a consequence of reciprocation, they were estimated as proportional to the concentrate flow Q_c which drives the pistons-rod assembly.

The incorporation of these practical issues into the Simulink model modified its predictions significantly as seen in Figure 8.10. The modelled feed pressure is now lower as are the product flows, and consequently, the simulated specific energy consumptions now approximate the measurements much better.

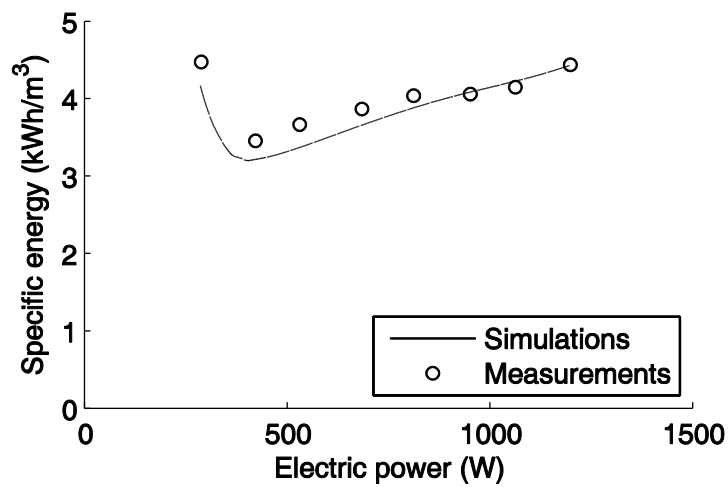
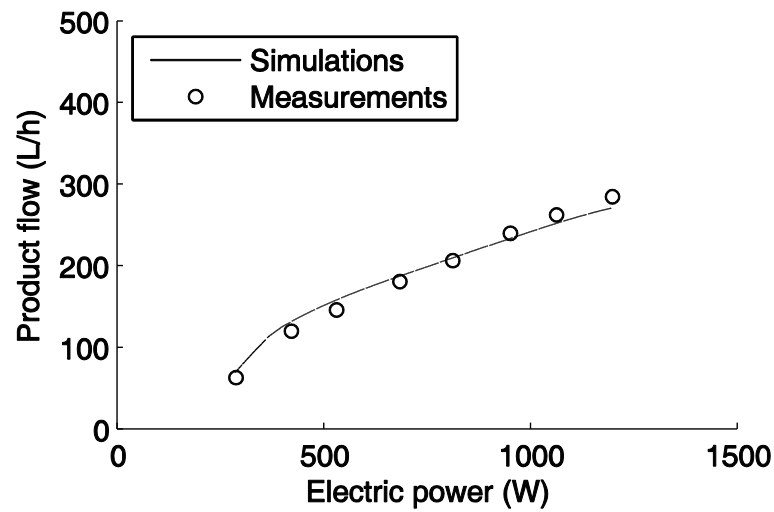
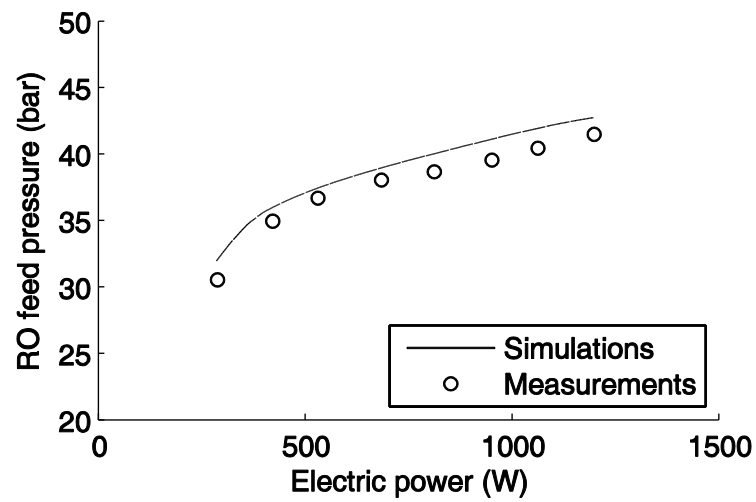


Figure 8.10 Revised model predictions

The modifications of the Simulink model are also reflected in the simulated energy flows around the system, which are illustrated in the Sankey diagram in Figure 8.11. These energy flows are very similar to the ones in Figure 8.9 (page 126) corresponding to the testing results. Thus, it is apparent that the adjusted model agrees very closely with the measurements, which supports the explanations given.

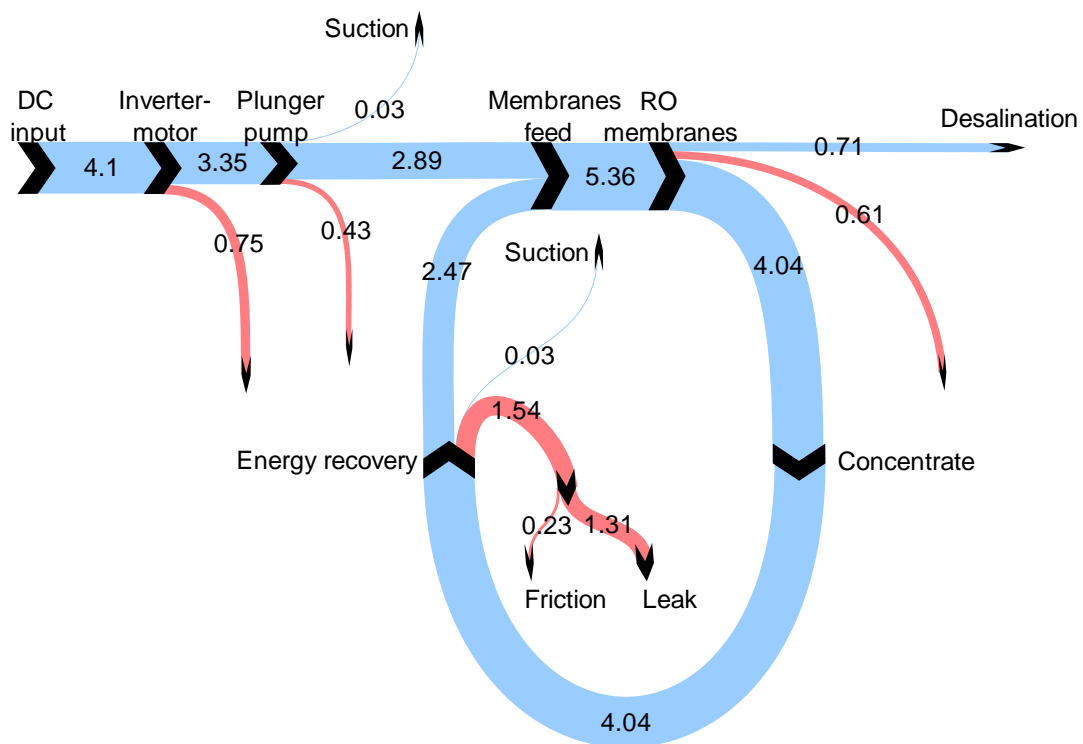


Figure 8.11 Sankey diagram of revised energy flows at 1196 W.
Values in kWh/m³

Chapter 9 Conclusions

This thesis described the concept development and prototype implementation of a new pressure intensifier for energy recovery in small-scale seawater reverse osmosis systems as well as the results of its successful practical demonstration. The following sections present the conclusions of this work.

9.1 Energy recovery for small-scale SWRO

A comprehensive review of the literature showed that brine-stream energy recovery has played a key role in lowering the energy consumption of SWRO. At the small scale, however, there are very few energy recovery devices available in the market, which has been partly responsible for the neglect of energy recovery practices in small systems, including most renewable-energy-powered SWRO systems. Consequently, there is still considerable room for innovative energy recovery designs at this level.

9.2 Mathematical analysis of pressure intensifiers

A generalised analysis applicable to pressure intensifiers for energy recovery in reverse osmosis applications was developed to gain a broad understanding of the capabilities of these devices. The analysis also allowed the study of its particular cases in a wider context.

The analysis uses the piston area ratio as a key variable and shows that it may be regarded as a continuum from below to above unity. Mathematical expressions for the product flow, freshwater recovery ratio and membranes feed pressure were derived and analysed across this continuum, identifying trends and implications.

The piston area ratio was used as a means of categorising devices: below, equal-to and above unity. These categories were then used to identify differences such as the requirement or otherwise of particular pumps within the system as well as viable ranges of operation. The generalised analysis was used in the specification of the piston area ratio of the new device and in its modelling within a reverse osmosis system.

9.3 New system configuration

The generalised analysis and modelling indicated the possibility of a system configuration that would be capable of sucking in seawater, which made possible the elimination of the low-pressure pump. The new configuration uses only one high-pressure pump and is therefore simpler than the Clark pump injection configuration.

9.4 Improved system efficiency

The new system configuration effectively replaces the motorised low-pressure pump of the basic Clark pump configuration with a high-pressure one. This could be for example a plunger pump or an axial-piston pump, both of which are capable of much higher efficiencies than small low-pressure centrifugal, diaphragm or Moineau pumps. This substitution makes energy efficiency improvements possible by reducing the losses of the motorised pumping component. This potential was quantified and the specific energy consumption of a commercial system consuming 3.2 kWh/m^3 could be reduced by 1 kWh/m^3 if a pump 18% more efficient were used (section 4.2).

9.5 New device concept

In order to realise the new configuration, a different approach to energy recovery was required. A new energy recovery device for seawater reverse osmosis systems was proposed and investigated. The device relies only on its piston area ratio to suck in and pressurise a portion of the seawater feed of the RO membranes; it is driven only by the energy it recovers from the concentrate. The new device concept is different from all known commercial devices and was also proposed by Folley et al. (2008), albeit in a direct-drive system; their work was primarily based on computer simulations. The work in this thesis covered the implementation of the concept and its practical operation within a SWRO system too.

9.6 Prototype implementation

A prototype of the new device was built. For implementation, the hardware of a standard Clark pump was used. The hardware was modified to redirect the main flows so as to reverse the roles of its two pairs of chambers. To achieve this, the valve gear of the original pump was reconfigured. The prototype is mechanically very similar to a Clark pump but its mode of operation is entirely different, and has been therefore referred to as a modified Clark pump.

9.7 First practical demonstration

To the knowledge of the author, the work described in this thesis is the first practical demonstration of the new energy recovery concept. The prototype built served effectively to recover energy from the concentrate and the whole system achieved its basic goal of desalinating seawater without the use of a low pressure pump. In the demonstration, the modified Clark pump sucked in seawater from a tank nearby through a cartridge filter without problems.

The energy consumption characteristic recorded with the modified Clark pump was relatively flat over a wide range of input power. This makes the concept of the new intensifier attractive for renewable-energy-powered SWRO systems without batteries, or for any other SWRO applications with fluctuating power inputs and no energy storage.

The specific energies recorded with the modified Clark pump were very respectable but they were not better than those reported for the standard Clark pump. This was primarily because of a compromise made on the piston area ratio imposed by the use of a Clark pump's hardware for implementation. Additionally, the nature of the modifications of the Clark pump led to a number of inefficiencies in the prototype that further increased the system's energy consumption.

9.8 Practical issues

After the tests, it became evident that there are a number of issues to be addressed in any future development of the concept. These are:

- The presence and extent of internal leaks needs further investigation and solution.
- The smooth operation of the pump must be restored. Irregular flows and pressures were observed during each stroke which may be due to poor timing of the operation of the reciprocation valve gear. The long flexible tubes and hoses used to reconfigure the pump for the test may also be affecting this timing and a closely coupled configuration should be sought.
- An internal source must be found for the small supply of water required to actuate the spool valve. Mains water was used in the testing.

- The firm attachment of the pistons to the rod may have increased friction within the pump and should be investigated.
- Alongside the optimisation of the modified Clark pump itself, the other components in the system should be selected to minimise overall specific energy consumption.
- The modified Clark pump sucked in its own seawater. However, applications requiring a larger suction head could present a challenge and result in cavitation. For instance, drawing seawater from a deep beach well would require installing the device close to seawater level.

9.9 *Alternative implementation*

As an alternative to the modified Clark pump, the new energy recovery concept could also be implemented using an arrangement consisting of an axial-piston pump (APP) in combination with an axial-piston motor (APM) of larger capacity. The arrangement would act as an energy recovery device with a piston area ratio $r_a < 1$ and would be placed instead of the modified Clark pump as shown in Figure 9.1.

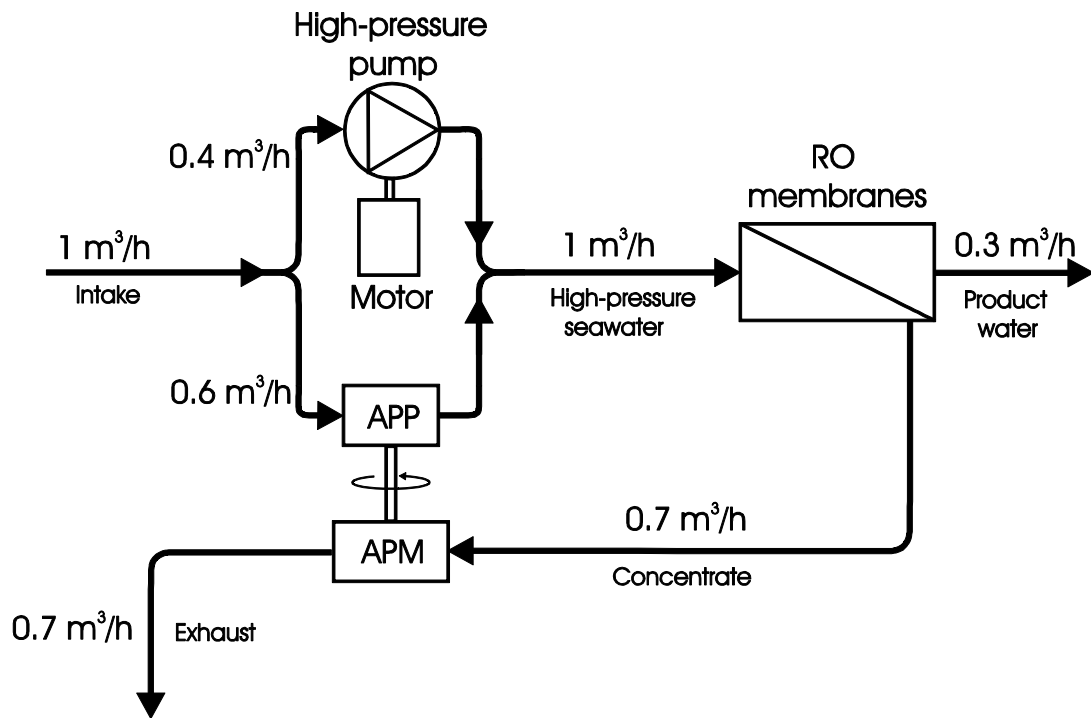


Figure 9.1 Alternative configuration

With the ready availability of axial-piston pumps and motors this setup could be easier to implement. However, it would not be expected to be more efficient than an optimised modified Clark pump. The generalised analysis presented in Chapter 5 would also be applicable to this setup but the angles of the swash plate of the two devices must be taken into consideration to incorporate them into the piston area ratio r_a appropriately.

9.10 Closing statement

This thesis has presented a novel option for energy recovery in small-scale SWRO systems. A mathematical model allowed development of a prototype device and system which successfully operated to desalinate seawater.

Publications

- Bermudez Contreras, A. and Thomson, M. (2008). Energy recovery for reverse osmosis desalination in Mexico. *Proceedings of the 1st IWA Mexico National Young Water Professionals Conference*, Mexico City, Mexico, International Water Association Mexico, 66-73. On-line available <http://hdl.handle.net/2134/5115> accessed (30 November 2009).
- Bermudez-Contreras, A. and Thomson, M. (2009). Modified operation of a small scale energy recovery device for seawater reverse osmosis. *Proceedings of the European Desalination Society Conference Desalination for the Environment - Clean Water and Energy*, Baden-Baden, Germany, 17-20 May 2009, European Desalination Society.
- Bermudez-Contreras, A. and Thomson, M. (2010). Modified operation of a small scale energy recovery device for seawater reverse osmosis. *Desalination and Water Treatment* **13**: 195-202. On-line available <http://hdl.handle.net/2134/5963> accessed (2 March 2010).
- Bermudez-Contreras, A., Thomson, M. and Infield, D. G. (2008). Renewable energy powered desalination in Baja California Sur, Mexico. *Desalination* **220**(1-3): 431-440. On-line available <http://hdl.handle.net/2134/5964> accessed (2 March 2010).
- Thomson, M. and Bermudez, A. (2006). *ADU - RES Work Package 6: Further Development of Integrated Plant Design - Deliverable 6.1: Energy Consumption Modelling*. European Commission, 6th Framework Programme, Co-ordination Action Autonomous Desalination Units Based on Renewable Energy Systems, September 2006. On-line available www.adu-res.org accessed (27 April 2009).

References

- Andrews, W. T. and Laker, D. S. (2001). A twelve-year history of large scale application of work-exchanger energy recovery technology. *Desalination* **138**(1-3): 201-206.
- Arp, L. J. and Varnum, J. M. (1970). *Fluid delivery device*. United States Patent 3530873.
- Barlow, R., McNelis, B. and Derrick, A. (1993). *Solar pumping :an introduction and update on the technology, performance, costs, and economics*. London, Intermediate Technology Publications.
- Bermudez Contreras, A. and Thomson, M. (2008). Energy recovery for reverse osmosis desalination in Mexico. *Proceedings of the 1st IWA Mexico National Young Water Professionals Conference*, Mexico City, Mexico, International Water Association Mexico, 66-73. On-line available <http://hdl.handle.net/2134/5115> accessed (30 November 2009).
- Bermudez-Contreras, A., Thomson, M. and Infield, D. G. (2008). Renewable energy powered desalination in Baja California Sur, Mexico. *Desalination* **220**(1-3): 431-440. On-line available <http://hdl.handle.net/2134/5964> accessed (2 March 2010).
- Buros, O. K. (2000). *The ABCs of Desalting*. International Desalination Association. On-line available: <http://www.elkhornslough.org/desal/ABCs.pdf> (accessed: 20/09/2006).
- Buros, O. K., El-Nashar, A. M. and Bakish, R. (1981). *The U.S.A.I.D. desalination manual*. International Desalination and Environmental Association (IDEA).
- Byrne, W. (1995). *Reverse osmosis - A practical guide for industrial users*. Tall Oaks Publishing.
- Carnegie Wave Energy Limited (2009). *CETO*. On-line available: <http://www.carnegiecorp.com.au/> accessed (22 October 2009).
- Carta, J. A., González, J. and Subiela, V. (2004). The SDAWES project: an ambitious R&D prototype for wind-powered desalination. *Desalination* **161**(1): 33-48.
- Charcosset, C. (2009). A review of membrane processes and renewable energies for desalination. *Desalination* **245**(1-3): 214-231.

- Childs, W. D. and Dabiri, A. E. (1999). Hydraulic driven RO pump & energy recovery system. *International Desalination and Water Reuse Quarterly* **9**(2): 21-29.
- Childs, W. D., Dabiri, A. E., Al-Hinai, H. A. and Abdullah, H. A. (1999). VARI-RO solar-powered desalting technology. *Desalination* **125**(1-3): 155-166.
- CRES (1998). *Desalination Guide Using Renewable Energies*. THERMIE - DG XVII, European Commission Report, CRES. Greece.
- Cruz, J. and Salter, S. (2006). Update on the design of an offshore wave powered desalination device. *Proceedings of the OWEMES European Seminar*, Civitavecchia (Rome), Italy, 20-22 April 2006, On-line available <http://192.107.92.31/test/owemes/38.pdf> accessed (21 October 2009).
- Dallas, S., Sumiyoshi, N., Kirk, J., Mathew, K. and Wilmot, N. (2009). Efficiency analysis of the Solarflow - An innovative solar-powered desalination unit for treating brackish water. *Renewable Energy* **34**(2): 397-400.
- Danfoss (2009). *SWPE seawater pump with energy recovery*. On-line available: <http://www.danfoss.com/Solutions/Reverse+Osmosis/ProductGroups/SWPEunit.htm> accessed (20 July 2009).
- Davies, P. A. (2005). Wave-powered desalination: resource assessment and review of technology. *Desalination* **186**(1-3): 97-109.
- Desalination & Water Reuse (2009). *Wave-powered desalination plant to produce bottled water*. On-line available: http://www.desalination.biz/news/news_story.asp?id=5074 accessed (13 October 2009).
- Doujak, E. and List, B. (2003). Application of PIV for the Design of Pelton Runners for RO-Systems. *Proceedings of the Renewable Energy Sources for Islands, Tourism and Water Desalination Conference*, Crete, Greece, 26-28 May 2003, EREC (European Renewable Energy Council), 533-540.
- Dow (2005). *FILMTEC Reverse Osmosis Membranes - Technical Manual*. July 2005. DOW Liquid Separations. On-line available: <http://www.dow.com/liquidseps/lit/techman.htm> (accessed: 28/02/2006).
- Dow (2009a). *Dow Chemical Company*. On-line available: <http://www.dow.com/> accessed (26 June 2009).
- Dow (2009b). *System Design: Membrane System Design Guidelines*. On-line available: http://www.dow.com/liquidseps/design/des_ronf_feed.htm accessed (22 February 2009).

- Dow Filmtec (1998). *Factors affecting RO membranes performance*. Dow Filmtec. On-line available: http://www.dow.com/liquidseps/lit/tech_inf.htm accessed (20 September 2009).
- Dow-ROSA (2005). *ROSA. Version 6.0.1*. Dow Liquid Separations.
- Economist.com (2008). Tapping the oceans. *The Economist - Technology Quarterly*.
- El-Dessouky, H. T. and Ettouney, H. M. (2002). *Fundamentals of Salt Water Desalination*. Amsterdam, Elsevier.
- Energy Information Administration (2009). *International Energy Statistics*. US Department of Energy. On-line available: <http://www.eia.doe.gov/international/> accessed (24 July 2009).
- Energy recovery Inc (2007). *PX Pressure Exchanger*. Energy recovery Inc. On-line available: <http://www.energyrecovery.com/> accessed (24 May 2009).
- Epp, C. and Papapetrou, M. (2005). *ADU - RES Work Package 2: Report on the Status of Autonomous Desalination Units Based on Renewable Energy Systems*. WIP - Renewable Energies. On-line available www.adu-res.org accessed (28 October 2005).
- Fabre, A. (2003). Wind turbines designed for the specific environment of islands case study: Experience of an autonomous wind powered water desalination system on the island of Therasia, Greece - Vergnet SA, France, in *Proceedings of Renewable Energy Sources for Islands, Tourism and Water Desalination Conference*. Crete, Greece, EREC (European Renewable Energy Council). 247-252.
- Folley, M., Peñate Suarez, B. and Whittaker, T. (2008). An autonomous wave-powered desalination system. *Desalination* **220**(1-3): 412-421.
- Folley, M. and Whittaker, T. (2009). The cost of water from an autonomous wave-powered desalination plant. *Renewable Energy* **34**(1): 75-81.
- Freris, L. and Infield, D. (2008). *Renewable energy in power systems*. Chichester, John Wiley.
- Garcia-Rodriguez, L. (2002). Seawater desalination driven by renewable energies: a review. *Desalination* **143**(2): 103-113.
- Garretson, O. L. (1950). *Hydraulic pumping unit*. United States Patent 2528131.
- GE (2009). *GE Water*. On-line available: www.gewater.com accessed (6 July 2009).

- Ghermandi, A. and Messalem, R. (2009). Solar-driven desalination with reverse osmosis: the state of the art. *Desalination and Water Treatment* (7): 285-296.
- Greenlee, L. F., Lawler, D. F., Freeman, B. D., Marrot, B. and Moulin, P. (2009). Reverse osmosis desalination: Water sources, technology, and today's challenges. *Water Research* **43**(9): 2317-2348.
- Gwillim, J. (1996). *Village Scale Photovoltaic Powered Reverse Osmosis*. Dulas Limited. Machynlleth, Wales. March 1996.
- Hicks, D. C. (2004). Communication to the Horizon Solutions Site. Update on: *The Delbuoy, a low-cost, low maintenance, wave-powered desalination unit*. Horizon Solutions Site. On-line available: http://www.solutions-site.org/artman/publish/article_60.shtml accessed (21 October 2009).
- Hicks, D. C., Mitcheson, G. R., Pleass, C. M. and Salevan, J. F. (1989). Delbouy: Ocean wave-powered seawater reverse osmosis desalination systems. *Desalination* **73**: 81-94.
- Hydranautics (2007). *RO animation*. On-line available: <http://www.membranes.com/> accessed (11 November 2009).
- Independent Natural Resources Inc. (2009). *The SEADOG pump*. On-line available: <http://inri.us/index.php/SEADOG> accessed (15 October 2009).
- Kalogirou, S. A. (2005). Seawater desalination using renewable energy sources. *Progress in Energy and Combustion Science* **31**(3): 242-281.
- Käufle, J. and Pohl, R. (2009). Seawater desalination (RO) as a wind powered industrial process — technical and economical specifics. *Proceedings of the European Desalination Society Conference Desalination for the Environment - Clean Water and Energy*, Baden-Baden, Germany, 17-20 May 2009, European Desalination Society.
- Keefer, B. G. (1980). *Reverse osmosis method and apparatus*. United States Patent 4187173.
- Keefer, B. G. (1984). *Multi-cylinder reverse osmosis apparatus and method*. United States Patent 4434056.
- Keefer, B. G., Hembree, R. D. and Schrack, F. C. (1985). Optimized matching of solar photovoltaic power with reverse osmosis desalination. *Desalination* **54**: 89-103.
- Koch (2000). *Reverse osmosis product catalogue*. Wilmington, Koch Membrane Systems.
- Koch (2009). *Koch Membrane Systems*. On-line available: <http://www.kochmembrane.com/> accessed (6 July 2009).

- Koch-ROPRO (2000). *ROPRO Version 6.1*. Fluid Systems, Koch Membrane Systems, .
- Kunczynski, Y. (2008). *Use of axial-piston motors for energy recovery in small-scale PV-powered seawater RO systems*. Personal communication. Bermudez Contreras. 31 December 2008. La Paz, Mexico.
- Kunczynski, J. K. (2006). *Hybrid, reverse osmosis, water desalinization apparatus and method with energy recuperation assembly*. United States Patent 20060065597.
- Kunczynski, Y. (2003). Development and Optimization of 1000-5000 GPD Solar Power SWRO. *Proceedings of the IDA World Congress*, Bahamas, 28 September-03 October 2003.
- MacHarg, J., Seacord, T. F. and Sessions, B. (2008). ADC baseline tests reveal trends in membrane performance. *International Desalination and Water Reuse Quarterly* **18**(2): 30-39.
- MacHarg, J. and Truby, R. (2004). West Coast researchers seek to demonstrate SWRO affordability. *International Desalination and Water Reuse Quarterly* **14**(3).
- Maratos, D. F. (2003). Technical feasibility of wavepower for seawater desalination using the hydro-ram (Hydram),. *Desalination* **153**(1-3): 287-293.
- Markvart, T. (2000). *Solar Electricity*. Chichester, Wiley.
- Mathew, K., Dallas, S., Ho, G. E. and Anda, M. (2000). A solar-powered village water supply system from brackish water. *Proceedings of the World Renewable Energy Congress VI*.
- McCormick, M. E. and Kraemer, D. R. B. (2001). Wave Energy, in *Encyclopedia of Ocean Sciences*. Steele. Oxford, Academic Press. 3187-3191.
- Medina San Juan, J. A. (2000). *Desalación de aguas salobres y del mar: Osmosis inversa*. Madrid, Mundi-Prensa.
- Miranda, M. d. S. (2003). *Small-Scale Wind-Powered Seawater Desalination without Batteries*. Ph. D. thesis. Loughborough University. On-line available: <http://staff.bath.ac.uk/eesmm/Thesis.html>.
- Miranda, M. S. and Infield, D. (2003). A wind-powered seawater reverse-osmosis system without batteries,. *Desalination* **153**(1-3): 9-16.
- Oklejas, R. A. and Oklejas, E. (1990). *Power recovery pump turbine*. United States Patent 4966708.

- Orchard, B. and Pauly, C. (2008). International Desalination Congress report. *World Pumps* **2008**(500): 28-32.
- Pankratz, T. (2008). *IDA desalination yearbook 2008-2009*. Global Water Intelligence. Oxford.
- Paulsen, K. and Hensel, F. (2005). Introduction of a new Energy Recovery System--optimized for the combination with renewable energy. *Desalination* **184**(1-3): 211-215.
- Permar, C. (1995). *Liquid treatment apparatus for providing a flow of pressurized liquid*. United States Patent 5462414.
- Phoenix Vessels Ltd (2000). *Pressure vessel technical diagram*. Gloucester.
- Pinkerton, H. E. (1979). *Fluid handling system*. United States Patent 4178240.
- Rahal, Z. (2001). *Wind powered desalination*. Ph.D. Thesis. Loughborough University.
- Reid, C. E. and Breton, E. J. (1959). Water and ion flow across cellulosic membranes. *Journal of Applied Polymer Science* **1**(2): 133-143.
- Richards, B. S. and Schäfer, A. I. (2002). Design considerations for a solar-powered desalination system for remote communities in Australia. *Desalination* **144**(1-3): 193-199.
- Riffel, D. B. and Carvalho, P. C. M. (2009). Small-scale photovoltaic-powered reverse osmosis plant without batteries: Design and simulation. *Desalination* **247**(1-3): 378-389.
- Schippers, J. C. (2007). *One-day intensive course on membrane fouling and pre-treatment in RO technology. Theory and practice*. Course notes. Halkidiki, Greece. 22 April 2007, European Desalination Society.
- Seacord, T. F., Coker, S. D. and MacHarg, J. (2005). Affordable desalination collaboration 2005 results. *International Desalination and Water Reuse Quarterly* **16**(2): 10-21.
- Shaddock, R. E. (1972). *Double-acting tandem piston pump*. United States Patent 3700360.
- Sharmila, N., Jaliha, P., Swamy, A. K. and Ravindran, M. (2004). Wave powered desalination system. *Energy* **29**(11): 1659-1672.
- Sing, R. (2006). *Hybrid membrane systems for water purification: Technology, systems design and operation*. Oxford, Elsevier.
- Smith, D. (2000). Battery-powered desalter relies on unique pressure pump. *International Desalination and Water Reuse Quarterly* **10**(3): 18-22.

- Spectra Watermakers (2005). *Clark pump field repair & rebuild manual*. 15-Feb-2005. On-line available: <http://www.spectrawatermakers.com/> accessed (06 Jun 2007).
- Spectra Watermakers (2009). Technology overview section. Spectra Watermakers. On-line available: <http://www.spectrawatermakers.com/> accessed (17 July 2009).
- Spiegler, K. S. and El-Sayed, Y. M. (1994). *A Desalination Primer: Introductory Book for Students and Newcomers to Desalination*. Balaban Desalination Publications.
- Stover, R. (2009). Retrofits to improve desalination plants. *Proceedings of the Desalination for the Environment - Clean Water and Energy Conference*, Baden-Baden, Germany, European Desalination Society.
- Stover, R. L. (2007). Seawater reverse osmosis with isobaric energy recovery devices. *Desalination* **203**(1-3): 168-175.
- Subiela, V. J., Fuente, J. A. d. I., Piernavieja, G. and Peñate, B. (2009). Canary Islands Institute of Technology (ITC) experiences in desalination with renewable energies (1996–2008). *Desalination and Water Treatment* (7): 220-235.
- Taylor, J. (1974). *Reverse-osmosis pump*. United States Patent 3825122.
- The Water Corporation (2009a). *Media backgrounder: Southern Seawater Desalination Project - general background info*. 30 June 2009. The Water Corporation. On-line available: http://www.watercorporation.com.au/m/media_detail.cfm?id=3551 accessed (24 July 2009).
- The Water Corporation (2009b). *Seawater desalination*. The Water Corporation. On-line available: <http://www.thinking50.com.au/go/developing-new-sources> accessed (24 July 2009).
- The Water Corporation (2009c). *Southern seawater desalination plant contract signed*. 30 June 2009. The Water Corporation. On-line available: http://www.watercorporation.com.au/m/media_detail.cfm?id=3547 accessed (24 July 2009).
- Thomson, M. (2003). *Reverse-Osmosis Desalination of Seawater Powered by Photovoltaics Without Batteries*. Ph.D. Thesis. Loughborough University. On-line available: <http://www-staff.lboro.ac.uk/~elmt/Thesis.htm> accessed (18 August 2005).
- Thomson, M. and Bermudez, A. (2006). *ADU - RES Work Package 6: Further Development of Integrated Plant Design - Deliverable 6.1: Energy Consumption Modelling*. European Commission, 6th Framework

- Programme, Co-ordination Action Autonomous Desalination Units Based on Renewable Energy Systems, September 2006. On-line available www.adu-res.org accessed (27 April 2009).
- Thomson, M. and Infield, D. (2005). Laboratory demonstration of a photovoltaic-powered seawater reverse-osmosis system without batteries. *Desalination* **183**(1-3): 105-111.
- Toray (2009). *Toray Group*. On-line available: <http://www.toray-membrane.com> accessed (6 July 2009).
- Toyobo (2009). *Toyobo Group*. On-line available: <http://www.toyobo.co.jp/> accessed (26 June 2009).
- Tzen, E., Epp, C. and Papapetrou, M. (2006). Co-ordination Action for Autonomous Desalination Units Based on RE Systems, ADU-RES. *Proceedings of the European Wind Energy Conference & Exhibition (EWEC)*, Athens, Greece, 27 February - 2 March 2006, online available <http://www.ewec2006proceedings.info/> accessed (22 March 2010).
- Tzen, E., Theofiloyianakos, D. and Kologios, Z. (2008). Autonomous reverse osmosis units driven by RE sources experiences and lessons learned. *Desalination* **221**(1-3): 29-36.
- UN-Water (2005). *Water for Life Decade 2005-2015*. United Nations Department of Public Information.
- Van der Bruggen, B. (2003). Desalination by distillation and by reverse osmosis -- trends towards the future. *Membrane Technology* **2003**(2): 6-9.
- Van der Bruggen, B. and Vandecasteele, C. (2002). Distillation vs. membrane filtration: overview of process evolutions in seawater desalination. *Desalination* **143**(3): 207-218.
- Wangnick, K. (2004). *2004 IDA Worldwide Desalting Plants Inventory - Report No. 18*. Wangnick Consulting GmbH.
- Went, J., Kroemke, F., Schmoch, H. and Vetter, M. (2009). Energy demand for desalination with solar powered reverse osmosis units. *Proceedings of the European Desalination Society Conference Desalination for the Environment - Clean Water and Energy*, Baden-Baden, Germany, 17-20 May 2009, European Desalination Society.
- WHO (2003). *Total dissolved solids in Drinking-water. Background document for development of WHO Guidelines for Drinking-water Quality*. Geneva, World Health Organization. On-line available.
- WHO (2008). *Guidelines for drinking-water quality*. Geneva, World Health Organization. On-line available:

http://www.who.int/water_sanitation_health/dwq/gdwq3rev/en/index.html
accessed (19 June 2009).

- Wilf, M., Awerbuch, L., Bartels, C., Mickley, M., Pearce, G. and Voutchkov, N. (2007). *The guidebook to membrane desalination technology: reverse osmosis, nanofiltration and hybrid systems process, design, applications and economics*. L'Aquila, Italy, Balaban Desalination Publications.
- Wilson, L. P. S. (1983). *Reverse osmosis liquid purification apparatus*. United States Patent 4367140.

Appendix A Testing data

Table A.1 Averaged data for all tests

Parameter	Input power	Specific energy consumption	Product flow	Feed pressure	Feed flow	Concentrate flow	Recovery ratio	Pressure drop
Symbol	DC_{in}	SEC	Q_p	P_f	Q_f	Q_c	RR	ΔP_{RO}
Units	(W)	(kWh/m ³)	(L/h)	(bar)	(L/h)	(L/h)	(%)	(bar)
Testing measurements	286	4.48	64	30.6	763	700	9	0.2
	419	3.46	121	35.0	891	770	14	0.2
	528	3.59	147	36.8	973	826	15	0.3
	682	3.76	182	38.1	1055	874	17	0.3
	810	3.90	207	38.7	1112	905	19	0.3
	949	3.94	241	39.6	1179	938	20	0.4
	1060	4.02	264	40.5	1239	976	21	0.4
	1196	4.18	286	41.5	1298	1012	22	0.5